

DELETION MUTATION OF GLNB AND GLNK GENES IN RHODOBACTER
CAPSULATUS TO ENHANCE BIOHYDROGEN PRODUCTION

A THESIS SUBMITTED TO
THE GRADUATE SCHOOL OF NATURAL AND APPLIED SCIENCES
OF
MIDDLE EAST TECHNICAL UNIVERSITY

BY

GÜLŞAH PEKGÖZ

IN PARTIAL FULFILLMENT OF THE REQUIREMENTS
FOR
THE DEGREE OF MASTER OF SCIENCE
IN
BIOTECHNOLOGY

SEPTEMBER 2010

Approval of the thesis:

**DELETION MUTATION OF GLNB AND GLNK GENES IN
RHODOBACTER CAPSULATUS TO ENHANCE BIOHYDROGEN
PRODUCTION**

submitted by **GÜLŞAH PEKGÖZ** in partial fulfillment of the requirements for the degree of **Master of Science in Biotechnology Department, Middle East Technical University** by,

Prof. Dr. Canan Özgen
Dean, Graduate School of **Natural and Applied Sciences** _____

Prof. Dr. İnci Eroğlu
Head of Department, **Biotechnology** _____

Prof. Dr. Ufuk Gündüz
Supervisor, **Biological Sciences Dept., METU** _____

Prof. Dr. İnci Eroğlu
Co-Supervisor, **Chemical Engineering Dept., METU** _____

Examining Committee Members:

Prof. Dr. Semra Kocabıyık
Biological Sciences Dept., METU _____

Prof. Dr. Ufuk Gündüz
Biological Sciences Dept., METU _____

Prof. Dr. İnci Eroğlu
Chemical Engineering Dept., METU _____

Assist. Prof. Dr. Gökhan Kars
Biology Dept., Selçuk University _____

Dr. Tuba Hande Ergüder
Environmental Engineering Dept., METU _____

Date: 06.09.2010

I hereby declare that all information in this document has been obtained and presented in accordance with academic rules and ethical conduct. I also declare that, as required by these rules and conduct, I have fully cited and referenced all material and results that are not original to this work.

Name, Last name: Gülşah Pekgöz

Signature:

ABSTRACT

DELETION MUTATION OF GLNB AND GLNK GENES IN RHODOBACTER CAPSULATUS TO ENHANCE BIOHYDROGEN PRODUCTION

Pekgöz, Gülşah

M.Sc., Department of Biotechnology

Supervisor: Prof. Dr. Ufuk Gündüz

Co-Supervisor: Prof. Dr. İnci Eroğlu

September 2010, 163 pages

Rhodobacter capsulatus is a photosynthetic, purple non-sulfur (PNS) bacterium that produces biohydrogen via photofermentation. Nitrogenase enzyme is responsible for hydrogen production; during fixation of molecular nitrogen into ammonium, hydrogen is produced. Since this process is an energetically expensive process for the cell, hydrogen production is strictly controlled at different levels. When ammonium is present in the environment, hydrogen production completely ceases. The key proteins in the regulation of nitrogenase by ammonium are two PII proteins; GlnB and GlnK.

‘Hyvolution’, 6th framework EU project, aims to achieve maximum hydrogen production by combining two hydrogen production processes; dark fermentation and photofermentation. In the first stage of the overall process, biomass is used for

hydrogen production in dark fermentation process. Then, the effluent of dark fermentation is further utilized by photosynthetic bacteria to produce more hydrogen. However, the effluent of dark fermentation contains high amount of ammonium, which inhibits photofermentative hydrogen production. In order to achieve maximum hydrogen production, ammonium regulation of nitrogenase enzyme in *R.capsulatus* has to be released. For this purpose, all P_{II} signal transduction proteins of *R.capsulatus* (GlnB and GlnK) were targeted to be inactivated by site-directed mutagenesis. The internal parts of *glnB* and *glnK* genes were deleted individually without using antibiotic cassette insertion. The successful *glnB* mutant was obtained at the end of mutagenesis studies. In the case of *glnK* mutation, the suicide vector was constructed and delivered into the cells. However, *glnK* mutant could not be obtained.

The effect of ammonium on *glnB* mutant *R.capsulatus* was investigated and compared with wild type. Biomass of the bacterial cultures, pH of the medium and amount of produced hydrogen were periodically determined. Moreover, the concentrations of acetic, lactic, formic and propionic acids in the medium were periodically measured. Both wild type and *glnB* mutant grew on acetate and effectively utilized acetate. Ammonium negatively affected hydrogen production of *glnB* mutant and wild type. The ammonium inhibition of hydrogen production did not release in *glnB* mutant due to the presence of active GlnK protein in the cell; hence, inactivation of one of P_{II} proteins was not enough to disrupt ammonium regulation of the cell. Moreover, kinetic analysis of bacterial growth and hydrogen production were done. Growth data fitted to the Logistic Model and hydrogen production data fitted to the Modified Gompertz Model.

Keywords: *R. capsulatus*, biohydrogen, ammonium inhibition, GlnB, GlnK, site-directed mutagenesis, kinetic modeling

ÖZ

RHODOBACTER CAPSULATUS'DA BİYOHİDROJEN ÜRETİMİNİN ARTTIRILMASI AMACIYLA GLNB VE GLNK GENLERİNİN ETKİSİZLEŞTİRİLMESİ

Pekgöz, Gülşah

M.Sc., Biyoteknoloji Bölümü

Tez Yöneticisi: Prof. Dr. Ufuk Gündüz

Ortak Tez Yöneticisi: Prof. Dr. İnci Eroğlu

Eylül 2010, 163 sayfa

Rhodobacter capsulatus fotofermentasyon yoluyla biyohidrojen üreten mor, sülfürsüz, fotosentetik bir bakteri türüdür. Bu organizmada, hidrojen üretiminden sorumlu enzim nitrojenaz'dır ve bu enzim aynı zamanda moleküler azottan amonyum sentezleyebilmektedir. Hidrojen ve amonyak üretimi hücre için yüksek miktarda enerji gerektiren bir tepkime olduğundan, bu enzim hücrede çeşitli seviyelerde sıkı bir şekilde kontrol edilmektedir. Hücreler ortamda amonyak varsa, hidrojen üretimini tamamen durdurmaktadır. Nitrojenaz enziminin amonyum tarafından kontrolünde görev alan anahtar proteinler, iki adet P_{II} sinyal iletim proteini: GlnB ve GlnK.

Altıncı çerçeve AB projesi olan 'Hyvolution' projesi, iki farklı hidrojen üretim süreci olan karanlık fermentasyon ile fotofermentasyonu birleştirerek maksimum hidrojen üretimini amaçlamaktadır. Bu bütünleşik sürecin ilk aşamasında, biyokütleden

karanlık fermentasyon ile hidrojen üretilmektedir. Sonraki aşamada, fotosentetik bakteriler karanlık fermentasyonun atık suyunu kullanarak ilaveten hidrojen üretmektedirler. Ancak, karanlık fermentasyonun atık suyu genelde fotofermentatif hidrojen üretimini engelleyecek kadar yüksek miktarlarda amonyum içermektedir. *R.capsulatus*'da maksimum seviyede hidrojen üretime ulaşılabilmesi için bu sorunun aşılması ve dolayısıyla nitrojenaz enzimi amonyum baskısından kurtarılmalıdır. Bu amaçla, bu çalışmada *R.capsulatus*'daki bütün P_{II} sinyal iletim proteinleri (GlnB ve GlnK) yönlendirilmiş mutagenез ile etkisiz hale getirilmeye çalışıldı. Bu iki proteinin hücre içindeki sentezinden sorumlu olan *glnB* ve *glnK* genlerinin içkısımlarından parçalar silinmiştir. Sonuçta, başarılı bir *glnB* mutanı elde edilmiştir. *glnK* mutasyonu çalışmalarında ise, intihar vektörü elde edilmiştir ve hücrelerin içerisine gönderilmiştir. Ancak, başarılı bir *glnK* mutanı elde edilememiştir.

Sonra, amonyumun *R.capsulatus glnB* mutantının hidrojen üretimine etkisi araştırılmıştır ve bu veriler yaban soyunkiler ile karşılaştırılmıştır. Büyüme, asitlik ve üretilen hidrojen miktarlarıyla ilgili veriler periyodik olarak toplanmıştır. Bunlara ek olarak, besiyeri içerisindeki asetik, laktik, formik ve propiyonik asit konsantrasyonları periyodik olarak belirlenmiştir. Hem yaban soy hem de mutant bakteri, asetat içeren besiyerinde başarılı bir şekilde büyümüştür. Amonyum, hem yaban soy hem de mutant bakterideki hidrojen üretimini olumsuz yönde etkilemiştir. *glnB* mutantında, aktif GlnK proteini bulunmaktadır. Bundan dolayı, nitrojenaz enzimi üzerindeki amonyum baskısı kalkmamıştır. P_{II} proteinlerinden bir tanesinin bozulması hücredeki amonyum regülasyonunun kalkması için yeterli olmamıştır. Ayrıca, yaban soy ve mutant bakterilerinin büyüme ve hidrojen üretim verilerinin kinetik analizleri yapılmıştır. Büyüme verilerinin Logistic Model'e, hidrojen üretimi verilerinin de Modifiye Gompertz Modeli'ne uyumlu olduğu gösterilmiştir.

Anahtar kelimeler: *R. capsulatus*, biyohidrojen, amonyak baskısı, GlnB, GlnK, yönlendirilmiş mutagenез, kinetik modelleme

To my family

ACKNOWLEDGEMENTS

First of all, I would like to express my deepest gratitude to my supervisor Prof. Dr. Ufuk Gündüz and to my co-supervisor Prof. Dr. İnci Erođlu for their continual guidance, advice and support throughout this study. I would also thank to Prof. Dr. Meral Yücel for her valuable ideas and criticism.

I would like to express my sincere gratitude to Prof. Dr. Kornel Kovacs and Assoc. Prof. Dr. Gabor Rakhely for their kindness in providing their research laboratories to accomplish the crucial part of my research.

I am grateful to Assist. Prof. Dr. Gökhan Kars and Dr. Ebru Özgür for their continual help and endless support.

I feel great appreciation to my dear friend Pelin Sevinç, who contributed a lot to this thesis in HPLC analyses and modeling results. My special thanks go to my labmates; Yaprak Dönmez, Zelha Nil, Esra Kaplan, Esra Güç, Sevilay Akköse, Burcu Özsoy, Tuğba Keskin and Gülistan Tansık for their endless friendship and moral support in difficult times.

I would also like to thank to members of METU Biohydrogen group; Endam Özkan, Nilüfer Afşar, Gökçe Avcıođlu, Dominic Deo Androga, Muazzez Gürgan and Efe Boran for their great help and suggestions. Moreover, my colleagues in the Department of Biotechnology of Szeged University deserve special thanks for their interest and great friendship.

I also feel great appreciation to the examining committee members for their contribution and comments.

I am deeply indebted to my mother Pervin Alpaslan and my brother Kürşat Pekgöz for their endless support, trust and never ending love throughout my life.

I feel great appreciation to my close friends Şaziye Deniz Oğuz, Eylem Kuzgun, Güven Kazım Altunkaya and Ceren Kazancı for their deep friendship and concern. Moreover, nice people of ‘Baraka’ and ‘METU Mountaineering and Winter Sports Club’ are greatly acknowledged for their sincere friendship and for making life more enjoyable.

This research study was supported by 6th framework European Union Project “Hyvolution”, Hungarian Academy of Sciences (ITC fellowship) and BAP Project.

TABLE OF CONTENTS

ABSTRACT	iv
ÖZ.....	.vi
ACKNOWLEDGEMENTS.....	ix
TABLE OF CONTENTS	xi
LIST OF TABLES	xiv
LIST OF FIGURES	xvi
LIST OF ABBREVIATIONS.....	xxi
CHAPTERS	1
1. INTRODUCTION.....	1
1.1. Hydrogen energy	1
1.2. Hydrogen production	2
1.3. Biohydrogen	3
1.3.1. Biophotolysis	4
1.3.2. Photofermentation.....	6
1.3.3. Dark fermentation	8
1.3.4. Integrated systems.....	10
1.4. Hyvolution Project.....	11
1.5. Objective of this study	12
2. LITERATURE SURVEY.....	14
2.1. Purple nonsulfur photosynthetic bacteria- <i>Rhodobacter capsulatus</i>	14
2.2. Hydrogen production by PNS bacteria	16
2.3. Enzymes in hydrogen metabolism.....	21
2.3.1. Hydrogenases.....	22
2.3.2. Nitrogenases	23
2.3.3. Regulation of nitrogenase.....	27
2.3.4. P _{II} Signal transduction proteins.....	30
2.3.5. Effect of ammonia on hydrogen production	33
2.3.6. Byproducts of hydrogen metabolism	34
3. MATERIALS AND METHODS.....	37

3.1. Bacterial strains	37
3.2. Plasmids	37
3.3. Growth media and conditions	40
3.4. Hydrogen production media and conditions.....	41
3.5. Hydrogen production setup	41
3.5.1. Sampling.....	43
3.5.2. Analyses	43
3.6. The preparation of vector constructs.....	45
3.6.1. Genomic DNA isolation	45
3.6.2. Plasmid DNA isolation.....	45
3.6.3. Agarose gel electrophoresis	46
3.6.4. Sequence and Primer design	47
3.6.5. Polymerase chain reaction (PCR) and Optimization of reaction conditions	50
3.6.6. Colony PCR.....	54
3.6.7. Sequence analysis	55
3.6.8. Restriction enzyme digestion.....	55
3.6.9. Extraction of DNA from agarose gel	56
3.6.10. Dephosphorylation of linearized plasmids	57
3.6.11. Phosphorylation of PCR products	57
3.6.12. Polishing the stick ends of the linear plasmids	58
3.6.13. Sticky or blunt end ligation.....	58
3.6.14. Preparation of constructs for inactivation <i>glnB</i> and <i>glnK</i>	59
3.6.15. Preparation of competent cells	59
3.6.16. Transformation of <i>E.coli</i>	60
3.6.17. Blue-White Screening	60
3.7. Construction of suicide vectors	61
3.8. Gene transfer into <i>R.capsulatus</i> by Conjugation and Selection.....	62
4. RESULTS AND DISCUSSION	66
4.1. Mutagenesis studies of <i>glnB</i> gene.....	66
4.1.1. Construction of the suicide vector for deletion inactivation of <i>glnB</i>	66
4.1.2. Delivery of the suicide vector for <i>glnB</i> deletion (pGBSUD) to <i>R.capsulatus</i> and selection/ screening of the double recombinants	73
4.1.3. Confirmation of <i>glnB</i> mutation by genetic methods	74
4.2. Mutagenesis studies for <i>glnK</i> gene	76

4.2.1. Construction of the suicide vector for deletion inactivation of <i>glnK</i>	76
4.2.2. Delivery of the suicide vector for <i>glnK</i> deletion (pGKSUD) to <i>R.capsulatus</i> and selection-screening of the double recombinants	82
4.3. Growth and hydrogen production of wild type and <i>glnB</i> mutant <i>R.capsulatus</i> on ammonium containing media	90
4.3.1. The effect of ammonium on the growth of wild type and <i>glnB</i> mutant <i>R.capsulatus</i>	90
4.3.1.1. Modeling of cell growth	93
4.3.2. pH variations in wild type and <i>glnB</i> mutant <i>R.capsulatus</i> at different ammonium levels ..	97
4.3.3. Hydrogen production profiles of wild type and <i>glnB</i> mutant <i>R.capsulatus</i> at different ammonium levels	99
4.3.3.1. Modeling of hydrogen production.....	103
4.3.4. Calculation of Substrate Conversion Efficiency, Yield, Molar Productivity, Light Conversion Efficiency and Product Yield Factor.....	106
4.3.5. Organic acid analysis of wild type and <i>glnB</i> mutant <i>R.capsulatus</i>	111
4.3.5.1. Acetate utilization.....	112
4.3.5.2. Lactic acid, formic acid and propionic acid formation	114
5. CONCLUSION.....	118
REFERENCES	120
APPENDICES	138
A. COMPOSITION OF GROWTH MEDIA	138
B. SOLUTIONS AND BUFFERS.....	141
C. OPTICAL DENSITY-DRY WEIGHT CALIBRATION CURVE	143
D. SAMPLE GAS CHROMATOGRAM.....	144
E. HPLC CHROMATOGRAM AND CALIBRATION CURVES	145
F. SAMPLE DNA SEQUENCE ANALYSIS	148
G. PRIMERS AND SEQUENCES	149
H. RESTRICTION ENDONUCLEASES AND DNA MODIFYING ENZYMES.....	151
I. LOGISTIC MODEL	152
J. MODIFIED GOMPertz MODEL	158
K. DNA LADDERS.....	163

LIST OF TABLES

TABLES

Table 1. 1 The summary of the main hydrogen production processes..	2
Table 2. 1 Classification of <i>Rhodobacter capsulatus</i>	15
Table 3. 1 The bacterial strains	38
Table 3. 2 The plasmids	39
Table 3. 3 Concentrations of nitrogen source in 30 mM acetate containing media.	41
Table 3. 4 List of primers for deletion of <i>glnB</i> and <i>glnK</i> genes, together with the restriction enzyme sites present in the primers	48
Table 3. 5 The primers for sequencing analysis of plasmids, originating from pBtSK and pK18 <i>mobSacB</i>	49
Table 3. 6 The primers for determination of the deletion in <i>glnB</i> and <i>glnK</i> genes	49
Table 3. 7 Components of the PCR reaction for <i>glnB</i> upstream, <i>glnK</i> upstream and <i>glnK</i> downstream fragments	52
Table 3. 8 The cycle conditions of the PCR reaction for <i>glnB</i> upstream fragment, <i>glnK</i> upstream and <i>glnK</i> downstream fragments.....	52
Table 3. 9 Components of the PCR reaction for <i>glnB</i> downstream fragment	53
Table 3. 10 The cycle conditions of the PCR reaction for <i>glnB</i> downstream fragment	53
Table 3. 11 The components of the PCR reaction for the screening of the potential mutants	54
Table 3. 12 The cycle conditions of the PCR reaction for the screening of the potential mutants	55
Table 4. 1 Comparison of experimental and logistic model constants of wild type <i>R.capsulatus</i> for different ammonium concentrations.....	96
Table 4. 2 Comparison of experimental and logistic model constants of <i>glnB</i> mutant <i>R.capsulatus</i> for different ammonium concentrations.....	96
Table 4. 3 Comparison of experimental values and Modified Gobertz Model constants of wild type <i>R.capsulatus</i> for different ammonium concentrations.	105
Table 4. 4 Comparison of experimental values and Modified Gobertz Model constants of <i>glnB</i> mutant <i>R.capsulatus</i> for different ammonium concentrations.	105

Table A. 1 The compositions of the BP media containing acetate and malate as sole carbon sources.....	139
Table A. 2 The composition of 10 x vitamin solution for 100 ml.....	140
Table A. 3 The composition of 10 x trace element solution for 100 ml.....	140
Table G. 1 Complete list of primers and their sequences	149

LIST OF FIGURES

FIGURES

Figure 1. 1 Hydrogen production by direct biophotolysis	5
Figure 1. 2 The electrons derived from water flow to hydrogen	5
Figure 1. 3 Hydrogen production by photofermentation.....	7
Figure 1. 4 Hydrogen production by dark fermentation.....	9
Figure 1. 5 The scheme of ‘Hyvolution Project’	11
Figure 2. 1 Microscopic picture of <i>R. capsulatus</i>	16
Figure 2. 2 The overall scheme of the carbon metabolism in PNS bacteria	17
Figure 2. 3 Acetate assimilation of PNS bacteria: (A) The citramalate cycle for <i>R. capsulatus</i> , (B) Ethylmalonyl-CoA pathway for <i>R. sphaeroides</i>	19
Figure 2. 4 The overall scheme of hydrogen production by PNS bacteria	20
Figure 2. 5 The general view of H ₂ related pathways in PNS bacteria	21
Figure 2. 6 Overall structure of N ₂ ase.....	25
Figure 2. 7 Schematic representation of the N ₂ ase Fe protein cycle.....	26
Figure 2. 8 The levels of ammonium regulation on N ₂ ase enzyme complex in <i>R. capsulatus</i>	29
Figure 2. 9 Nitrogen regulation (Ntr) system of enteric bacteria	31
Figure 2. 10 Scheme illustrating the potential variability of P _{II} targets.....	33
Figure 2. 11 PHA biosynthesis in the context of microbial metabolism.	35
Figure 3. 1 Anaerobic cultures of wild type <i>R. capsulatus</i> cultures.....	40
Figure 3. 2 The schematic representation of hydrogen production setup.....	42
Figure 3. 3 The experimental setup of hydrogen production.....	43
Figure 3. 4 Schematic representation of conjugation between <i>E. coli</i> S17-1 and <i>R. capsulatus</i> cells	63
Figure 3. 5 The mechanism of the suicide vector (pK18mobSacB).....	65
Figure 4. 1 Genomic DNA of <i>R. capsulatus</i> (A), agarose gel electrophoresis results of the amplification of <i>glnB</i> upstream fragment (~1kb) (B) and <i>glnB</i> downstream fragment (~1kb) (C).....	67
Figure 4. 2 10 kb fragment from <i>R. capsulatus</i>	68

Figure 4. 3 The plasmid containing <i>glnB</i> upstream insert (pGBBU1) (A) and agarose gel result of colony PCR for the amplification of the insert (B).	69
Figure 4. 4 The plasmid containing <i>glnB</i> downstream insert (pGBBD1) (A) and agarose gel result of colony PCR for the amplification of the insert (B).	70
Figure 4. 5 The suicide plasmid (pK18 <i>mobsacB</i>) containing ~1kb <i>glnB</i> downstream insert (pGBSD1) (A). Agarose gel results of linearized pK18 <i>mobsacB</i> (~5700 bps) (B) and linearized pGBSD (~6700 bps) (C).....	71
Figure 4. 6 The map of the final construct; the suicide plasmid containing ~2kb insert; both <i>glnB</i> upstream and downstream fragments (pGBSUD1) (A). Agarose gel results of linearized pGBSUD (~7700 bps) (B) and double digested pGBSUD (C) with excised insert.....	72
Figure 4. 7 Single recombinant colonies of <i>R.capsulatus</i> on BP agar containing kanamycin	74
Figure 4. 8 Agarose gel results of the colony PCR of wild type <i>R.capsulatus</i> (A), <i>glnB</i> mutant <i>R.capsulatus</i> (B).	75
Figure 4. 9 Agarose gel results of the amplification of <i>glnK</i> upstream fragment (~1kb) (A) and <i>glnK</i> downstream fragment (~1kb) (B).....	76
Figure 4. 10 10 kb fragment from <i>R.capsulatus</i> . The upstream (U) and downstream (D) fragments of <i>glnK</i> and the deletion region (✖) are indicated.	77
Figure 4. 11 The plasmid containing <i>glnK</i> upstream insert (pGKBU1) (A) and agarose gel result of colony PCR for the amplification of the insert (B).	78
Figure 4. 12 The plasmid containing <i>glnK</i> downstream (pGKBD1) (A) and the agarose gel result of colony PCR for the amplification of the insert (B).	79
Figure 4. 13 The suicide plasmid (pK18 <i>mobsacB</i>) containing ~1kb <i>glnB</i> downstream insert (pGKSD1) (A). Agarose gel results of linearized pK18 <i>mobsacB</i> (~5700 bps) (B) and linearized pGKSD (~6700 bps) (C)..	80
Figure 4. 14 The map of final construct; the suicide plasmid containing ~2kb insert; both <i>glnB</i> upstream and downstream fragments (pGBSUD1) (A). Agarose gel results of linearized pGKSUD (~7700 bps) (B) and double digested pGKSUD (C) with excised insert.....	81
Figure 4. 15 Single recombinant colonies of <i>R.capsulatus</i> on BP agar containing kanamycin	82
Figure 4. 16 A typical agarose gel result of the PCR reaction for the screening of <i>glnK</i> deletion.	83
Figure 4. 17 Biomass of wild type <i>R.capsulatus</i> in different ammonium levels	92
Figure 4. 18 Biomass of <i>glnB</i> mutant <i>R.capsulatus</i> in different ammonium levels	92

Figure 4. 19 The logistic growth model of wild type <i>R.capsulatus</i> for 1 mM NH ₄ Cl containing medium.....	95
Figure 4. 20 pH measurements of wild type <i>R.capsulatus</i> in different ammonium levels	98
Figure 4. 21 pH measurements of <i>glnB</i> mutant <i>R.capsulatus</i> in different ammonium levels.....	99
Figure 4. 22 Hydrogen production profile of wild type <i>R.capsulatus</i> in different ammonium levels	100
Figure 4. 23 Hydrogen production profile of <i>glnB</i> mutant <i>R.capsulatus</i> in different ammonium levels	101
Figure 4. 24 The Modified Gombertz Model of wild type <i>R.capsulatus</i> for 1 mM NH ₄ Cl containing medium.....	104
Figure 4. 25 Substrate conversion efficiency values for wild type and <i>glnB</i> mutant <i>R.capsulatus</i> for different ammonium concentrations.....	107
Figure 4. 26 Molar productivity values for wild type and <i>glnB</i> mutant <i>R.capsulatus</i> for different ammonium concentrations	108
Figure 4. 27 Yield values for wild type and <i>glnB</i> mutant <i>R.capsulatus</i> for different ammonium concentrations.....	109
Figure 4. 28 Light conversion values for wild type and <i>glnB</i> mutant <i>R.capsulatus</i> for different ammonium concentrations	110
Figure 4. 29 Product yield factor values for wild type and <i>glnB</i> mutant <i>R.capsulatus</i> for different ammonium concentrations	111
Figure 4. 30 Acetic acid consumption by wild type <i>R.capsulatus</i> in different ammonium levels	113
Figure 4. 31 Acetic acid consumption by <i>glnB</i> mutant <i>R.capsulatus</i> in different ammonium levels	113
Figure 4. 32 Lactic acid formation by wild type <i>R.capsulatus</i> in different ammonium levels	115
Figure 4. 33 Lactic acid formation by <i>glnB</i> mutant <i>R.capsulatus</i> in different ammonium levels	115
Figure 4. 34 Formic acid formation by wild type <i>R.capsulatus</i> in different ammonium levels	116
Figure 4. 35 Formic acid formation by <i>glnB</i> mutant <i>R.capsulatus</i> in different ammonium levels	116
Figure 4. 36 Propionic acid formation by wild type <i>R.capsulatus</i> in different ammonium levels	117

Figure 4. 37 Propionic acid formation by <i>glnB</i> mutant <i>R.capsulatus</i> in different ammonium levels	117
Figure C. 1 Calibration curve and the regression trend line for <i>Rhodobacter capsulatus</i> (DSM 1710) dry weight versus OD660.....	143
Figure D. 1 A sample chromatogram for GC analysis of the collected gas.....	144
Figure E. 1 A Sample HPLC analysis chromatogram. Peak 1 (mobile phase- H ₂ SO ₄), Peak 2 (lactic acid), Peak 3 (formic acid) and Peak 4 (acetic acid).....	145
Figure E. 2 The acetic acid calibration curve	146
Figure E. 3 The lactic acid calibration curve	146
Figure E. 4 Formic acid calibration curve	147
Figure E. 5 Propionic acid calibration curve	147
Figure F. 1 A sample sequence analysis	148
Figure I. 1 The logistic growth model of <i>R.capsulatus</i> wild type in 2 mM glutamate (control) containing medium.....	152
Figure I. 2 The logistic growth model of <i>R.capsulatus</i> wild type in 2 mM NH ₄ Cl containing medium.....	153
Figure I. 3 The logistic growth model of <i>R.capsulatus</i> wild type in 3 mM NH ₄ Cl containing medium.....	153
Figure I. 4 The logistic growth model of <i>R.capsulatus</i> wild type in 5 mM NH ₄ Cl containing medium.....	154
Figure I. 5 The logistic growth model of <i>R.capsulatus</i> wild type in 8 mM NH ₄ Cl containing medium.....	154
Figure I. 6 The logistic growth model of <i>R.capsulatus glnB</i> mutant in 2 mM glutamate (control) containing medium	155
Figure I. 7 The logistic growth model of <i>R.capsulatus glnB</i> mutant in 1 mM NH ₄ Cl containing medium.....	155
Figure I. 8 The logistic growth model of <i>R.capsulatus glnB</i> mutant in 2 mM NH ₄ Cl containing medium.....	156
Figure I. 9 The logistic growth model of <i>R.capsulatus glnB</i> mutant in 3 mM NH ₄ Cl containing medium.....	156
Figure I. 10 The logistic growth model of <i>R.capsulatus glnB</i> mutant in 5 mM NH ₄ Cl containing medium.....	157
Figure I. 11 The logistic growth model of <i>R.capsulatus glnB</i> mutant in 8 mM NH ₄ Cl containing medium.....	157

Figure J. 1 The Modified Gompertz Model of <i>R.capsulatus</i> wild type in 2 mM glutamate (control) containing medium.....	158
Figure J. 2 The Modified Gompertz Model of <i>R.capsulatus</i> wild type in 2 mM NH ₄ Cl containing medium.....	159
Figure J. 3 The Modified Gompertz Model of <i>R.capsulatus</i> wild type in 3 mM NH ₄ Cl containing medium.....	159
Figure J. 4 The Modified Gompertz Model of <i>R.capsulatus</i> wild type in 5 mM NH ₄ Cl containing medium.....	160
Figure J. 5 The Modified Gompertz Model of <i>R.capsulatus glnB</i> mutant in 2 mM glutamate (control) containing medium	160
Figure J. 6 The Modified Gompertz Model of <i>R.capsulatus glnB</i> mutant in 1 mM NH ₄ Cl containing medium.....	161
Figure J. 7 The Modified Gompertz Model of <i>R.capsulatus glnB</i> mutant in 2 mM NH ₄ Cl containing medium.....	161
Figure J. 8 The Modified Gompertz Model of <i>R.capsulatus glnB</i> mutant in 3 mM NH ₄ Cl containing medium.....	162
Figure J. 9 The Modified Gompertz Model of <i>R.capsulatus glnB</i> mutant in 5 mM NH ₄ Cl containing medium.....	162
Figure K. 1 Fermentas GeneRuler 50 bp DNA Ladder (50-1000 bp) and 1 kb DNA Ladder (250-10,000 bp).....	163

LIST OF ABBREVIATIONS

<i>A. vinelandii</i>	<i>Azotobacter vinelandii</i>
ADP	Adenosine diphosphate
AMP	Adenosine monophosphate
ATase	Adenylyl transferase
ATP	Adenosine triphosphate
BP	Biebl and Pfennig
CIAP	Calf Intestinal Alkaline Phosphatase
CO ₂	Carbondioxide
DMSO	Dimethyl sulfoxide
DNA	Deoxyribonucleic acid
e	Constant (2.718282)
<i>E. coli</i>	<i>Escherichia coli</i>
Fd	Ferredoxin
Fe	Iron
gdw	Gram dry weight of bacteria
GS	Glutamine synthetase
H	Cumulative hydrogen produced (mmol/L)
H ₂	Molecular hydrogen
H ₂ ase	Hydrogenase enzyme
H _{max,e}	Experimental maximum cumulative hydrogen production (mmol/L)
H _{max,m}	Hydrogen cumulative hydrogen production obtained by Modified Gompertz Model (mmol/L)
HPLC	High pressure liquid chromatography
hup ⁻	Uptake hydrogenase deficient
IPTG	Isopropyl β-D-1-thiogalactopyranoside
k _c	Specific growth rate constant obtained by logistic model, (1/h)

Km	Kanamycin
LB	Luria Broth
MCS	Multiple Cloning Site
mM	Millimolar
Mo	Molybdenum
N ₂	Molecular nitrogen
N ₂ ase	Nitrogenase enzyme
NAD	Nicotinamide adenine dinucleotide phosphate
NH ₄	Ammonium
NH ₄ Cl	Ammonium chloride
Ni	Nickel
O ₂	Oxygen
OD	Optical density
pBtSK	pBluescript SK (+)
PCR	Polymerase Chain Reaction
PHA	Polyhydroxyalkanoates
PHB	Polyhydroxybutyrate
<i>phb</i> ⁻	Polyhydroxybutyrate deficient
P _i	Orthophosphate
PNK	T4 Polynucleotide Kinase Enzyme
PNS	Purple nonsulphur
r	Extent of the fit
<i>R.capsulatus</i>	<i>Rhodobacter capsulatus</i>
<i>R.sphaeroides</i>	<i>Rhodobacter sphaeroides</i>
RE	Restriction enzyme
R _{max,e}	Experimental maximum hydrogen production rate (mmol/L.h)
R _{max,m}	Maximum hydrogen production rate obtained from Modified Gompertz Model (mmol/L.h)
<i>Rs.rubrum</i>	<i>Rhodospirillum rubrum</i>
S	Sulphur
TCA	Tricarboxylic acid

UTase	Uridylytransferase
UTP	Uridine-5'-triphosphate
UV	Ultraviolet
Va	Vanadium
X-GAL	Bromo-chloro-indolyl-galactopyranoside
$X_{\max,e}$	Experimental maximum bacterial concentration (gdw/L)
$X_{\max,m}$	Maximum bacterial concentration obtained by logistic model (gdw/L)
$X_{o,e}$	Experimental initial bacterial concentration (gdw/L)
$X_{o,m}$	Initial bacterial concentration obtained by logistic model (gdw/L)
λ_e	Experimental lag time (h)
λ_m	Lag time obtained from Modified Gompertz Model (h)
μ_{\max}	Specific growth rate constant obtained by exponential model (1/h)

CHAPTER 1

INTRODUCTION

1.1. Hydrogen energy

Fossil fuels have been considered as the most important energy source, since recently almost 80 % of the energy demand is obtained from fossil fuels (Das and Veziroglu, 2001). There are many predictions about the depletion time of fossil fuels, but the important point is the fact that there is high energy demand and limited amount of fossil sources left on the earth. Besides, today, environmental pollution is a great concern for the world, mainly due to rapid industrialization and urbanization. Burning any fossil fuel produces carbon dioxide, which contributes to the "greenhouse effect" and warms the Earth. Due to these drawbacks of fossil fuels, increasing focus is being placed on clean and renewable energy. There are numerous alternative energy carriers, such as bioethanol, biogas or biohydrogen which might replace the fossil fuels in the near future. Few important directions have to be considered regarding these carriers: a) they should be produced from renewable sources; b) they must be environmentally sound, i.e. during their utilization the emission of hazardous materials (usually CO₂) must be minimized. Photobiological hydrogen production, which is the production of hydrogen by biological systems, could be a potentially environmentally acceptable energy production method because hydrogen gas is renewable using the primary energy source, sunlight, and completely recycled without CO₂ emission (Asada and Miyake, 1999).

1.2. Hydrogen production

Hydrogen has the largest energy content per weight of any known fuel, and can be produced by various means (Hallenbeck and Benemann, 2002; Das and Veziroglu, 2001). The summary of the main hydrogen production processes and their status of development can be seen in Table 1.1 (Rosen et al., 1992). Nowadays, the mostly applied hydrogen production methods are electrolysis of water or steam reformation of methane (Levin and Love, 2004). In addition to these, some of these methods have also reached maturity in the application; such as steam reforming of natural gas, catalytic decomposition of natural gas, partial oxidation of heavy oils, coal gasification and steam-iron coal gasification. Other methods, including photochemical processes, thermochemical, photochemical, photoelectrochemical and photobiological processes, are under intense research and development (Momirlan and Veziroglu, 2002). Biohydrogen production, using microorganisms for hydrogen production, is an exciting new area of technology development that offers the potential production of usable hydrogen from a variety of renewable resources.

Table 1. 1 The summary of the main hydrogen production processes (Rosen et al., 1992). The stage of development is represented by letters ‘R’and ‘D’, indicating ‘research’ and ‘development’.

Production process	Status
Steam reforming of natural gas	Mature
Catalytic decomposition of natural gas	Mature
Partial oxidation of heavy oil	Mature
Coal gasification	R and D—Mature
Steam-iron coal gasification	R and D
Water electrolysis	Mature
Thermochemical cycles (pure)	R and D
Thermochemical cycles (hybrid)	R and D
Photochemical processes	Early R and D
Photoelectrochemical processes	Early R and D
Photobiological processes	Early R and D

Fuel-cell powered vehicles are considered as the main application of the hydrogen in the near future. Many different vehicles and small equipments have been developed, but optimization studies are still going on by manufacturing companies (Akkerman et al., 2002). In order to increase the applicability of hydrogen energy, large scale production has to be maintained in a feasible way. Still, there are no commercially available large scale biohydrogen production systems, but successful prototypes are under process.

1.3. Biohydrogen

Biohydrogen is a feasible way for producing hydrogen. There are many advantages of biohydrogen over conventional H₂ production methods. Most of the currently applied methods are energy intense and not necessarily environment friendly. Whereas, biological production processes are less energy intense since they are applied at moderate temperatures and pressures (Benemann, 1997; Sasikala et al., 1993). The feasibility of the biohydrogen systems can be enhanced by using various carbon sources from waste waters of refineries or agricultural production units, such as, olive mill waste water (Eroglu et al., 2006), waste water of sugar refinery (Yetis et al., 2000) and waste water of milk industry (Turkarslan et al., 1998).

The ultimate energy source of biohydrogen is the sun, either directly the solar energy is used or indirectly, carbon compounds are used to derive energy. All of the biological hydrogen production techniques involve either hydrogenases or nitrogenases enzymes with particular characteristics, which will be discussed further (Hallenbeck and Ghosh, 2009). There are two reasons for the generation of hydrogen by microorganisms; first, they get out of the excess reducing equivalents or second, they produce hydrogen as a byproduct in nitrogen fixation reaction (Meherkotay and Das, 2008).

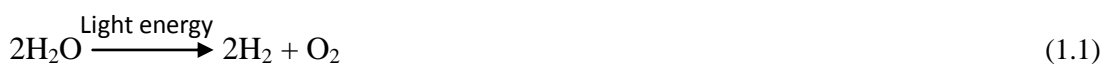
Biohydrogen production processes can be classified (Debabrata and Veziroglu, 2001) as follows:

- i. Biophotolysis of water using algae and cyanobacteria.
- ii. Photofermentation of organic compounds by photosynthetic bacteria.
- iii. Dark fermentative hydrogen production from organic compounds,
- iv. Hybrid systems using photosynthetic and fermentative bacteria.

All of these processes of hydrogen production have their particular advantages and disadvantages, which will be discussed in the following sections.

1.3.1. Biophotolysis

Microalgae and cyanobacteria possess two photosystems. A green algae or cyanobacterium performs photosynthesis by their uses solar energy to split water and produce oxygen and hydrogen (Equation 1.1), which is called ‘Direct Biophotolysis’. Ferredoxin (Fd) is reduced, which can in turn reduce a hydrogenase or nitrogenase, both of which are oxygen sensitive. Hence, hydrogen is produced by either of these enzymes, which will be discussed later. So, the sunlight can be directly converted into chemical energy by direct biophotolysis (Figure 1.1), which is also called ‘photoautotrophic hydrogen production’.



In photosynthesis of algae and cyanobacteria, Fd is reduced immediately after light appears. In this moment, cells contain an excess of NAD(P)H formed by dark anaerobic metabolism. Therefore, to get rid of the excess reducer, reduced Fd is oxidized by hydrogenase. Hydrogen and oxygen are evolved simultaneously (Tsygankov, 2007). The route of electrons is shown in Figure 1.2.

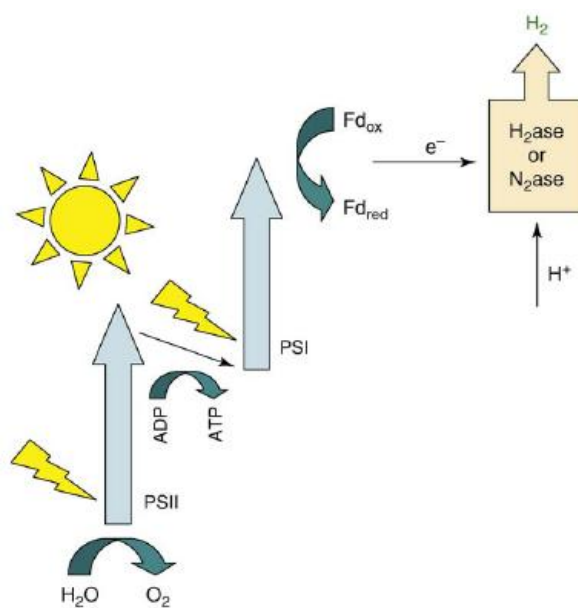


Figure 1. 1 Hydrogen production by direct biophotolysis (Hallenbeck and Ghosh, 2009)

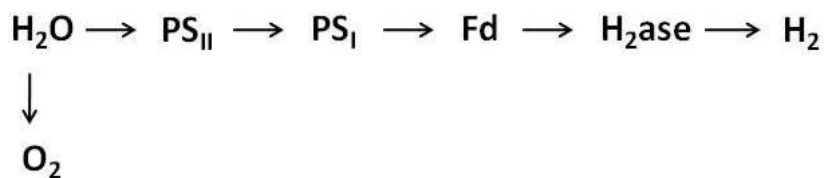


Figure 1. 2 The electrons derived from water flow to hydrogen

The hydrogen production by photolysis of water is advantageous because the substrate is abundant (H_2O) and the products are simple (H_2 and CO_2). But this process has some limitations to be solved in order to achieve efficient hydrogen production (Hallenbeck and Benemann, 2002). First, the light conversion efficiency has to be improved; conversion efficiencies for direct biophotolysis are below 1%. Moreover, the costs of the photobioreactors are high due to the impermeable materials that are being used in the structure. The main drawback of photoautotrophic hydrogen production process is oxygen inhibition; the hydrogenase enzyme is very sensitive to oxygen. The oxygen produced in biophotolysis inactivates the H_2 -producing systems in cyanobacteria and green algae, leading to lower yields of biohydrogen (Hallenbeck and Ghosh, 2009). There are attempts to achieve oxygen tolerant hydrogenase activity through classical mutagenesis techniques (Ghirardi et al., 1997) and mutants that are O_2 tolerant for H_2 production were reported to be obtained (Seibert, 2001). Moreover, the usage of heterocystous cyanobacteria, which are composed of hydrogen evolving and oxygen evolving cell types, were applied (Benemann and Weare, 1974). Even though the oxygen limitations of this process would have been overcome, the requirement to separate hydrogen gas from oxygen gas increases the overall cost (Melis, 2002)

1.3.2. Photofermentation

The bacteria, which harbor only one photosystem, are not able to split water and directly produce oxygen and hydrogen. However, in the conditions of oxygen absence, these bacteria are able to use organic compounds to derive electrons. The light energy is used to overcome the positive free energy of activation. Purple non-sulfur (*Rhodobacter*) and purple sulfur bacteria (*Chromatium* or *Thiocapsa*) produce hydrogen by photofermentation (Basak and Das, 2007; Kovacs et al., 2000). Phototrophic organisms are the potential microbial systems for biohydrogen production (Akkerman et al., 2002; Fascetti et al., 1998).

Purple non-sulfur bacteria perform anaerobic photosynthesis, which does not lead to the release of O₂. They are able to use reduced compound (organic acids) with the help of light energy, which is called photofermentation (Figure 1.3). The electrons, derived from organic acids, are delivered to nitrogenase enzyme. Nitrogenase, which is the enzyme responsible for hydrogen production in photosynthetic bacteria, converts electrons and protons into H₂. In addition to nitrogenases, hydrogenases may also be present, functioning either in the production of H₂ or in the consumption of H₂ (Miyamoto, 1997). The overall reaction can be seen in Equation 1.2.

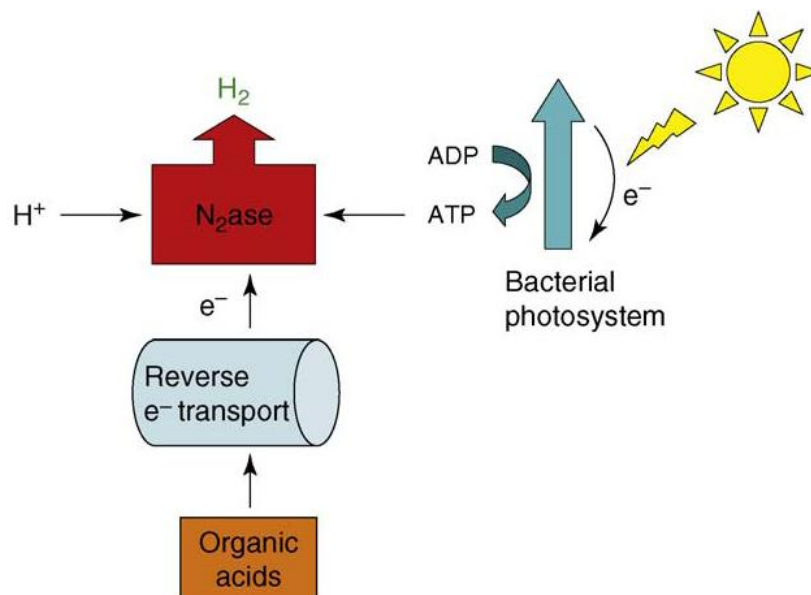
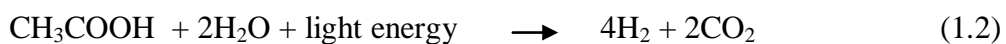


Figure 1. 3 Hydrgen production by photofermentation (Hallenbeck and Ghosh, 2009)



The major benefits as compared to the direct biophotolysis are as follows (Das and Veziroglu, 2001):

- i. high theoretical conversion yields, approaching 100 %,
- ii. anaerobic photosynthesis has no O₂ evolving activity, so there is no inhibition of hydrogen production by oxygen,
- iii. capability to use wide spectrum of light,
- iv. ability to consume organic substrates (mainly, organic acids) from various wastes, such as food process wastes, agricultural wastes, distillery effluent and more. Thus, it is also suitable for waste water treatment.

There are some challenges in photofermentation such as increasing productivity and decreasing the photobioreactors' cost. The process of hydrogen production by photofermentation requires anaerobic environment, so oxygen impermeable but light permeable photobioreactors must be developed (Fedorov et al., 1998). Further research is necessary to increase feasibility of photofermentation process.

1.3.3. Dark fermentation

In dark fermentation process, many different bacteria catalyze energy rich carbon compounds into hydrogen and other side-products (mainly organic acids and alcohols). H₂ and carbon dioxide (CO₂) are the main gas evolved during dark fermentation, but lower amounts of methane (CH₄), hydrogen sulfide (H₂S) and carbon monoxide (CO) are also observed.

The main percentage of microbial hydrogen production is by the anaerobic metabolism of pyruvate, formed during the catabolism of various substrates. The pyruvate produced by systems are used in the absence of oxygen to give acetylCoA and either formate or Fd, which can derive H₂ (Hallenbeck and Benemann, 2002). The general scheme of dark fermentation can be seen in Figure 1.4. The enzyme

which catalyzes the hydrogen production is hydrogenase. At the same time, uptake hydrogenases, which are the enzymes consuming H₂ produced in order to remove the excess reducing power, can be present in the cell. In that case, the real hydrogen production yields are lower (Kovacs et al., 2004).

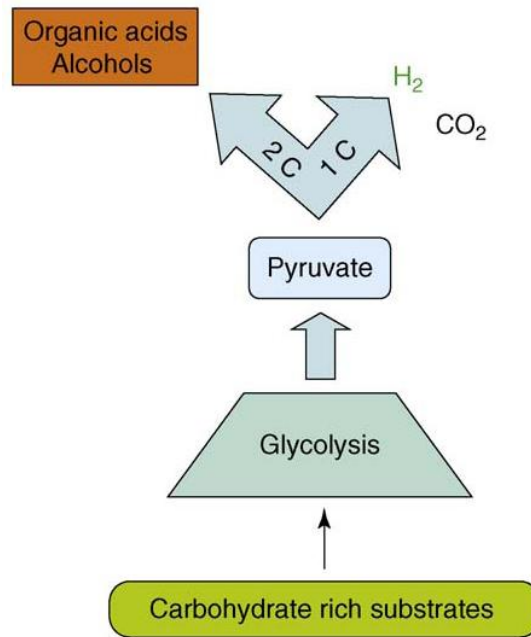


Figure 1. 4 Hydrogen production by dark fermentation (Hallenbeck and Ghosh, 2009)



It is possible to utilize variety of wastewater or agriculture remainings in the fermentation process (Kapdan and Kargi, 2006). It produces valuable products such as butyric, lactic and acetic acids (Equation 1.3).

1.3.4. Integrated systems

In dark fermentation, the carbon source can only be reduced to organic acids (acetic acid, butyric acid, lactic acid etc.), since the further reduction is not feasible thermodynamically due to positive free energy change (Basak and Das, 2007). It is very well known that organic acids are utilized by photosynthetic bacteria by photofermentation to H₂ and CO₂. The processes, in which sequential dark fermentation is followed by photofermentation (or light fermentation), are called 'integrated systems'. With this application, the hydrogen is produced from both of the processes; hence the overall hydrogen yield can be improved to a great extent (Nath and Das, 2004; Hawkes et al., 2002; Momirlan and Veziroglu, 1999).

Glucose is converted into 2 moles of acetate with the release of 4 moles of H₂ in dark fermentation (Equation 1.3). After further decomposition of 2 moles of acetate into CO₂ and H₂ by purple non sulphur (PNS) bacteria, additional 8 moles of H₂ is produced (Meherkotay and Das, 2008). The theoretical conversion of glucose to H₂ is 12 moles (Miyake et al., 1990; Basak and Das, 2007) (Equation 1.4). The overall equations of dark fermentation and photofermentation are given below:



1.4. Hyvolution Project

The Hyvolution Project, “nonthermal production of pure hydrogen from biomass”, is an integrated project, funded by European Union in the Sixth Framework Programme. The aim is to develop a blue-print for cost effective hydrogen production process using various local biomass (Claassen and Vrije, 2006). Pretreatment and logistics of biomass, thermophilic fermentation, photofermentation, gas upgrading, system integration, societal integration and training are the main work packages of the Project. The scheme of the Project is given in Figure 1.5.

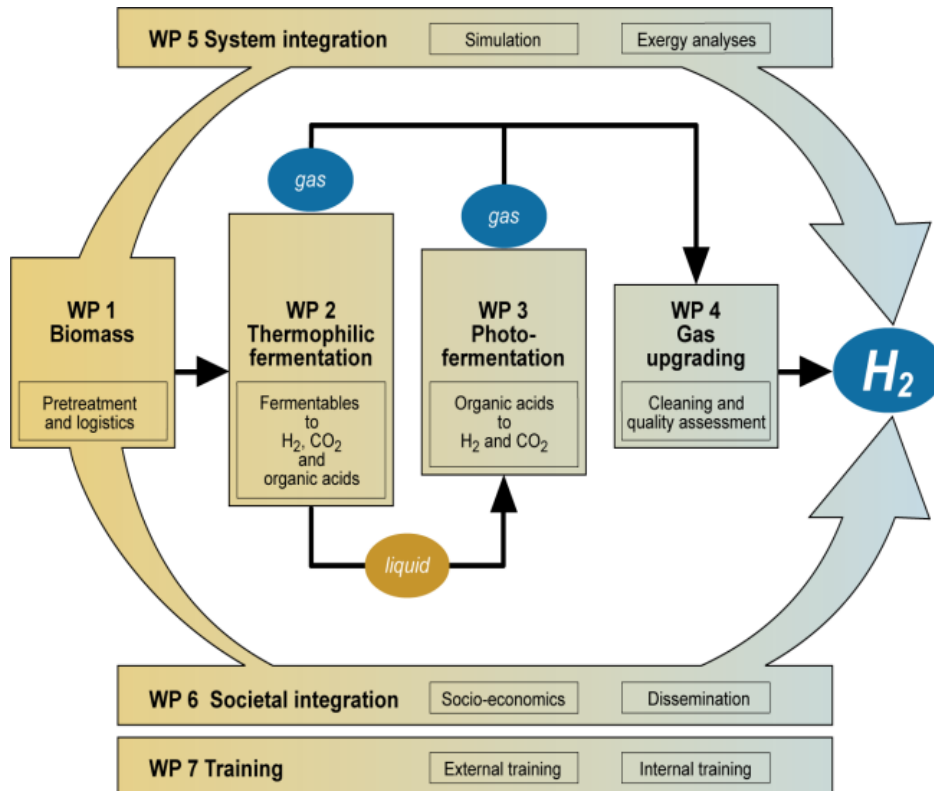


Figure 1. 5 The scheme of ‘Hyvolution Project’

(<http://www.biohydrogen.nl/hyvolution/25446/5/0/20>, Last access date: July 27, 2010)

In the first stage of 'Hyvolution', the biomass, which is pretreated properly, is used in thermophilic dark fermentation process. *Caldicellulosiruptor saccharolyticus*, which is able to consume different carbon compounds such as cellulose, xylan and pectin with efficient hydrogen production (Niel et al., 2002; Kadar et al., 2004), is used in the dark fermentation. The carbon compounds are converted into acetate, H₂ and CO₂. In the second stage, the effluent of this stage (dark fermenter effluent), which is rich in acetate, is delivered into a photobioreactor. By photofermentation, the acetate is converted into H₂ and CO₂ by PNS bacteria, *Rhodobacter capsulatus* or *Rhodobacter sphaeroides* (Afsar et al., 2009; Özgür et al., 2010; Nath et al., 2006; Eroglu et al., 2006; Miyake et al., 1984).

In the future, hydrogen is predicted to be an important energy carrier and to replace coal or electricity. Therefore, hydrogen economy, which is growing very rapidly, is thought to be the dominating economy of the energy in the future. Recently, most of the hydrogen technologies are based on fossil fuels, which are limited and environment polluting. In order to achieve a sustainable and clean hydrogen economy in the future, the renewable sources have to be applied for hydrogen production. The idea of 'Hyvolution' relies on the exploitation of bacteria, which are able to utilize biomass for growth and H₂ production. The novel approach of the combination of thermophilic and photosynthetic bacterial bioprocesses is adopted in order to achieve the highest H₂ production efficiency in small scale, cost effective industries. A new technology of a small-scale sustainable hydrogen production from local biomass will be developed at the end of the project (Claassen and de Vrije, 2005).

1.5. Objective of this study

In the integrated biohydrogen production systems, combining dark fermentation with photofermentation, the effluent of the dark fermentation is used in photofermentation. The effluent of dark fermentation contains high concentrations of ammonium together with acetate. This is a problem in integrated H₂ production

systems, since high ammonium inhibits H₂ production by photofermentation due to the repression of nitrogenase (N₂ase) enzyme activity and synthesis. In order to increase the efficiency of integrated systems, H₂ has to be also produced from photofermentation. For this purpose, either excess ammonium has to be removed from the effluent, which would not be feasible due to the integration of another step into the overall process, or some modifications in the organism has to be applied in order to obtain a strain, which can produce H₂ independent from ammonium levels.

In the present study, GlnB and GlnK proteins, which are the important elements in ammonium dependent regulation of the nitrogenase expression and activity, were targeted to be inactivated and the results of this inactivation process were examined. A strain, which is able to produce H₂ at high NH₄ concentrations, was aimed to be produced. For this aim, deletion mutations of *glnB* and *glnK* genes were performed by constructing relevant vectors. The deletions were done in frame, in order to keep downstream genes functional.

CHAPTER 2

LITERATURE SURVEY

In this chapter, *R.capsulatus*, which is a purple non sulphur (PNS) photosynthetic bacterium, is described. Moreover, H₂ production mechanism together with the enzymes involved in PNS bacteria are issued. The regulatory mechanisms on these enzymes and the effects of ammonium on H₂ production are distinguished.

2.1. Purple nonsulfur photosynthetic bacteria- *Rhodobacter capsulatus*

Purple non sulphur photosynthetic bacteria represent a non-taxonomic group of microorganisms, which shows remarkable metabolic diversity. PNS bacteria i.e. *R.capsulatus*, can grow as five different modes of growth; photoautotrophic, photoheterotrophic, chemoorganotrophic by aerobic respiration, chemoorganotrophic by fermentation and chemolithotrophic (with H₂ electron donor and oxygen as electron acceptor) (Klipp et al., 2004).

PNS bacteria are able to grow in different growth modes, depending on available conditions such as: degree of anaerobiosis, availability of carbon source (CO₂ for autotrophic growth, organic compounds for heterotrophic growth) and availability of light source (for phototrophic growth) (Basak and Das, 2007).

‘Nonsulphur’ term indicates that PNS bacteria are not able to use hydrogen sulphide (as with sulphur bacteria) as an electron donor in photoautotrophic growth. PNS bacteria is observed in yellowish brown to greenish and deep brown color in the

presence of light and in the absence of oxygen. On the other hand, whenever the environment becomes oxygenic, the carotenoids are altered into ketocarotenoids and the color of the culture turns into red (Pellerin and Gest, 1983).

Rhodobacter capsulatus is a gram negative, photosynthetic, purple non sulphur bacterium. It is a rod shaped bacterium, with the cell size of 0.5-1.2 µm. It is able to move by the aid of polar flagella. The cells are divided by binary fission, have vesicular photosynthetic membranes. Similar to all other *Rhodobacter* species, the cells require thiamine, and biotin and a different third vitamin as growth factors. Its optimum growth pH is between 6 and 9, optimum temperature is between 25°C and 35°C (Sasikala et al., 1993). The taxonomical order of *Rhodobacter capsulatus* is given in Table 2.1. Besides, microscopic images of *R.capsulatus* is given in Figure 2.1.

Table 2. 1 Classification of *Rhodobacter capsulatus* (Imhoff et al., 1984)

Super Kingdom	<i>Prokaryota</i>
Kingdom	<i>Monera</i>
Sub kingdom	<i>Eubacteria</i>
Phylum	<i>Gracilicutes</i>
Class	<i>Photosynthetic eubacteria</i>
Order	<i>Rhodospirillates</i>
Family	<i>Rhodospirillaceae</i>
Genus	<i>Rhodobacter</i>
Species	<i>capsulatus</i>

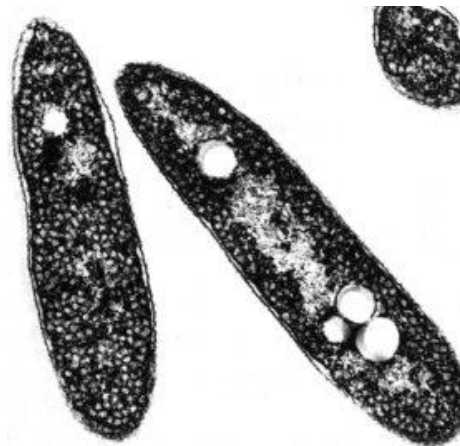


Figure 2. 1 Microscopic picture of *R capsulatus*

(<http://www.iet.uni-duesseldorf.de/Frameseiten/Photobiotechnology&topframenav.htm>,
Last access date: July 27, 2010)

2.2. Hydrogen production by PNS bacteria

In PNS bacteria, the mostly preferred metabolic mode is photoheterotrophic mode; which is both suitable for the best growth and hydrogen production. In photoheterotrophic mode, H_2 is produced under the illuminance and in the absence of oxygen. However, the bacteria are able to change the metabolic mode with respect to different factors. In a bacterial culture medium, in which the carbon/ nitrogen ratio is high (nitrogen limitation), the bacteria remove the excess energy in the form of H_2 . For production of hydrogen, the enzyme systems (hydrogenases and nitrogenases), carbon metabolism and photosynthetic membrane apparatus are all connected to each other with ATP, hydrogen ions (H^+) and electrons (e^-) (Koku et al., 2002).

The overall scheme of the carbon metabolism in PNS bacteria is represented in Figure 2.2. Carbon compounds are oxidized in anaerobic light dependent citric acid cycle (TCA cycle), first discovered by Gest et al. (1949).

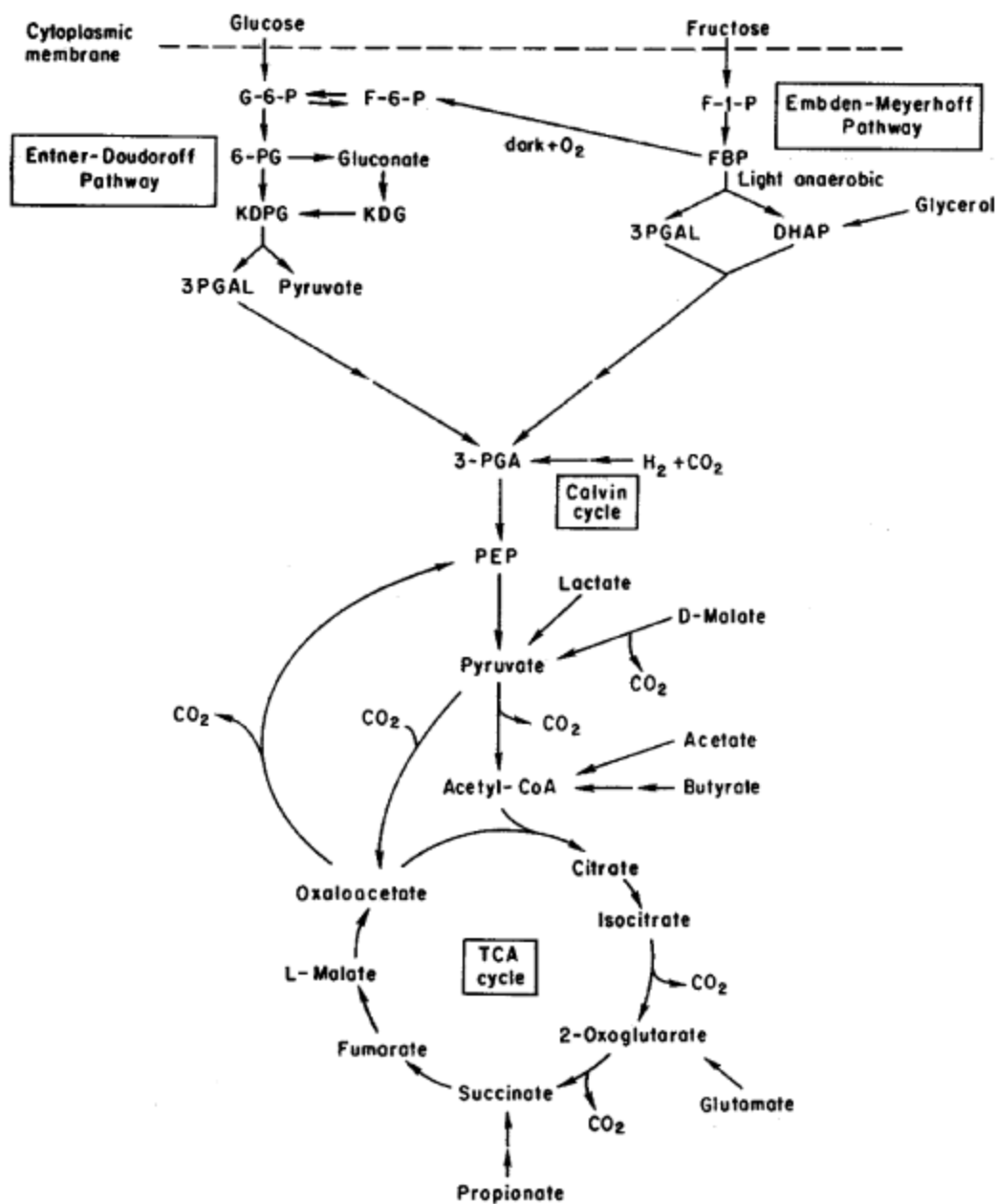
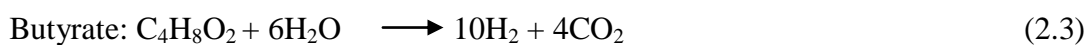


Figure 2. 2 The overall scheme of the carbon metabolism in PNS bacteria (Koku et al., 2002)

PNS bacteria can utilize different carbon compounds for hydrogen production; such as acetate, malate, lactate, butyrate and glucose. The theoretical conversion reactions of these carbon sources are given in Equation 2.1, 2.2, 2.3 and 2.4.



‘Ethylmalonyl-CoA pathway’ (Figure 2.3B) is responsible for assimilation of the acetate in *R.sphaeroides* (Alber et al., 2006; Erb et al., 2008). This pathway shares common enzymes with a competitive biopolymer biosynthesis pathway (Poly-3-hydroxybutyrate, PHB). The acetate catabolism of *R.capsulatus* is by a special pathway called ‘citramalate cycle’ (Figure 2.3A) (Kars et al., 2009).

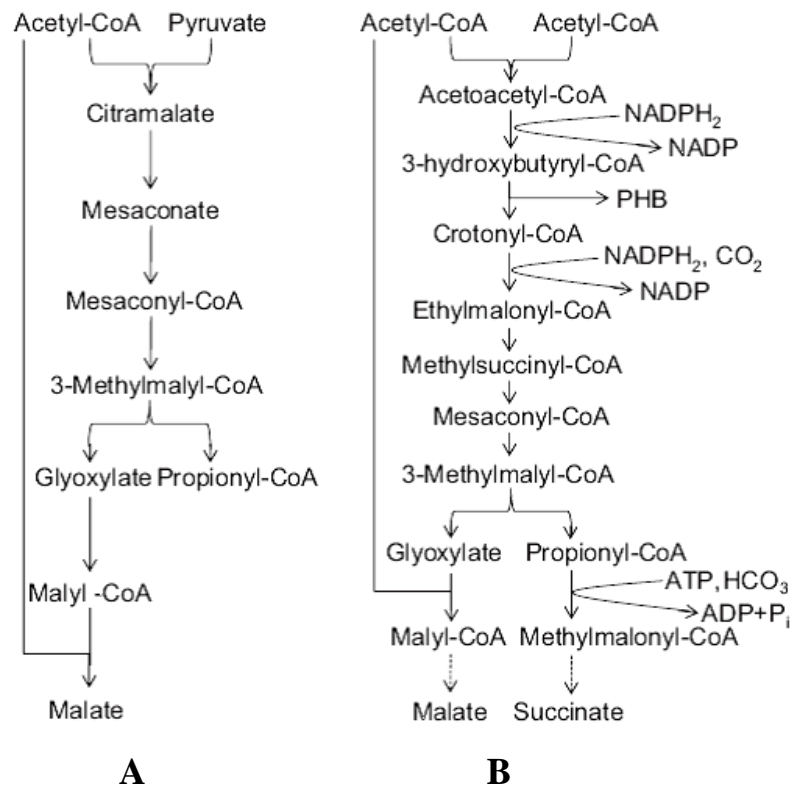


Figure 2. 3 Acetate assimilation of PNS bacteria: (A) The citramalate cycle for *R.capsulatus*, (B) Ethylmalonyl-CoA pathway for *R.sphaeroides* (Kars and Gündüz, 2010)

The H_2 metabolism in PNS bacteria is schematically represented in Figure 2.4 (Koku et al., 2002) and Figure 2.5 (Kars and Gunduz, 2010). The organic compounds are catabolized by TCA cycle and resulting electrons are transferred to the electron carriers in the membrane (Koku et al., 2002). In the photosynthetic apparatus, electrons are transferred between membrane electron transfer chain and ATP's are formed with the aid of proton motive force, which formed across the membrane due to the transport of H^+ . Then, electrons, hydrogen ions and ATP's are delivered to nitrogenase enzyme to be converted into H_2 . Nitrogenase, which originally functions to fix nitrogen from molecular nitrogen (N_2), still can catalyze the reaction in the absence of N_2 (Sasikala et al., 1990)

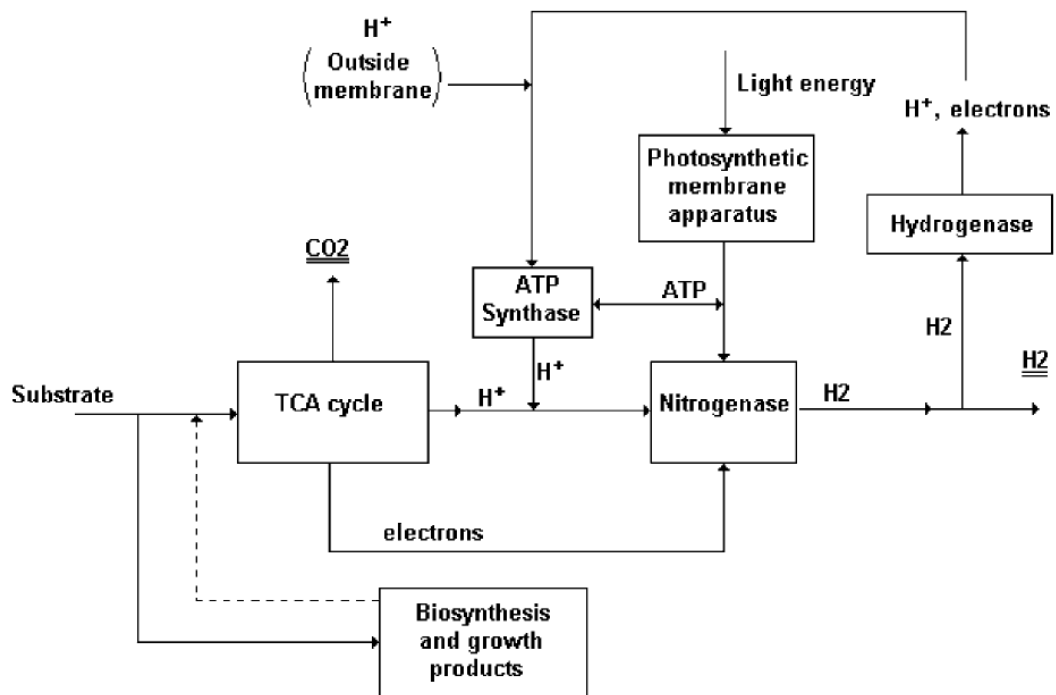
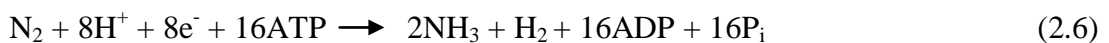
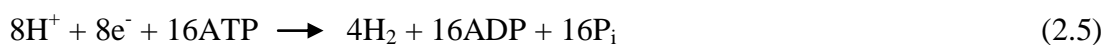


Figure 2. 4 The overall scheme of hydrogen production by PNS bacteria (Koku et al., 2002)

The reaction catalyzed in the absence of N_2 (Equation 2.5) yields 4 times more moles of H_2 than in the presence of N_2 (Equation 2.6) with the expense of the same amount of ATP.



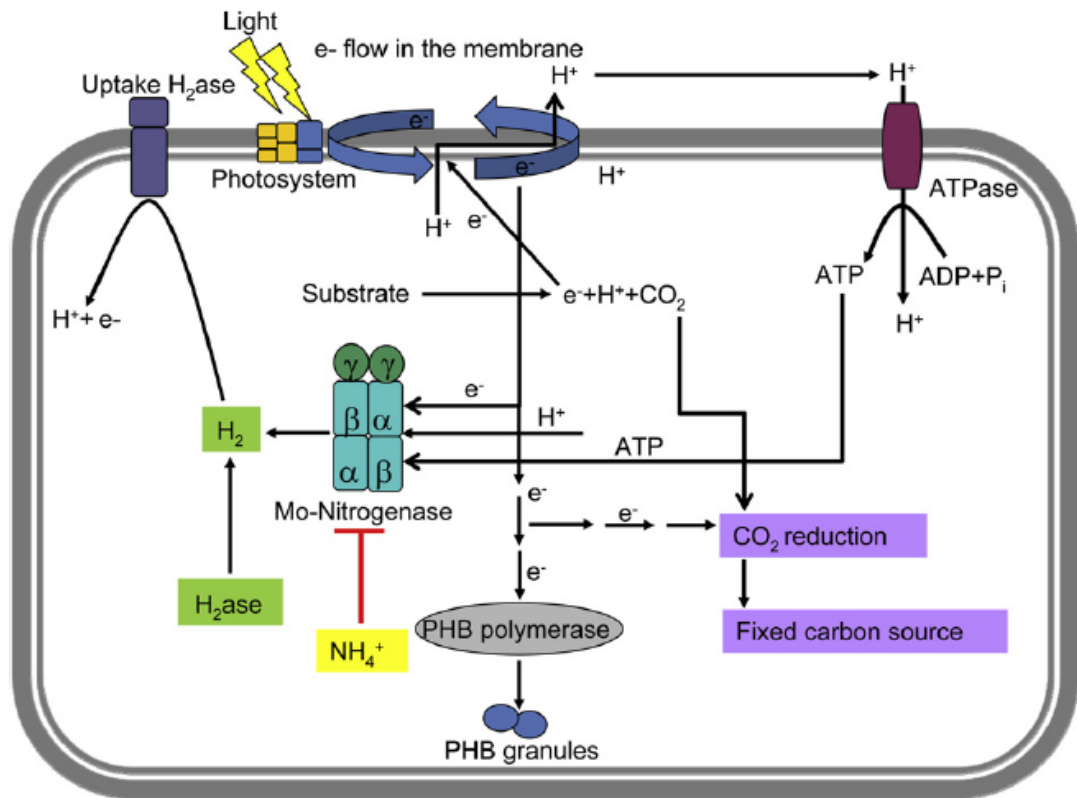


Figure 2. 5 The general view of H₂ related pathways in PNS bacteria (Kars and Gündüz, 2010)

In addition to nitrogenase, uptake hydrogenase is also present in PNS bacteria; it consumes H₂ and decreases H₂ production efficiency (Figure 2.5). The net H₂ yield is H₂ produced by nitrogenase minus H₂ used by uptake hydrogenase (Vignais et al., 1985).

2.3. Enzymes in hydrogen metabolism

There are two main enzymes in H₂ metabolism; hydrogenases (H₂ase) and nitrogenases (N₂ase).

2.3.1. Hydrogenases

The key enzyme in biohydrogen metabolism is H₂ase, which catalyzes both generation and decomposition of H₂ depending on the needs of the organism (Kovacs et al., 2000; Vignais et al., 2001). The simple reaction catalyzed by H₂ase is given in Equation 2.7.



The functions of H₂ases are quite diverse in various organisms. In dark fermentation, H₂ases are mainly responsible for H₂ production and organic acid production (Woodward et al., 2000). In nitrogen fixing bacteria, i.e. PNS bacteria, various H₂ases are present, both producing and consuming H₂, whereas H₂ production is based on N₂ase. The main function of H₂ases in PNS bacteria is to consume H₂ as generally being accepted as the “metabolic antagonist” of N₂ase (Klemme, 1993). So, the term H₂ase are mostly used for uptake H₂ases in PNS bacteria. Hence, H₂ production in PNS bacteria by H₂ases can be considered as negligible (Meyer et al., 1978; Vignais et al., 1985; Benemann et al., 1974).

The functional variation of H₂ases is related with the cellular location of the enzymes. For example, H₂ producing H₂ases are generally found in the cytosol, whereas the uptake H₂ases are present in periplasmic space or in the membrane. Cytoplasmic bidirectional H₂ases also consume H₂. The energy requirement of the cell changes with changing environment conditions. With the aid of various H₂ases, the cell can react efficiently to the changes in energy requirement of the cell, which is resulting from the environmental factors (Vignais and Meyer, 2001).

Most of the H₂ases are metalloenzymes, containing nickel (Ni) and/or iron (Fe) atoms in their structure. The classification is based on the type of metal atom they contain. Three classes of H₂ases are identified; [Fe]-H₂ases, [NiFe]-H₂ases, and the

metal-free H₂ases (Basak and Das, 2007; Vignais et al., 2001). On the other hand, H₂ases can be also regarded as ‘reversible’ and ‘uptake’ H₂ases (Valdez-Vazquez and Poggi-Varaldo, 2009). Reversible H₂ases bidirectionally catalyze the formation and deformation of H₂ (Equation 2.7), according to the redox status of the cell. Uptake H₂ases oxidizes H₂ into electrons and hydrogen ions (Chen et al., 1978). Uptake H₂ase is membrane bound and causes decreases in the H₂ production, since it consumes H₂ molecules produced by N₂ase (Hall et al., 1995). In *R.capsulatus*, H₂ase enzyme is membrane bound and mainly functions as an H₂ uptake (consumption) enzyme (Uyar, 2008). The electrons derived from H₂ uptake are transferred to ferredoxins and cytochromes.

Similar to many metalloenzymes, H₂ases are sensitive to various factors, including oxygen, high temperature and some other factors. Oxygen has a drastic effect on H₂ase. It does not affect the structural integrity of [NiFe] hydrogenases but reversibly inactivates their catalytic function (Buhrke et al., 2005). In green algae, H₂ production immediately ceases (from several seconds to a few minutes), due to the oxygen release by photosynthesis (Melis, 2002).

2.3.2. Nitrogenases

The H₂ production by PNS bacteria is by means of N₂ase enzyme, which is a two protein component enzyme system that catalyzes biological reduction of dinitrogen (N₂) into ammonium with the hydrolysis of ATP (Burris, 1991). Since the energy barrier of the reaction is high due to the strong N-N triple bond of N₂, N₂ase requires a great deal of chemical energy, released from the hydrolysis of ATP, and reducing agents, such as dithionite *in vitro* or ferredoxin *in vivo*. Proton reduction to H₂ is an obligatory reaction of N₂ase when it reduces N₂. Moreover, N₂ase can also reduce protons to H₂ in the absence of dinitrogen. The reaction catalyzed by N₂ase can be seen in Equation 2.5 and 2.6. From the perspective of H₂ production, the theoretical

H₂ yield of N₂ase is four times better in the absence of N₂ (Equation 2.5) than in the presence of N₂ (Equation 2.6) as indicated before.

The classification of N₂ases is mainly based on the cofactor metal atom present in the active site of the enzyme. A recent N₂ase was discovered from *Streptomyces thermoautotrophicus*. This N₂ase contains two components; first component is CO-dehydrogenase, which oxidizes CO₂ into CO and reduces O₂ into superoxide anion radical (O₂⁻). The second component oxidizes O₂⁻, supplies electrons to N₂ and reduces MoFeS active site (Ribbe et al., 1997). There are three more classes of N₂ases, which are distinguished on the basis of the presence of Mo (molybdenum), V (vanadium) or Fe (iron) atoms in the active site (Igarashi and Seefeldt, 2003). The conventional N₂ase is MoFe N₂ase. However, Mo atom is replaced by either V atom or Fe atom in the active site of vanadium-iron and iron-iron (Fe-only) classes of N₂ases, respectively.

All nitrogen fixing bacteria contains molybdenum–iron (MoFe) N₂ase. However, in the absence of molybdenum in the environment, some organisms such as *R.capsulatus* and *A.vinelandii* activate an alternative Mo-independent N₂ase, which contains vanadium-iron or iron-iron atoms. They are inhibited in the presence of molybdenum (Dixon and Kahn, 2004; Eady, 1996; Robson et al., 1986).

N₂ases are composed of two proteins, which are named according to their metal atom; dinitrogenase, also called MoFe protein, is the catalytic site of the enzyme for reduction of the substrate and dinitrogenase reductase, also called Fe protein, passes electrons to dinitrogenase in an ATP dependent manner and bind to nucleotide (Rees and Howard, 2000). Dinitrogenase protein contains [8Fe-7S] metal cluster, called P cluster, whereas dinitrogenase reductase contains [4Fe-4S] metal cluster (Igarashi and Seefeldt, 2003). The structure of N₂ase is given in Figure 2.6 (Dixon and Kahn, 2004).

The gene systems encoding different N_2 ases are present. The *nifHDK* operon encodes the subunits of N_2 ase; *nifH* encodes two dinitrogenase reductase subunits and *nifD* -*nifK* encode subunits of dinitrogenase. *nifA* is the transcriptional activator of *nifHDK* operon (Henson et al., 2004). The vanadium-iron N_2 ase is encoded by *vnf* gene system and Fe-only N_2 ase is encoded by *anf* gene system (Siemann et al., 2002; Eady, 1996).

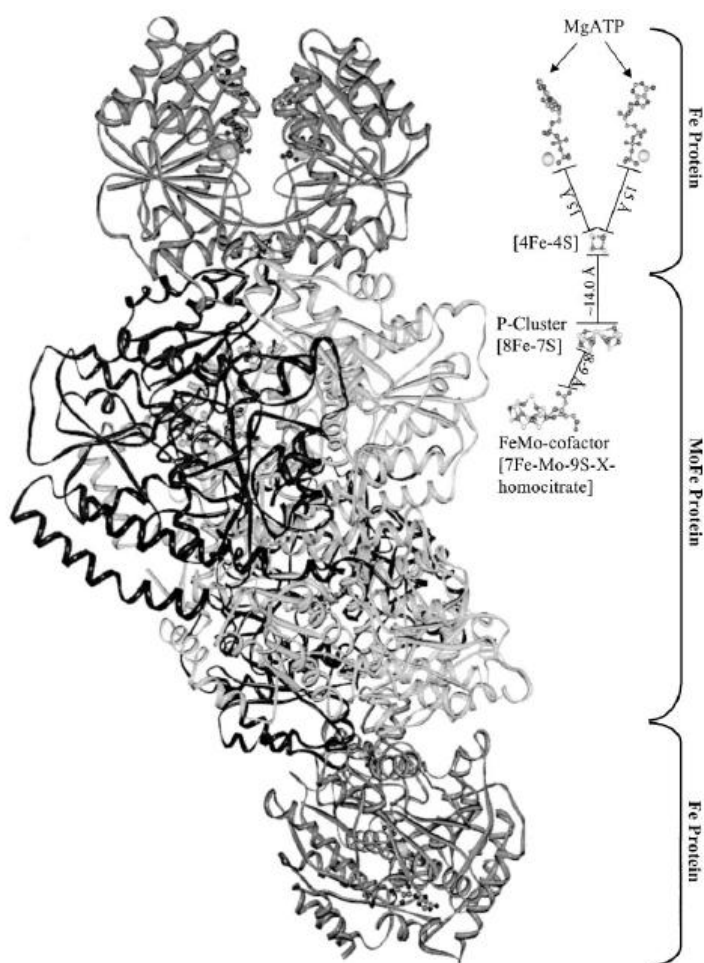


Figure 2. 6 Overall structure of N_2 ase. The middle protein is MoFe protein, top and bottom proteins are Fe proteins (Igarashi and Seefeldt, 2003).

MoFe protein associates with one half of the Fe protein which is reduced in the [4Fe-4S] cluster and bound to 2 molecules of MgATP (Igarashi and Seefeldt, 2003). The association of the proteins causes the hydrolysis of ATP molecules without dissociation from Fe protein. One electron is first transferred to P cluster and then to FeMo cofactor of MoFe protein. The substrate is bound to the FeMo cofactor and reduced. The oxidized Fe and MoFe proteins dissociate after the electron transfer. Fe protein cycles and delivers other electrons to MoFe protein by being reduced by an electron transfer protein (ferredoxin or flavodoxin) (Chatelet and Meyer, 2001; Hallenbeck and Gennaro, 1998). The cycling of Fe protein is represented in Figure 2.7.

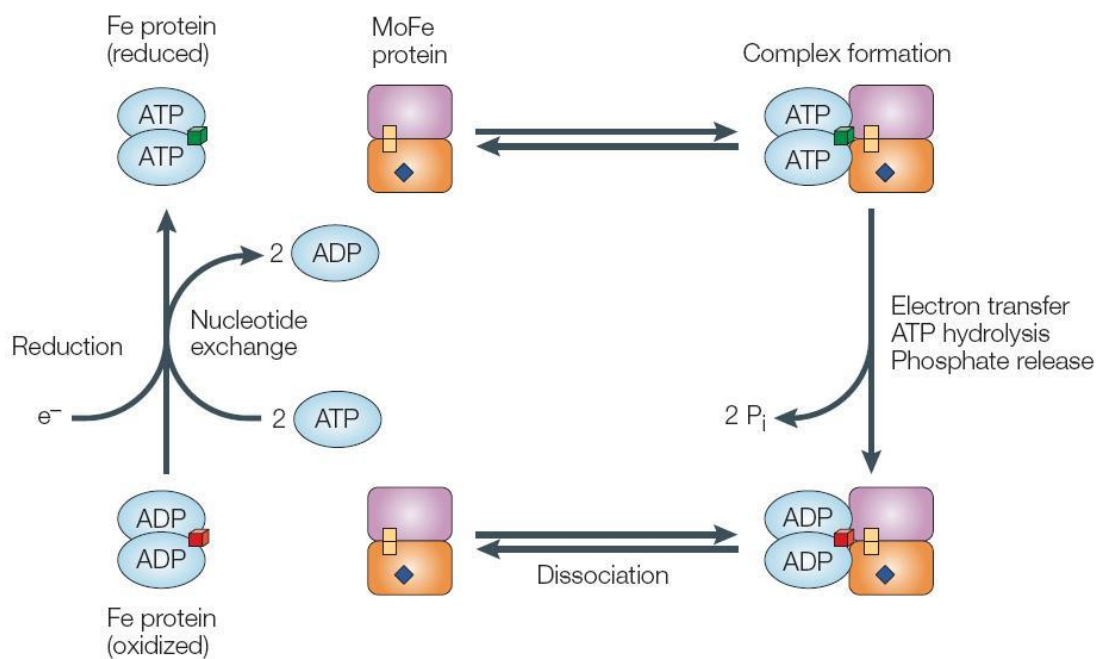


Figure 2. 7 Schematic representation of the N₂ase Fe protein cycle. The Fe protein dimer is in light blue color and the small cube inside representing the [4Fe-4S] cluster (reduced form of [4Fe-4S] cluster is in green and oxidized form is in red color). The α and β subunits of the MoFe protein are purple and orange squares. The

small yellow cubes inside MoFe protein represent P clusters and the blue diamond inside represents FeMo cofactor (Dixon and Kahn, 2004).

2.3.3. Regulation of nitrogenase

As indicated before, nitrogen fixing process is energetically expensive for the cell. So, this process; hence hydrogen production is strictly controlled by many factors. The necessity to respond to the concentrations of fixed nitrogen and external oxygen, and to provide sufficient energy for nitrogen fixation, comprises the common regulatory principles among nitrogen fixing bacteria (Dixon and Kahn, 2004). In *R.capsulatus*, N₂ase is regulated by various environmental factors such as ammonium (NH₄), molybdenum, O₂ and light (Masepohl et al., 2002). Ammonium, which is the end product of nitrogen fixation reaction, has drastic inhibitory effects both on the expression and the activity of N₂ase by the aid of multilevel ammonium regulatory mechanism (Masepohl et al., 2004).

Nitrogen fixation and regulation over N₂ase in *R.capsulatus* have been extensively studied by Masepohl, Drepper, Klipp and their colleagues (Masepohl et al., 2004). In *R.capsulatus*, there are three proposed levels of ammonium regulation on N₂ase enzyme complex (Figure 2.8) (Masepohl et al., 2002). The first level of control is the 'Global Nitrogen Regulation System', shortly 'Ntr' system, which is well defined in enteric bacteria (Gussin et al., 1986). Ntr system is responsible for measurement of cellular nitrogen status of the cell and Ntr system of *R.capsulatus* is thought to be similar to the Ntr system of enteric bacteria (Ninfa and Atkinson, 2000). NifA is the master regulator of nitrogen fixation (Rudnick et al., 1997) in diazotrophic species of proteobacteria. In those organisms, the two-component NtrB-NtrC regulatory system, which provides global control in response to the nitrogen source, controls NifA expression (Dixon and Kahn, 2004). At this level of control, transcription of *nifA1*, *nifA2* and *anfA* genes, which are the transcriptional activators of structural genes of N₂ases, are regulated. *nifA1* and *nifA2* activate transcription of *nif* genes together with RNA polymerase containing σ^{54} sigma factor, moreover they can substitute for each

other (Masepohl et.al, 1988). The key regulator at this level is NtrB protein which can act both as a kinase and phosphatase. When there is no NH₄ in the environment, NtrB molecule is in its active form and it activates NtrC molecule by phosphorylation. Once NtrC is active, it can go and activate the transcription from *nifA1*, *nifA2* and *anfA*, which encode NifA1, NifA2 and AnfA that are the transcriptional activators of structural genes of nitrogenases (*nif* genes). Thus, in the absence of NH₄, *nif* genes are transcribed. Whenever there is NH₄ in the cells, the regulatory GlnB protein, one of P_{II} signal transduction protein (discussed later), binds to NtrB and inactivates it. In this form, NtrB cannot activate NtrC protein. Therefore, no transcription of NifA activators takes place, resulting in the failure in transcription of structural *nif* genes in the presence of NH₄ (Figure 2.8, Level 1).

In the second level of NH₄ regulation, which is independent of Ntr system, is on the control of the activity of NifA transcriptional activators. Paschen et al. (2001) observed that NifA mediated *nifH* expression is still inhibited by NH₄ even though NifA protein is accumulated in the cell by overexpression from constitutive promoters. In the presence of NH₄, P_{II} regulatory proteins (GlnB and GlnK) inhibit the activity of NifA1 and NifA2. In many diazotrophic bacteria, such as *Azorhizobium caulinodans* (Michel-Reydellet and Kaminski 1999), *A. vinelandii* (Little et al., 2000), *Rs.rubrum* (Zhang et al., 2000) and *R.capsulatus* (Drepper et al., 2003) and more, it was shown that P_{II} proteins (GlnB and GlnK) regulate NifA activity (Figure 2.8, Level 2).

Third level of regulation is based on the post-translational control of nitrogenase activity. The cell is capable to switch off the nitrogenase activity in response to NH₄ addition by reversible ADP-ribosylation of Fe protein (dinitrogenase reductases) of N₂ase. This type of regulation is mediated by a two-enzyme system. *draT* encodes dinitrogenase reductase ADP ribosyltransferase (DRAT) protein, which inactivates Fe protein of N₂ase by ADP-ribosylation. The activation of Fe protein is performed by dinitrogenase reductase activating glycohydrolase (DRAG) protein, which is the gene product of *draG* (Masepohl et al., 1993; Drepper et al., 2003; Yakunin and

Hallenbeck, 1998). Similar to other levels of regulation, this level of regulation is also controlled by GlnB and GlnK proteins (Figure 2.8, Level 3).

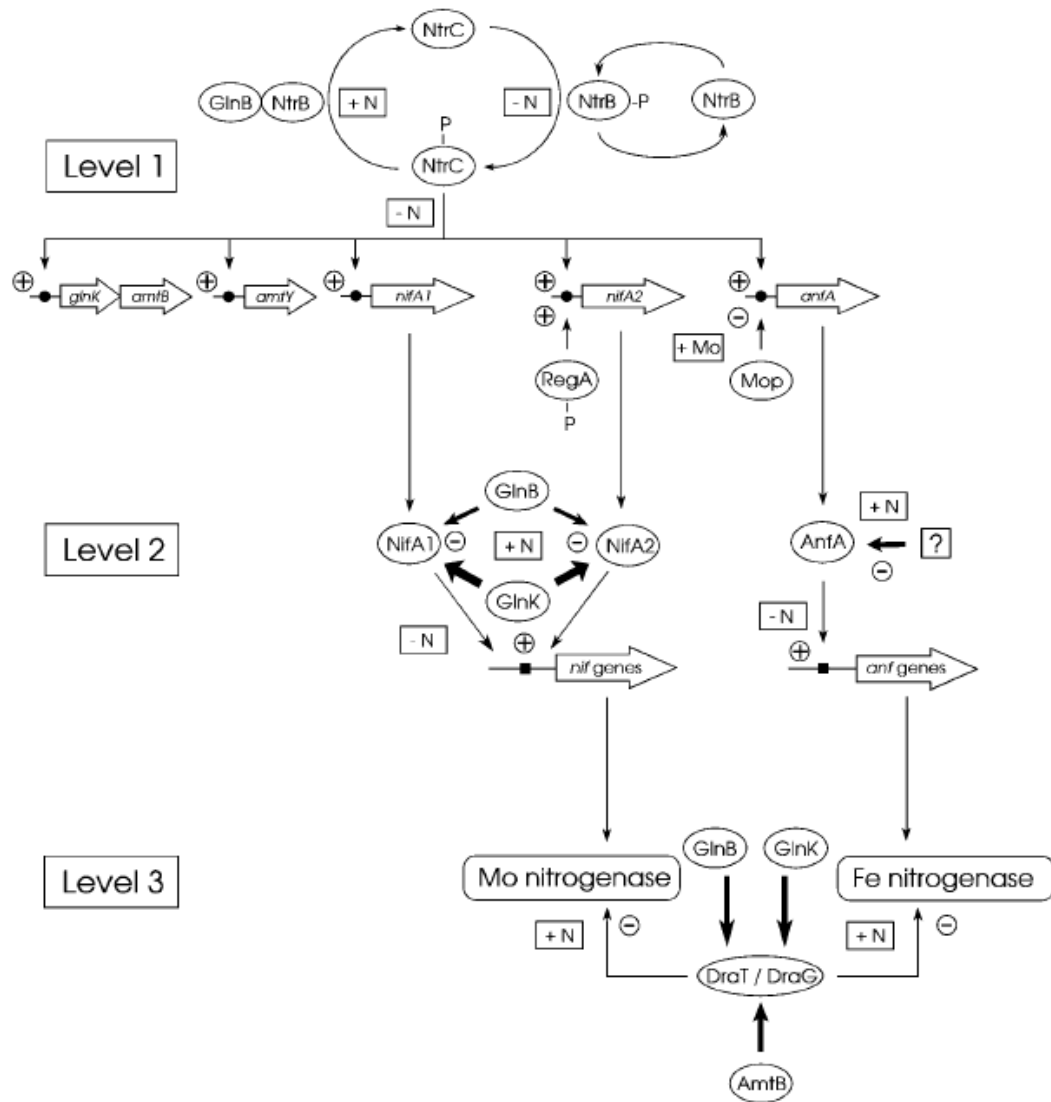


Figure 2. 8 The levels of ammonium regulation on N_2 ase enzyme complex in *R. capsulatus*. Availability of NH_4 is represented by [+N] and [-N], respectively meaning presence and absence of NH_4 . (Masepohl et al., 2002)

2.3.4. P_{II} Signal transduction proteins

P_{II} signal transduction proteins play widespread crucial roles in microbial nitrogen regulation. They function as the central processing unit (CPU) for the integration of signals of carbon and nitrogen status, and use this information to control nitrogen assimilation (Ninfa and Atkinson, 2000; Forchhammer, 2004). P_{II} proteins functions in the transcriptional regulation of nitrogen-regulated (Ntr) genes when the cells are under N₂ase repressing conditions, hence they regulate N₂ases. Moreover, they regulate activity of glutamine synthetase (GS), which is the main enzyme in nitrogen assimilation, by modulating adenylation state of it (Blauwkamp and Ninfa, 2002).

The nitrogen status of the cell is sensed by Ntr system. Glutamine to α -ketoglutarate concentration represents nitrogen to carbon balance of the cell (Senior, 1975). The signal of nitrogen status is delivered to P_{II} proteins and the NtrB protein by *glnD* gene product, bidirectional uridylyltransferase/uridylylremoving (UTase/UR) enzyme, which catalyzes the uridylylation and deuridylylation of P_{II} (central cycle in Figure 2.9). Hence, UTase/UR can be considered as intracellular nitrogen sensor (Jiang et al., 1998). When there is no ammonium present, UTase uridylylates P_{II} at tyrosine residue at position 51. The resulting uridylylated P_{II} (P_{II}-UMP)₃ is now inactive; thus it cannot interact with target NtrB protein to inactive. The active NtrB protein successfully activates transcriptional activators of structural N₂ase genes. When ammonium becomes available, uridylylremoving (UR) enzyme activates P_{II} by removing UMP group attached. P_{II} interact with NtrB, prevent activation of NtrC and further proteins. The connection between changes in the intracellular nitrogen status and the activity of the transcriptional activator protein NtrC is achieved.

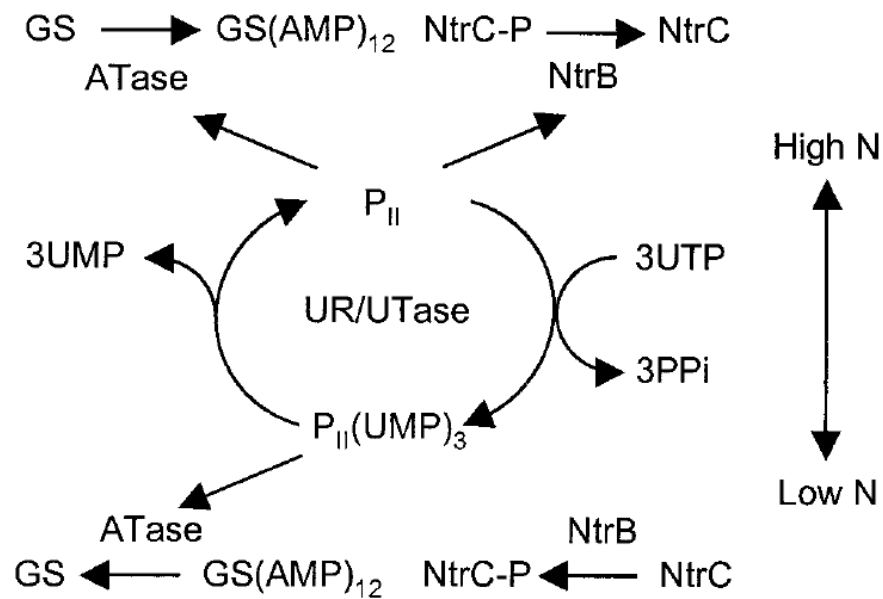


Figure 2. 9 Nitrogen regulation (Ntr) system of enteric bacteria. The activities of both GS and NtrC are regulated in response to the intracellular nitrogen status. UTase catalyzes the uridylylation and deuridylylation of P_{II} . ATase catalyzes the adenylation and deadenylation of GS. NtrB catalyzes the phosphorylation and dephosphorylation of NtrC (Arcondeguy and Merrick, 2001)

In addition to the N_2ase regulation, P_{II} proteins control nitrogen assimilation by GS, which is responsible for most of ammonium assimilation, in response to nitrogen status of the cell (Westby et al., 1987). The reaction catalyzed by GS is given in Equation 2.8. When ammonium is available, the activity of GS is limited in order to keep the rate of nitrogen assimilation balanced with carbon assimilation in response to [glutamine] to [α -ketoglutarate] ratio. The complete regulation of GS is by means of regulation its transcription and activity by reversibly adenylation (Ninfa and Atkinson, 2000). ATase, which is encoded by *glnE* gene, is one of P_{II} targets. ATase catalyzes the addition/removal of adenylyl groups to a tyrosine residue of the subunits in GS; resulting either active GS or inactive GS (GS-AMP). When there is available NH_3 , ATase adenylylates GS, resulting into 'inactive' GS (GS-AMP). However, in the absence of NH_3 , ATase removes AMP group from GS and activates

it. Determination of the direction catalyzed by ATase is by means of P_{II} protein, depending on the uridylylation state of it. P_{II} results adenylylation of GS, whereas P_{II}-UMP results deadenylylation of GS (Figure 2.9).



There are accumulated evidences about the functions of P_{II} proteins in the transport of nitrogen compounds. In some bacteria, P_{II} mutants are not able to utilize nitrate as the only nitrogen source, suggesting the possible role of P_{II} in nitrate utilization (Amar et al., 1994; Wray et al., 1994). Moreover, the strict structural linkage between *glnK* and *amtB* genes; *amtB*, which encodes high affinity ammonium transporter, is invariably present in the downstream of *glnK* within the same operon. It was shown by Javelle et al. (2004) that AmtB transport protein is able to form complex with GlnK regulatory protein, hence inactivating ammonium transport. This regulation is mediated by uridylylation/deuridylylation state of GlnK, which represents the variations in intracellular glutamine concentration.

Further known and proposed targets of P_{II} proteins are illustrated in Figure 2.10, summarizing revealed information and predictions.

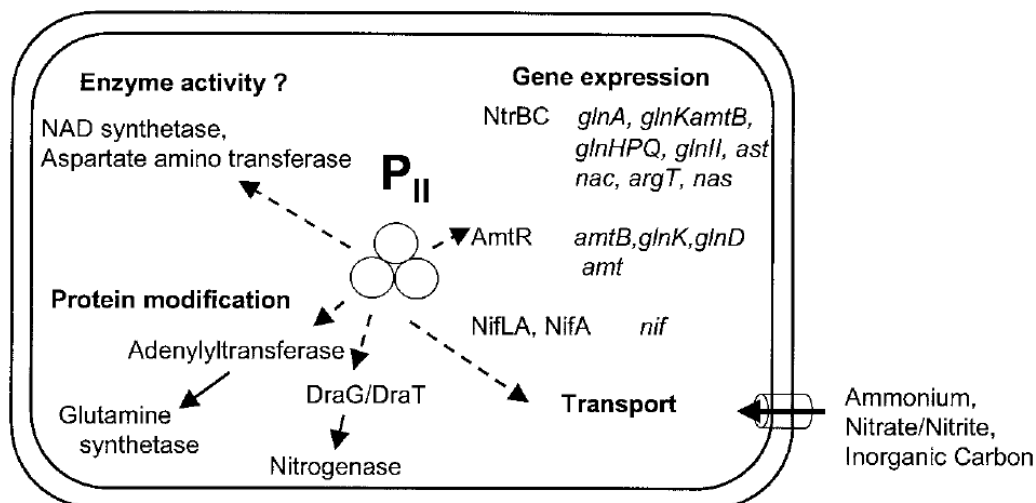


Figure 2. 10 Scheme illustrating the potential variability of P_{II} targets (Arcondeguy and Merrick, 2001)

2.3.5. Effect of ammonia on hydrogen production

As mentioned in above, the N₂ase is under intense regulation; hence H₂ production is, too. Presence of NH₄ in the medium reduces H₂ production by PNS bacteria. Akköse et al. (2009) demonstrated that H₂ production in *R.sphaeroides* decreased as the NH₄ concentration in the media increased and moreover it ceased when the NH₄ concentration was higher than 2 mM.

The negative effect of NH₄ on H₂ production of *Rhodospseudomonas palustris* grown on acetate was also reported by Oh et al. (2004). Similar result was observed; presence of NH₄ reduced the rate of H₂ production and cumulative H₂ production. Moreover, comparisons of various nitrogen sources indicated that yeast extract and glutamate are better nitrogen sources than NH₄ with respect to H₂ production.

Presence of NH₄ was also reported to decrease H₂ production of *R.capsulatus* on acetate medium (Hyvolution confidential, (2007). Deliverable3.2: Hydrogen

production capacity and substrate utilization data of tested strains). Similar pattern of negative effect was observed for *R. capsulatus*. As the NH_4Cl concentration increased from 1 mM to 8 mM, H_2 production decreased drastically.

2.3.6. Byproducts of hydrogen metabolism

Byproducts are associated with H_2 production mechanism (Figure 2.4 and 2.5). In H_2 production process, biomass is considered as byproduct. Photosynthetic cells are quite rich in protein and co-factors and vitamins (Rocha et al., 2001), so the biomass of photosynthetic bacteria can be used as fertilizer, supplementary animal food etc.

Another important byproduct of H_2 metabolism is Polyhydroxyalkanoates (PHAs). They are a class of natural polyesters and are accumulated in the cells as the granules. By accumulating PHAs, the cells store carbon and reducing powers (Aldor and Keasling, 2003). Polyhydroxybutyrate (PHB) is a PHA. It is a bacterial storage material in stress conditions, typically accumulated in stationary phase for further utilization in starvation (Yamagishi, 1995; Yiğit et al., 1999). Due to its thermoplastic feature and biodegradability, it is considered as one of the candidates to replace conventional plastics from petroleum (Khatipov et al., 1998; Fuller, 1995; Steinbuechel, 1991). The PHB synthesis takes place in the cell and it is accumulated in the form of granules, especially when the cell is in a high carbon/ nitrogen concentration environment (conditions limiting growth). In addition to the lack of nitrogen, the absence of sulphur or phosphorous also lead PHB accumulation (Brandl et al., 1989; Brandl et al., 1991; Liebergesell et al., 1991; Hustede et al., 1993).

When the photosynthetic bacteria are grown in anaerobic conditions, PHB synthesis and accumulation depend on carbon and nitrogen availability, and pH of the medium. Acetate was found to be the best carbon source and ammonium in high concentrations was found to be the best nitrogen source for the highest PHB productivity in *R. sphaeroides*. Gross et al. (1992) reported that *R. sphaeroides* accumulated 24 % (w/w) PHB. Moreover, high pH was found to enhance PHB

production (Khatipov et al., 1998). The PHA biosynthesis pathway is given in Figure 2.11.

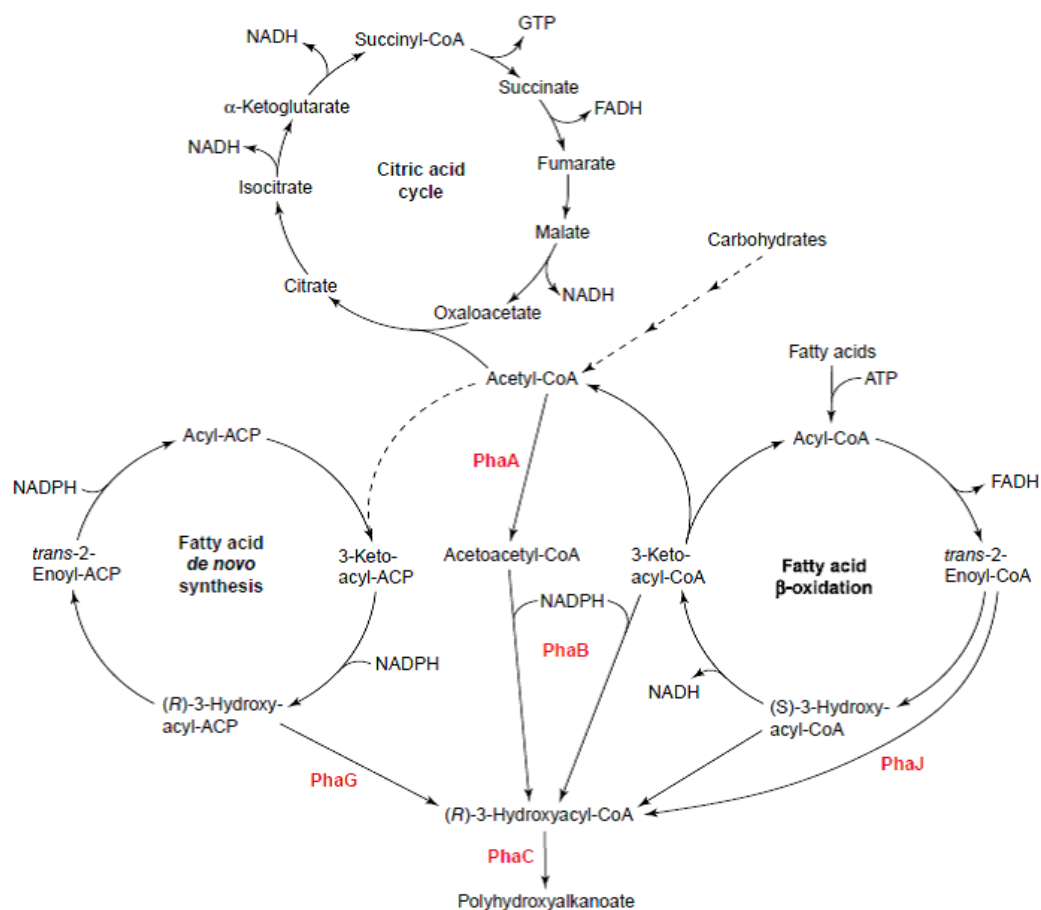


Figure 2. 11 PHA biosynthesis in the context of microbial metabolism. The major enzymes in PHA biosynthesis are PhaA (3-ketothiolase), PhaB ((R)-3-ketoacyl-CoA reductase), PhaC (PHA synthase), PhaG ((R)-3-hydroxyacyl ACP:CoA transacylase) and PhaJ ((R)-specific enoyl-CoA hydratase). In the case of PHB biosynthesis, PhaB is acetoacetyl-CoA reductase enzyme (Aldor and Keasling, 2003).

The synthesis of PHB is similar to H₂ production in a way that PHB synthesis process also removes excess reducing equivalents in the cell. Hence, PHB synthesis and H₂ production are competitive processes. Kim et al. (2006) obtained a *phb*⁻ mutant of *R.sphaeroides* and compared the maximum H₂ production of this strain with wild type strain. They observed that the H₂ production of mutant strain was 1.3 times higher than the H₂ production of wild type. On the other hand, the ability of the cell to accumulate and reuse PHB enables cells to be more resistant to stress conditions. When stress tolerance of *Pseudomonas* sp. was analyzed in PHB accumulating and non-accumulating conditions, it was shown that *Pseudomonas* sp., which accumulated PHB granules, were more resistant to stress than other cells, which did not accumulated PHB (Ayub et al., 2004).

Carotenoid pigments are another valuable byproduct of H₂ metabolism. Carotenoids are required in photosynthesis by transferring absorbed light to bacteriochlorophyll and in protecting the cell from the photooxidative effect of sunlight (Yiğit et al., 1999).

CHAPTER 3

MATERIALS AND METHODS

In this chapter, the experimental methods used in the present study were described. The bacterial strains/ the plasmids used and obtained were listed. The hydrogen production experiment, including the media composition and the setup, were detailed. Moreover, recombinant DNA procedures, which were applied for the construction of the plasmid vectors, were explained.

3.1. Bacterial strains

All of the bacterial strains used in this study are listed in Table 3.1. The microorganism used in this study for hydrogen production and for genetic manipulations is *Rhodobacter capsulatus* DSM1710, which is the wild type strain, was obtained from Deutsche Sammlung von Mikroorganismen (DSM, Braunschweig Germany). The genetic manipulations in this organism were performed with the help of *Escherichia coli* strains. One of the strains used for general cloning purposes is *E. coli* XL1Blue strain, which is suitable for blue-white screening. The other *E. coli* strain S17-1 (λ pir) used for conjugation in order to deliver the interested plasmid into with *R. capsulatus* DSM1710.

3.2. Plasmids

The cloning vector pBluescript SK (+) (pBtSK) and the suicide vector pK18mobsacB were the plasmids used in this study. The plasmids pGBBU, pGBBD, pGKBU, pGKBD, pGBSD, pGKSD, pGBSUD and pGKSUD were obtained in the

present study. All the plasmids used and obtained in this study are listed in Table 3.2 and their maps are given in related sections.

Table 3. 1 The bacterial strains

Organism/ Strain	Characteristics	References
<i>E.coli</i> XL1Blue	$\Delta(mcrA)183$, $\Delta(mcrCB-hsdSMR-mrr)$ 173, <i>endA1</i> , <i>supE44</i> , <i>thi-1</i> , <i>recA1</i> , <i>gyrA96</i> , <i>relA1 lac</i> [F' <i>proAB lacIqZ</i> Δ M15 Tn10 (Tetr)]c	Stratagene
<i>E.coli</i> S17-1 (λ pir)	294 (<i>recA pro res mod</i>) Tpr, Smr (pRP4-2-Tc::Mu-Km::Tn7), λ pir	Herrero et al, 1990
<i>R.capsulatus</i> DSM1710	wild type strain	Deutsche Sammlung von Mikroorganismen (DSM, Braunschweig Germany).
<i>glnB</i> <i>R.capsulatus</i>	<i>glnB</i> mutant strain	Present study

Table 3. 2 The plasmids

Plasmid	Characteristics	Reference
pK18 <i>mobsacB</i>	<i>Km^r</i> , <i>sacB</i> , <i>RP4 oriT</i> , <i>ColE1 ori</i>	Schafer et al, 1994
pBluescript SK (+) (pBtSK)	<i>Amp^r</i> , cloning vector	Stratagene
pGBBU	pBtSK containing <i>glnB</i> upstream fragment	This work
pGBBD	pBtSK containing <i>glnB</i> downstream fragment	This work
pGKBU	pBtSK containing <i>glnK</i> upstream fragment	This work
pGKBD	pBtSK containing <i>glnK</i> downstream fragment	This work
pGBSD	pK18 <i>mobsacB</i> having 1kb <i>glnB</i> downstream	This work
pGBSUD	pK18 <i>mobsacB</i> having 2kb <i>glnB</i> upstream &downstream	This work
pGKSD	pK18 <i>mobsacB</i> having <i>glnK</i> downstream	This work
pGKSUD	pK18 <i>mobsacB</i> having 2kb <i>glnK</i> upstream &downstream	This work

3.3. Growth media and conditions

During molecular genetics experiments, *Rhodobacter capsulatus* DSM1710 was grown under continuous illumination at 30°C in Biebl and Pfennig (BP) minimal medium (Biebl and Pfennig, 1981), in which malate (7.5 mM) and glutamate (10.0 mM) were used as carbon and nitrogen sources, respectively. The vitamin solution (thiamin, niacin and biotin), trace elements solution and ferric citrate solution were added (Appendix A). The media were prepared and sterilized by autoclaving. The vitamin solution and trace element solution were sterilized by filtering with 0.2 µm sterile filters, added into the cooled medium after autoclaving.



Figure 3. 1 Anaerobic cultures of wild type *R. capsulatus* cultures

E.coli strains were grown in Luria Broth (LB) medium at 37 °C with antibiotics in the following concentrations (µg/mL) when necessary: ampicillin 100; kanamycin 25; and tetracycline 10.

Solid media were prepared by including 1.5 % (w/v) agar into the BP medium and autoclaving. After the medium cooled to a moderate temperature, the vitamin solution, ferric citrate solution and trace elements solutions were added and immediately poured into sterile plastic petri plates.

3.4. Hydrogen production media and conditions

In hydrogen production experiments, BP media containing acetate as the carbon source was used with 30 mM concentration. When acetate was used as carbon source, the buffer capacity of the medium was increased 6 fold in order to compensate pH variations. In the case of nitrogen source, glutamate (2 mM) was used in the control medium and different concentrations of ammonium chloride (Table 3.3) was used in the other media in order to examine the effect of ammonium ion on H₂ production.

Table 3. 3 Concentrations of nitrogen source in 30 mM acetate containing media.

BP medium	Concentrations of nitrogen source
1	1mM NH ₄ Cl
2	2mM NH ₄ Cl
3	3mM NH ₄ Cl
4	5mM NH ₄ Cl
5	8 mM NH ₄ Cl
6 (control)	2mM glutamate

3.5. Hydrogen production setup

For both wild type and mutant *glnB⁻ R.capsulatus*, 55 ml glass photobioreactors, sterilized by autoclaving, were used for hydrogen production with the medium composition described in Appendix A. The media were inoculated from the same mother culture with 10 % inoculation volume. The opening of the bottles were tightly closed with plastic septa and covered with parafilm and teflon seal tape. The time of inoculation is accepted as ‘zero time’. Before connecting to gas collection

tubes, the cultures were flushed with argon gas in order to provide anaerobic environment in the photobioreactor. The whole system was placed in a cooling incubator. The cultures were incubated at 30 °C under the illuminance of 2100-2200 LUX, which was provided by 100 watt tungsten lamps from the distance of 30-40 cm. The light intensity was checked every day after the sampling by a luxmeter (Lutron LX-105 Light Meter). The conversion factor is 1 W/m²= 17.5 lux (Uyar, 2008).

The hydrogen produced was collected in collection tubes. In the setup, which is developed by Uyar et al (2008), the photobioreactors are connected to gas collection tubes by empty cables. The gas produced by the cultures passes through the cables and replaces the water in the gas collection tubes. So, the total gas was measured with the help of volumetric labels on the gas collection tubes (Figure 3.2).

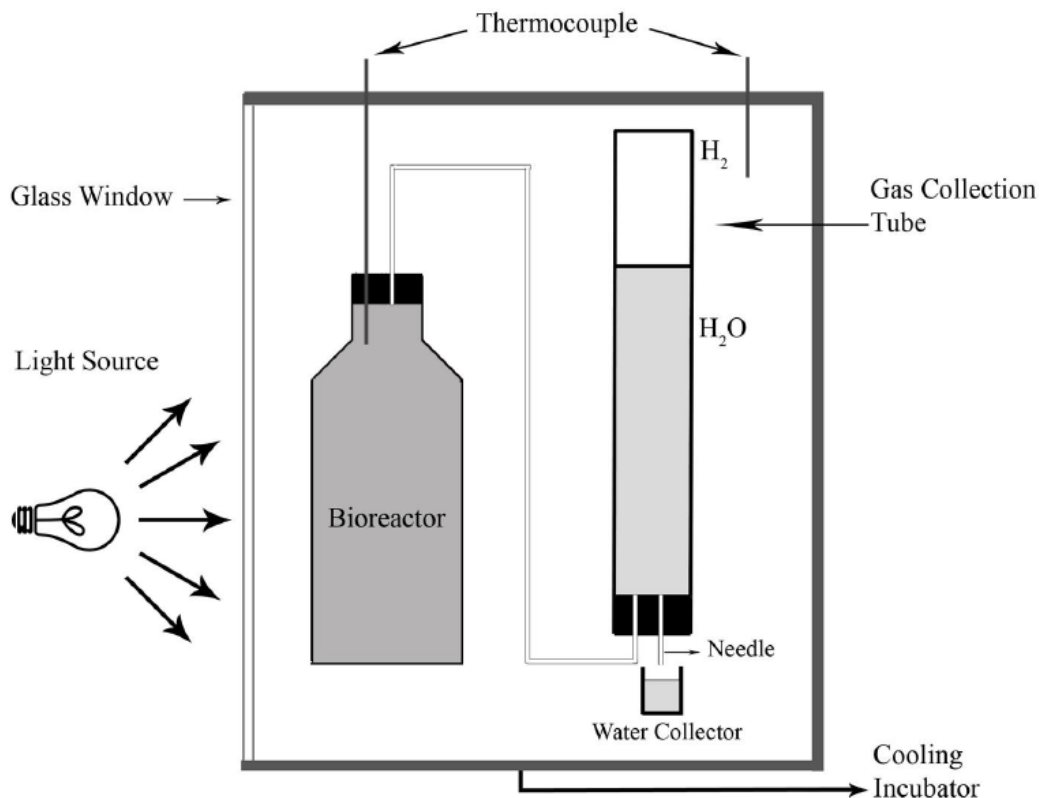


Figure 3. 2 The schematic representation of hydrogen production setup (Sevinç, 2010)



Figure 3. 3 The experimental setup of hydrogen production

3.5.1. Sampling

In time intervals (approximately, in every 24 hours), samples were taken from the cultures for pH and cell density analyses. In order to prevent the negative pressure that might appear in the photobioreactor after sampling, the cultures were fed with same volume of basal medium (BP medium without carbon and nitrogen sources) (Appendix A).

3.5.2. Analyses

pH of the cultures was initially arranged to 6.3-6.4. The samples taken each day were analyzed by pH meter (WTW series InoLab pH/Cond720, Germany).

Bacterial growth of the culture was detected by measuring the optical density of the cultures at 660 nm by spectrophotometer (Shimadzu UV-1208). The medium was used as blank. Graph of dry cell weight versus OD_{660} developed by Uyar (2008, page

211) was used to transform the absorbance to the dry cell weight. The calibration curve of dry cell weight versus OD₆₆₀ is given in Appendix C.

The composition of the gas was detected by a gas chromatography having a thermal conductivity detector and equipped with a Supelco Carboxen 1010 column (Agilent Technologies 6890N, USA). The samples were taken from the top of the photobioreactors by a gas-tight syringe (Hamilton, 22 GA 500 μ L gas tight No. 1750). The carrier gas was argon with a flow rate of 26 ml/min and the temperature sets for oven, injector and detector were 140 °C, 160 °C and 170 °C, respectively. A typical sample gas chromatogram is given in Appendix D.

The samples taken from the bioreactors were centrifuged to precipitate cells. The supernatants were stored at -20 °C for organic acid analysis. The supernatants of the samples were filtered by 45 μ m nylon filters (Millipore, 13 mm) to remove impurities that might be present in the solution. Organic acid analyses were performed by High Pressure Liquid Chromatography (HPLC) (Shimadzu LC 20A-Prominence Series). The analyses were done by an Alltech IOA-1000 (300 mm x 7.8 mm) HPLC column. 10 μ l samples were injected to the system with an autosampler (Shimadzu SIL-10AD) and the detection of organic acids was determined by an UV detector (Shimadzu FCV-10AT) at 210 nm. The oven temperature was adjusted to 66°C. As the mobile phase, 0.085 M H₂SO₄ was used. Flow rate of mobile phase was adjusted to 0.4 ml/min.

The concentrations of acetic acid, lactic acid, formic acid, propionic acid and butyric acids were detected by HPLC. The calibration curves for all of the organic acids were obtained manually with the aid of different concentrated solutions of each organic acid. The concentrations of the organic acids were determined from the peak areas by calibration curves. A sample HPLC chromatogram and a sample calibration curve are given in Appendix E.

3.6. The preparation of vector constructs

3.6.1. Genomic DNA isolation

The genomic DNA of *R. capsulatus* DSM1710 was isolated by GenElute Bacterial Genomic DNA Kit (Sigma- Aldrich) with the instructions given in the user guide. According to the protocol, 1.5 ml of overnight-grown bacterial culture was centrifuged at 12,000-16,000 x g for 2 minutes. The supernatant was discarded and the pellet was resuspended in 180 µl of Lysis Solution T. 20 µl of Proteinase K Solution was added to the cell suspension, mixed and incubated at 55 °C for 30 minutes. 200 µl of Lysis Solution C was added to the mixture, vortexed and incubated at 55 °C for 10 minutes. So, cell lysis was completed. Meanwhile, column was prepared by adding 500 µl of Column Preparation Solution to the binding column and spinning at 12,000 x g for 1 minute. The flow-through was discarded. 200 µl of ethanol was added to the lysate and vortexed; a homogenous mixture was obtained. This ethanol mixture was then transferred onto the prepared binding column and spinned at 6,500 x g for 1 minute. The column was transferred into a new collection tube, 500 µl of Wash Solution 1 was added onto the column and the column was spinned at 6,500 x g for 1 minute. After spinning, the column was again transferred into a new collection tube, 500 µl of Wash Solution Concentrate was added onto the column. In order to let the column to dry, the column was centrifuged at 6,500 x g for 3 minutes. Finally, the column was transferred into a new collection tube, 200 µl of Elution Solution was placed directly onto the center of the column. After spinning down the column at 6,500 x g for 1 minute, genomic DNA was efficiently harvested in the eluate. The genomic DNA was stored at -20 °C.

3.6.2. Plasmid DNA isolation

The plasmid DNA of *E. coli* was isolated by GenElute Plasmid Miniprep Kit (Sigma- Aldrich) with the instructions given in the user guide. According to the protocol, 2-3 ml of overnight culture was centrifuged at 12,000 x g for 1 minute. The supernatant

was discarded and the pellet was completely dissolved in 200 μ l of Resuspension Solution. The cells are lysed by adding 200 μ l of Lysis Solution onto the resuspended cells and immediate mixing of the contents by several inversions. The cell debris was then precipitated by adding 350 μ l of the Neutralization/ Binding Solution. After gentle mixing, the cell debris was precipitated by spinning at 12,000 x g for 10 minutes. In order to prepare the column, 500 μ l of Column Preparation Solution was added onto the Miniprep column and centrifuged at 12,000 x g for 1 minute. The flow-through was discarded. The cleared lysate without cell debris was transferred onto the prepared column and centrifuged at 12,000 x g for 1 minute. 750 μ l of the diluted Wash Solution was added onto the column and centrifuged at 12,000 x g for 1 minute. The column was transferred into a new collection tube, 100 μ l of Elution Solution was added onto and spun at 12,000 x g for 1 minute. Plasmid DNA was obtained in the eluate and stored at -20 °C.

3.6.3. Agarose gel electrophoresis

Agarose gel electrophoresis was performed according to the procedure described in Short Protocols in Molecular Biology (Ausubel et.al., 1990). For examination of genomic DNA and plasmid DNA in agarose gel electrophoresis, 1 % (w/v) agarose gel; for PCR products and restriction enzyme digested fragments, 2 % (w/v) agarose gel was used. 1 or 2 gr of agarose was melted in 100 ml TAE Buffer (Appendix B). After cooling molten agarose to 50-60 °C, ethidium bromide (Appendix B) was added and poured onto the tray. The samples were mixed with loading dye and applied to the wells formed in the gel. Generuler 50 bp and 1kb DNA ladders and Generuler Ladder Mix (Fermentas) were used in agarose gel electrophoresis as DNA marker. The electrophoresis was applied at 90 V for one hour. DNA bands were visualized by a software UV transilluminator and photographed by Vilber Lourmat Gel Imaging System.

3.6.4. Sequence and Primer design

Since the genome of *R.capsulatus* DSM1710 is not sequenced yet, the genome sequence of another strain (SB1003) was used for sequence information. Two different 10 kilobasepairs (kb) sequences including *glnB* and *glnK* genes were obtained and all of the genes in these sequences were annotated with the help of BLAST program. The genes were annotated and cloning were simulated by using Clone Manager Software. The sequences of *glnB* and *glnK* genes are given in Appendix G.

In order to achieve exact sequences of *glnB* and *glnK* genes of DSM1710 strain, primers were designed, the PCR fragments were obtained and sequenced. This sequence information was the specific sequence of DSM1710 strain. Using these sequence information, new set of primers were designed for site directed mutagenesis (inactivation of the genes by deletion of the internal fragments) of upstream and downstream fragments of *glnB* and *glnK* genes (Table 3.4). Restriction enzyme recognition sites were incorporated to the primers. All of the primers used in this study were designed in the Clone Manager software and the complete list of primers is in Appendix G.

In the sequencing analysis of plasmids, universal primers, which have binding sites in the plasmids, were used. T3 and T7 primer set was used for sequencing of the plasmids that were obtained from pBtSK plasmid. The primers, M13 fw and M13rev, were used when the vectors originated from the pK18mobSacB plasmid were sequenced. The sequences of these primers are given in Table 3.5.

Table 3. 4 List of primers for deletion of *glnB* and *glnK* genes, together with the restriction enzyme (RE) sites present in the primers

Amplicon	Primer Name	Sequence	RE Site
<i>glnB</i> upstream	OGLNBU-F2 (forward)	CTGCAG-AACGCATCTCCTCGGTCAAG	<i>Pst</i> I
<i>glnB</i> upstream	OGLNBU-R2 (reverse)	TCTAGA- CACCTCGATCACGCTCAGCC	<i>Xba</i> I
<i>glnB</i> downstream	OGLNB3F (forward)	GGATCC-GAGGACGCGGTCTGAGACTT	<i>Bam</i> HI
<i>glnB</i> downstream	OGLNB4R (reverse)	TCGCGTGTTCAGGATACCG	
<i>glnK</i> upstream	OGLNKU-F2 (forward)	GGATCC- GAAGCCCTTGATTTCCGTCAC	<i>Bam</i> HI
<i>glnK</i> upstream	OGLNKU-R2 (reverse)	GAATTC-GCGGCAGTCGGTCTCGTAATC	<i>Eco</i> RI
<i>glnK</i> downstream	OGLNK1F (forward)	CTGCAG-CCTTGGTGACGAAGAAGTAG	<i>Pst</i> I
<i>glnK</i> downstream	OGLNK2R (reverse)	TCTAGA-GACGAAGCGCTGTAAGAACC	<i>Xba</i> I

Table 3. 5 The primers for sequencing analysis of plasmids, originating from pBtSK and pK18*mobSacB*

Plasmid	Universal Primer Name	Sequence
pBtSK	T3 (forward)	AATAACCCTCACTAAAG
	T7 (reverse)	AATACGACTCACTATAG
pK18 <i>mobSacB</i>	M13 fw (forward)	CGCCAGGGTTTTCCAGTCACGAC
	M13rev (reverse)	AGCGGATAACAATTCACACAGGA

In order to screen the potential mutants and to examine the presence of the deletion sites in *glnB* and *glnK* genes, another set of primers were designed (Table 3.6). These primers were used in colony PCR.

Table 3. 6 The primers for determination of the deletion in *glnB* and *glnK* genes

Amplification	Primer Name	Sequence
<i>glnB</i> internal part	OGNB5F (forward)	GCCGCCCAAACAGTTTACAC
	OGLNB6R (reverse)	CGCCTTCATCAGATCGAGAG
<i>glnK</i> internal part	OGLNK5F (forward)	TCAGCACGGAGAGCATGTTC
	OGLNK6R (reverse)	TTCCGCCGCGCAACTTACAC

In the present study, deletion inactivation of the genes to insertional mutagenesis was preferred, because any presence of an antibiotic cassette present in the mutant bacteria possesses a potential biosafety risk. On the other hand, there is no such a risk in the mutants containing deleted genes.

In the same operon with *glnB* and *glnK* genes, there are some other genes coming after *glnB* and *glnK*. When deletion mutation takes place in the *glnB* and *glnK* genes, the downstream genes might also be inactivated due to a frame shift mutation. In order to prevent this to occur, the primers were designed in a way to keep the amino acid reading frame as original. This ensures that the downstream genes would be kept active after deletion mutation.

3.6.5. Polymerase chain reaction (PCR) and Optimization of reaction conditions

Upstream and downstream fragments of *glnB* and *glnK* genes (~1 kb) were individually obtained by PCR with the primers designed. The PCR reactions were prepared in 50 µl volumes and reactions were performed by Thermal Cyclers (Apollo™ ATC 401 Thermal Cycler and Thermo Thermal Cycler).

In the optimization, various types of polymerases were used for different purposes. For amplification of upstream and downstream fragments of *glnB* and *glnK* genes, either Phusion High-Fidelity DNA polymerase (Finnzymes) or Pfu DNA polymerase (Fermentas) was used, since they are able to amplify the new strand with high fidelity and create blunt end DNA molecules. In the PCR reactions, which were performed in the screening of potential mutants, DyNAzyme II DNA polymerase (Finnzymes) was used.

In PCR optimization, the most critical factors are annealing temperature of the reaction, the magnesium ion concentration in the reaction mixture, the type of the polymerase enzyme and the concentration of DNA template. For determining the

most efficient annealing temperatures for amplification upstream and downstream fragments of *glnB* and *glnK*, gradient PCR was used, in which different annealing temperatures can be applied in the same PCR reaction. After several optimization experiments, the annealing temperatures were determined as following; 63 °C for *glnB* upstream, 66 °C for *glnK* upstream and 61 °C for *glnK* downstream.

Optimum magnesium ion concentrations were determined by testing different concentrations in several PCR reactions. The optimum final MgSO₄ concentrations for *glnB* upstream, *glnK* upstream and *glnK* downstream fragments were determined as follows; 2, 1 and 2 mM. The optimum final MgCl₂ concentration for *glnB* downstream was determined as 1.5 mM.

After evaluation of Pfu or Phusion for amplification of fragments, it was determined that the *glnB* upstream, *glnK* upstream and *glnK* downstream fragments were optimally amplified by Pfu DNA, whereas Phusion DNA polymerase was used for the amplification of *glnB* downstream fragment.

After optimization of DNA template concentration, 10 times diluted genomic DNA was used as template in some of these PCR reactions.

The reaction components and cycle conditions for amplification of *glnB* upstream, *glnK* upstream and *glnK* downstream fragments are given in Table 3.7 and Table 3.8. The reaction components and cycle conditions for the amplification of *glnB* downstream fragment is given in Table 3.9 and Table 3.10.

After optimization experiments, high yields of PCR products was obtained. So, these PCR fragments were efficiently isolated from agarose gels and used in downstream cloning procedures.

Table 3. 7 Components of the PCR reaction for *glnB* upstream, *glnK* upstream and *glnK* downstream fragments

Component	Concentration	Volume (μl)
Nuclease free water		36.5
Pfu Buffer	10 x	5
dNTP	(2 mM)	5
Primer 1	(10 μ M)	1.0
Primer 2	(10 μ M)	1.0
Genomic DNA as template	10 x diluted	1
Pfu enzyme	(2.5 U/ μ l)	0.5
TOTAL VOLUME		50

Table 3. 8 The cycle conditions of the PCR reaction for *glnB* upstream fragment, *glnK* upstream and *glnK* downstream fragments

Cycle Step	Temperature ($^{\circ}$C)	Time (min)	Number of Cycles
Initial denaturation	95	3	1
Denaturation	95	1	30
Annealing	61-66	1	
Extension	73	3	
Final extension	72	5	1

Table 3. 9 Components of the PCR reaction for *glnB* downstream fragment

Component	Concentration	Volume (μl)
Nuclease free water		28.5
Phusion HF Buffer	5 x	10
dNTP	(2 mM)	5
Primer 1	(10 μ M)	2.5
Primer 2	(10 μ M)	2.5
Genomic DNA as template		1
Phusion enzyme	(2 U/ μ l)	0.5
TOTAL VOLUME		50

Table 3. 10 The cycle conditions of the PCR reaction for *glnB* downstream fragment

Cycle Step	Temperature ($^{\circ}$C)	Time	Number of Cycles
Initial denaturation	98	30 sec	1
Denaturation	98	7 sec	30
Annealing	61	30 sec	
Extension	72	30 sec	
Final extension	72	5 min	1

3.6.6. Colony PCR

This PCR type was applied in the screening of the deletion sites in the potential mutants. In this type of PCR, 25-30 μ l of sterile nuclease free water was put into an eppendorf tube. A toothpick was touched to the colony, which was being investigated to be a successful mutant, and dissolved in the water. This cell suspension was incubated at 95 °C for 10 minutes in order to lyse the cells. During the incubation, the suspension was vortexed to achieve complete lysis of the cells. After cooling, the cell lysate was used as DNA template in the PCR reaction. The primers used in colony PCR are listed in Table 3.5. DyNAzyme DNA polymerase was used for colony PCR. The components and the cycle conditions of the colony PCR reaction for the screening are given in Table 3.11 and 3.12. These PCR reactions are used to amplify the internal parts of the genes. The optimum annealing temperature of the colony PCR for the screening of *glnB* mutants and *glnK* mutants were determined as 55 °C and 57 °C. The final MgCl₂ concentration was 1.5 mM.

Table 3. 11 The components of the PCR reaction for the screening of the potential mutants

Component	Concentration	Volume (μ l)
Nuclease free water		15.5
DyNAzyme Buffer	10 x	3
dNTP	(2 mM)	3
Primer 1	(10 μ M)	3
Primer 2	(10 μ M)	3
Cell lysate as template		2
DyNAzyme enzyme	(2 U/ μ l)	0.5
TOTAL VOLUME		30

Table 3. 12 The cycle conditions of the PCR reaction for the screening of the potential mutants

Cycle Step	Temperature (°C)	Time	Number of Cycles
Initial denaturation	98	30 sec	1
Denaturation	95	1 min	30
Annealing	55-57	1 min	
Extension	72	1 min	
Final extension	72	5 min	1

3.6.7. Sequence analysis

Sequencing of the DNA molecules were performed for the amplified PCR products, plasmids ligated with these PCR products and genomic DNA of the potential mutants. For sequencing the PCR products, the corresponding gel band was extracted from the agarose gel and sent to sequencing. For the sequencing of plasmids and genomic DNA's, isolation kits were applied and isolated sample were sent to sequencing. The concentrations of samples were detected by NanoDrop. For sequencing, either the specific primers, which had been used in amplification, or some general primers of the plasmids were used (Table 2.5). The sequencing analyzes were done by MACROGEN company in Korea and RefGen company in METUTECH.

3.6.8. Restriction enzyme digestion

For restriction enzyme digestion, fast digest restriction enzymes from Fermentas Company was preferred. The volume for restriction enzyme digestion reaction was 20 µl. In an eppendorf tube, 15 µl of nuclease free water was added. Onto the water, 2-5 µl of plasmid was included, whose concentration had been decided to be

satisfactory from its agarose gel electrophoresis result. Then, 2 μ l of 10 x Fast Digest Buffer and finally, 1 μ l of Fast Digest Restriction Enzyme were added. If double digestion was done, second enzyme was also included to the reaction mixture with the same amount. Excess glycerol, which comes from the enzyme solution, increases star activity and causes nonspecific digestion of DNA. So, the volume of total enzyme present in the digestion mixture was kept minimum. The digestion reaction was completed with 5 minutes incubation at 37 °C. The enzymes were thermally inactivated at either 65 °C or 80 °C, depending on the property of the enzymes. In order to check the efficiency of the digestion, 2 μ l of the digested reaction mixture was ran on the agarose gel. All of the restriction enzymes used in this study are listed in Appendix H.

3.6.9. Extraction of DNA from agarose gel

In some cases, DNA molecules were extracted from the gel, in order to acquire PCR products for further cloning steps and/ or to acquire digested DNA fragments/ plasmids. For this purpose, Silica Bead DNA Gel Extraction Kit (Fermentas) was used. According to the protocol, DNA gel slide containing the interested DNA fragment were excised with a razor blade and placed into an eppendorf. The weight of the gel slide was recorded. During this time, UV damage was avoided as keeping the UV exposure minimal. Onto the gel slide, 3:1 volume of Binding Buffer to the gel slice (v/w) was added and incubated at 55 °C until the gel slice was completely dissolved in the buffer. Resuspended Silica Powder Suspension was added onto the melted agar solution (approximately, 5-6 μ l), then binding of DNA to silica matrix was allowed at 55 °C for 5 minutes. The mixture was spinned for 5 seconds to form a pellet. The supernatant was discarded and the pellet was resuspended in 500 μ l of Washing Buffer. This washing step was repeated 3 times. After the last washing step, the pellet was air-dried at room temperature for 10 minutes. The dried pellet was dissolved in 15 μ l water and the suspension was incubated at 55 °C for 5 minutes. Finally, in order to remove residual silica powder, the suspension was centrifuged with maximum speed and the supernatant was carefully transferred into a new

ependorff. Then, it was run in agarose gel electrophoresis to examine the purity and the concentration of the extracted DNA fragment.

3.6.10. Dephosphorylation of linearized plasmids

The digested plasmids were dephosphorylated by Calf Intestinal Alkaline Phosphatase (CIAP) (Fermentas), in order to prevent self ligation of the plasmids in the ligation reaction. Preventing self-ligation is important both in improving the yield of properly ligated product and in reducing the background of improperly self-ligated contaminant. For the reaction, onto the restriction enzyme mixture of the plasmid digestion (~ 20 μ l), which had been thermally inactivated, 1 μ l of CIAP (1 u/ μ l) was added. Then, the mixture was incubated at 37°C for 10 minutes. The dephosphorylation reaction was stopped by thermal inactivation at 85 °C for 10 minutes. The buffers for restriction enzyme digestion are suitable for CIAP enzyme, so there was no need to purify the DNA from restriction enzyme digestion mixture and run the dephosphorylation reaction in CIAP buffer. Direct addition of CIAP was enough.

3.6.11. Phosphorylation of PCR products

For efficient ligation of the vector and the insert in the ligation reaction, the ‘insert’ molecules should have phosphate group at the 5’ ends. Thus, addition of phosphate groups to the ends of the PCR products was required. So, the extracted PCR products were treated with T4 Polynucleotide Kinase Enzyme (PNK) (Fermentas).

The PCR products were generally extracted from the agarose gel before added into the ligation reaction mixture. After gel extraction, the PCR product was harvested in a volume of 10-12 μ l. Onto this, 2 μ l of buffer type, (suitable both for PNK and T4 Ligase), 5 μ l of ATP (10 mM) and 1 μ l of PNK (10 u/ μ l) were added and the total volume of the reaction mixture was completed to 20 μ l. Then, the mixture was incubated at 37 °C for 30 minutes. The reaction was stopped by heat inactivation at 70 °C for 10 minutes.

3.6.12. Polishing the stick ends of the linear plasmids

After the most restriction enzyme digestion reactions, the vector was linearized with the stick ends. In the cases, where the blunt and ligation was planned to be performed, there was need to transform sticky ends of the linear vector into blunt ends. For this purpose, Klenow Fragment, which is the large subunit of the fragment of DNA Polymerase I, was used. It is able to blunt DNA molecules by filling the 5' overhangs with 5'=>3' polymerization activity or by removing the 3' overhangs with 3'=>5' exonuclease activity. For polishing, the digested plasmid mixture (~ 10 µl) was combined with; 1 µl of a reaction buffer, which is suitable for Klenow treatment, 1 µl of dNTP (2 mM), 1 µl of Klenow Fragment (10 u/µl) and the reaction mixture was completed to 20 µl. Then, the mixture was incubated at 37 °C for 10 minutes. The reaction was stopped by heat inactivation at 70 °C for 10 minutes.

3.6.13. Sticky or blunt end ligation

For the blunt end ligation of the amplified PCR fragments to linear pBtSK (cloning vector) and for the sticky end ligation of the fragments excised from the plasmids to the suicide plasmid; T4 DNA Ligase was used, which originates from the T4 bacteriophage. The T4 DNA Ligase is suitable both for sticky and blunt end ligation. The ligation reaction mixture contained 2 µl of 10X T4 DNA Ligase Buffer, 10 µl of kinase treated insert, 5 µl of linear vector and 0.8 µl of T4 DNA Ligase (5 u/µl); the reaction volume was completed to 20 µl with nuclease-free water. The amount of insert was preferred to be more than the vector for high efficiency. The concentration of the insert and the vector was predicted from the agarose gel electrophoresis results, by comparing the brightness of the bands with the brightness of the DNA marker band.

The T4 DNA Ligase is most active in 25 °C. For successful sticky end ligation reactions, there has to be a balance between the melting temperature of the DNA fragments and the reaction temperature. If the reaction temperature is high enough to disrupts hydrogen bonding in the sticky ends, the ligation efficiency decreases. For

blunt end ligation, the reaction mixture was incubated at 18 °C for overnight or at room temperature for two hours. For sticky end ligation, the reaction mixture was incubated at room temperature for one hour. The small aliquot of the ligation mixture was transformed to competent *E.coli*.

3.6.14. Preparation of constructs for inactivation *glnB* and *glnK*

After the amplification of the upstream and downstream of *glnB* and *glnK* genes by PCR, the fragments were individually cloned into pBtSK (+), giving raises to pGBBU, pGBBD, pGKBU and pGKBD plasmids. Then, downstream fragments of *glnB* and *glnK* were excised from the relevant plasmids (pGBBD and pGKBD) and cloned into the suicide vector (pK18*mobsacB*), yielding the pGBSD and pGKSUD plasmids. By ligating these plasmids with upstream fragments of *glnB* and *glnK*, which were excised from pGBBU and pGKBU; the final constructs for inactivation of *glnB* and *glnK* were obtained: pGBSUD and pGKSUD. The clones were checked by colony PCR. The plasmids were analyzed by restriction enzyme digestion and sequence analysis.

3.6.15. Preparation of competent cells

The competent cell aliquots of *E.coli* XL1Blue and S17-1 were prepared to be used in transformation of the ligation mixtures. According to the procedure, the optimal OD value for competent cell preparation is 0.4 and 0.6. For this purpose, a stock culture was used to streak an LB agar plate which contains necessary antibiotic. After overnight incubation, a few grown colonies were inoculated into 500 µl of Super optimal medium (SOB) and the culture was incubated at 20-22 °C for 1 day. From this culture, differently diluted inoculations (1, 10 and 100 %) were performed and the OD₆₆₀ values were monitored. The culture, whose OD value was between 0.4 and 0.6, were selected to be used in preparation of competent cells. According to the procedure, the culture was divided into two and centrifuged at 4 °C at 7000 rpm for 10 minutes. The supernatants were discarded and each pellet was dissolved in 8 ml of TB buffer. The cell solution was incubated in ice for 10 minutes and then,

centrifuged at 6,000-7,000 rpm for 10 minutes, the supernatants were discarded. Again, each pellet was dissolved in 2 ml of TB buffer and 150 μ l DMSO and incubated in ice for 10 minutes. 100 μ l aliquots were prepared in cold-sterile eppendorf tubes, dipped into liquid nitrogen and stored at -80 °C. 3-4 days after the preparation of the competent cells, the transformation efficiency were checked by transforming 1 μ l of pBtSK plasmid (1 ng/ μ l); a good competent cell gives 10^8 colonies/ μ l of plasmid.

3.6.16. Transformation of *E.coli*

For transformation, an eppendorf of competent cell (100 μ l) was taken from -80 °C and waited in ice for 15 minutes. DNA to be transformed (most of the time, 10 μ l of ligation reaction mixture) was added onto competent cells and mixed gently. The transformation mixture was incubated in ice for 30 minutes. The heat shock was applied by incubating the cells at 42 °C for 90 seconds. SOC medium was immediately added and the transformed cells were allowed to recover by incubating them at 37 °C for 1 hour with 500 rpm shaking. After incubation, 200 μ l of the cell suspension was spreaded onto LB agar plate containing necessary antibiotic; ampicillin (100 μ g/ml) for pBtSK or kanamycin (25 μ g/ml) for pK18*mobSacB*. If the colonies were selected on the basis of Blue-white screening, the cells were spreaded onto LB agar plates that also contain IPTG (25 μ g/ml) and X-GAL (25 μ g/ml). The rest of the cell suspension was pelleted with low speed centrifugation (4,000-5,000 rpm) for one minute, 600 μ l of the supernatant was discarded. The resulting pellet was suspended in the remaining supernatant (200 μ l) and spreaded onto LB agar plate. Spreaded plates were incubated at 37 °C for overnight.

3.6.17. Blue-White Screening

In the cloning of PCR products to pBtSK cloning plasmid, Blue-White screening was performed. In the cloning of PCR products to the pBtSK cloning vector, the successful clones, containing the insert, was easily differentiated from the self-

ligated plasmids, containing no insert. The LB agar plates, which contained X-GAL (25 µg/ml), were inoculated after transformation. If the ligation was successful, the bacterial colonies were observed 'white'; if not, they were observed 'blue'.

pBtSK encodes α subunit of LacZ protein, having the 'Multiple Cloning Site (MCS)', and the host *E.coli* XL1Blue strain encodes the Ω subunit. β -galactosidase enzyme is functional in the presence of both α and Ω subunits. X-GAL is a colourless modified galactose sugar and can be hydrolyzed by β -galactosidase enzyme; resulting in blue colored colonies. IPTG induces the Lac operon. In the case of successful ligation of the insert to the linear pBtSK, which is cleaved at MCS; α subunit of β -galactosidase is disrupted. This leads β -galactosidase enzyme to be nonfunctional, so that X-GAL cannot be metabolized to a colorful compound and the colony appears in white. If the ligation is unsuccessful or the pBtSK is self-ligated, the β -galactosidase enzyme is functional, since α subunit is not disrupted. The colony is observed in blue color.

After transformation, both blue and white colonies were observed on the surface of agar. A number of white colonies were selected. Then, the presence and the direction of insert were confirmed by colony PCR and sequence analysis.

3.7. Construction of suicide vectors

For inactivation of *glnB* and *glnK* gene in *R.capsulatus*, the internal parts of these genes were deleted by homologous recombination taking place between the gene to be inactivated and the deleted gene in the designed suicide vector.

Initially, the upstream and downstream fragments of *glnB* and *glnK* were individually amplified by PCR. These fragments were individually cloned into the cloning vector (pBluescript) to be further used in downstream cloning protocols. The resulting plasmid vectors were named as pGBBU, pGBBD, pGKBU and pGKBD.

In order to obtain the suicide vector containing deleted *glnB* gene, the downstream fragment was excised from pGBBD and ligated into the suicide vector (pK18*mobSacB*) and resulting plasmid was named as pGBSD. Then, the upstream fragment was excised from pGBBU and ligated into pGBSD next to the downstream fragment. Hence, the suicide vector, which contains internally deleted *glnB* gene, was obtained.

Similar to *glnB*, the downstream fragment of *glnK* was excised from pGKBD and ligated into the suicide vector, resulting in the vector named as pGKSD. Then, the upstream fragment was excised from pGKBU and ligated into pGKSD next to the downstream fragment. So, suicide vector, containing internally deleted *glnK* gene, was obtained.

3.8. Gene transfer into *R.capsulatus* by Conjugation and Selection

In order to deliver the constructs into *R.capsulatus*, the constructs were first transformed into *E.coli* S17-1(λ pir). This *E.coli* strain is able to conjugate with *R.capsulatus* cells, since it provides *tra* genes, which are needed for transfer. *mob* gene, which is also required for transfer of the construct, were supplied by the construct itself (pK18*mobSacB* plasmid contains *mob* region). Through conjugation between donor cells (*E.coli* S17-1) and recipient cells (*R.capsulatus* DSM1710), constructs were transferred into *R.capsulatus* cells. According to the procedure (Donohue and Kaplan, 1991), both *E.coli* and *R.capsulatus* were activated from -80 °C stocks. After activation and reinoculation of the cultures, their growth densities were monitored by OD₆₆₀ values and they were obtained in the log phase of their growth curves; OD₆₆₀ is between 0.4-0.6 for *E.coli* and is 0.5-0.7 for *R.capsulatus*. To remove antibiotic and to harvest cells, 4 ml of *E.coli* culture was centrifuged at 5,000 rpm for 5 minutes (All centrifugation steps were performed at 4°C). The pellet was dissolved in 4 ml LB and combined with 40 ml *R.capsulatus* culture (1:10 ratio). The *E.coli* and *R.capsulatus* mixture was centrifuged at 10,000 x g for 10 minutes, the supernatant was discarded and the pellet was dissolved in 200-300 μ l of BP. The concentrated cell mixture was spotted onto LB agar plate and incubated at 30-32 °C

for 6 hours. After incubation, the cells were collected from the surface of the agar by a sterilized spatula and dissolved in 1 ml of BP medium. From this cell mixture, 200-300 μ l of aliquots were spread onto BP agar plates containing Km²⁵. *E.coli* cells were easily eliminated, since *E.coli* S17-1 strain is proline auxotroph and cannot grow in BP minimal medium. Moreover, non-conjugated *R.capsulatus* cells were eliminated, since they are not resistant to kanamycin and could not grow in the presence of kanamycin. The successfully conjugated *R.capsulatus* cells, which received the plasmids from *E.coli* cells, were able to form colonies in BP agar. The colonies formed on the agar after 3-4 days of incubation (Donohue and Kaplan, 1991). The conjugation is schematically represented in Figure 3.4.

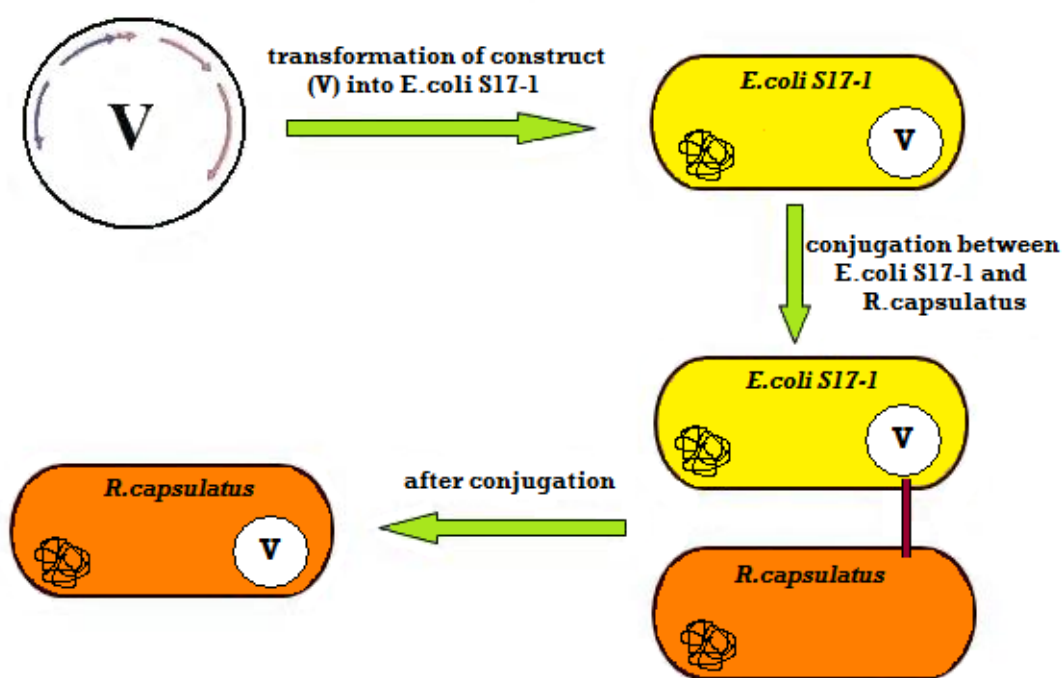


Figure 3. 4 Schematic representation of conjugation between *E.coli* S17-1 and *R.capsulatus* cells

Once the construct was delivered into *R.capsulatus* cell, targeted genes were deleted by means of homologous recombination between the construct, containing deleted gene with homologous arms, and the genomic DNA of the cell (Figure 3.5). In the cells, there happens recombination event between the homologous arms of the plasmid and genomic DNA. With this recombination, entire plasmid was inserted into the genomic DNA. These single recombinants were selected based on kanamycin resistance, since the plasmid contained kanamycin resistance gene. These colonies, which formed on kanamycin containing plates, were selected and passaged in non-selective liquid BP medium for 4-5 times, in order to allow cells to undergo the second recombination. With the second recombination, the inserted plasmid was excised from the DNA and the deleted gene of the plasmid was exchanged with the active gene of the genomic DNA. The double recombinants were selected by the selection mechanism of pK18*mobsacB* suicide vector, in which there is a *sacB* gene whose gene product converts sucrose to a toxic compound. Spreading the passaged cells onto sucrose containing BP plates eliminated single recombinants, since they could not survive in the presence of sucrose due to the presence of *sacB* gene in their genomic DNA. Thus, only the double recombinants could form colonies on sucrose containing plates, which were either wild type or the expected mutant strain. The mutant strains were further selected and confirmed by the length of the PCR product of the interested gene and the sequence results of these PCR products.

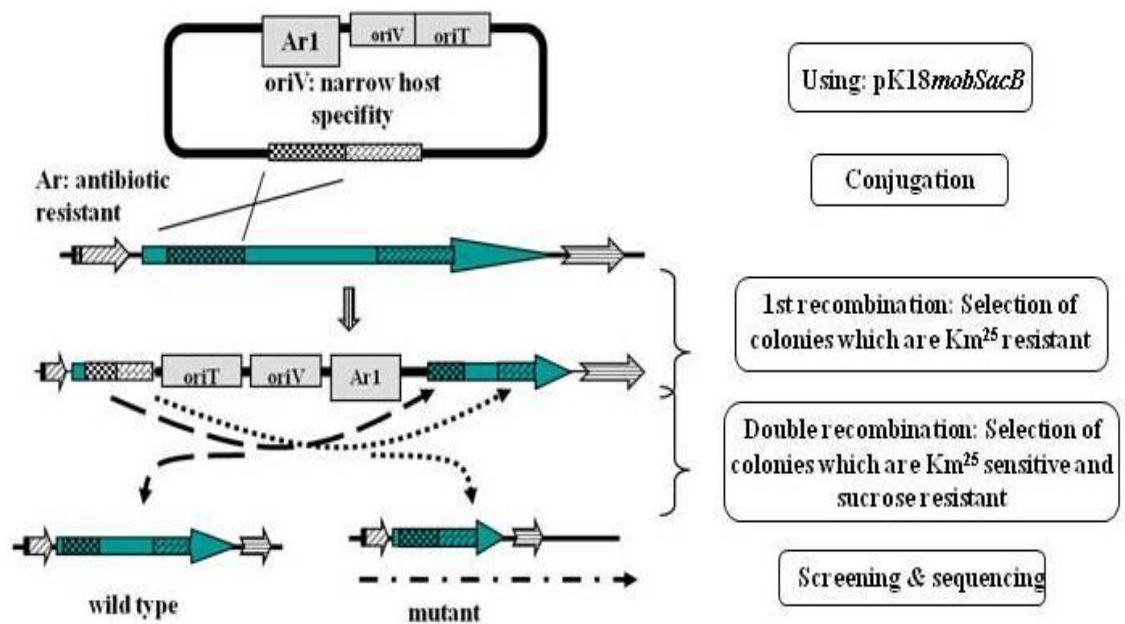


Figure 3. 5 The mechanism of the suicide vector (pK18mobSacB)

As the result, either the wild type containing the active gene or the mutant type containing deleted gene was obtained with the percentage of 45 % to 55 %, respectively. After the exchange of the genes by a two step homologous recombination, the targeted genes (*glnB* and *glnK*) were inactivated.

CHAPTER 4

RESULTS AND DISCUSSION

4.1. Mutagenesis studies of *glnB* gene

In this chapter, the results for the final suicide plasmid construct preparations, the delivery of the plasmids into *R.capsulatus* cells and selection of the mutant were given. Moreover, a *glnB* mutant was successfully selected and its H₂ production profile was examined with respect to the wild type strain.

4.1.1. Construction of the suicide vector for deletion inactivation of *glnB*

For inactivation of *glnB* gene in *R.capsulatus*, the internal part of the gene was deleted by homologous recombination taking place between the gene to be inactivated and the deleted gene in the designed suicide vector.

The genome sequencing project of the *R.capsulatus* DSM1710 is not completed yet, so the sequence information of *R.capsulatus* was obtained from the completed genome sequence of *R.capsulatus* SB1003. However, the exact sequence of DSM1710 has to be known before primer design and the primers have to be designed based on exact sequence of this strain. If there is any difference between the primer sequence and corresponding DSM1710 sequence, this difference in the primers leads the entire amplified DNA fragments to contain a false nucleotide. So that, before designing primers for the amplification of upstream and downstream fragments, two sets of primers was designed to sequence *glnB* and *glnK* genes. The two genes to be deleted (*glnB* and *glnK*) were amplified with PCR and the exact sequences of these genes of *R.capsulatus* DSM1710 were obtained by sequence analyses of the PCR

amplicons. The primers for amplification of upstream and downstream fragments were then designed based on the exact sequence information.

As the start of the deletion strategy, genomic DNA of *R.capsulatus* DSM1710 was isolated from the fresh culture (Figure 4.1A) and used as DNA template in Polymerase Chain Reaction (PCR) in order to amplify both upstream and downstream fragments of *glnB* gene, but not the internal deletion part (226 bps). The agarose gel electrophoresis results of amplifications of *glnB* upstream and downstream is given in Figure 4.1B-C. The locations of the *glnB* upstream and downstream fragments together with the deletion site are shown in Figure 4.2.

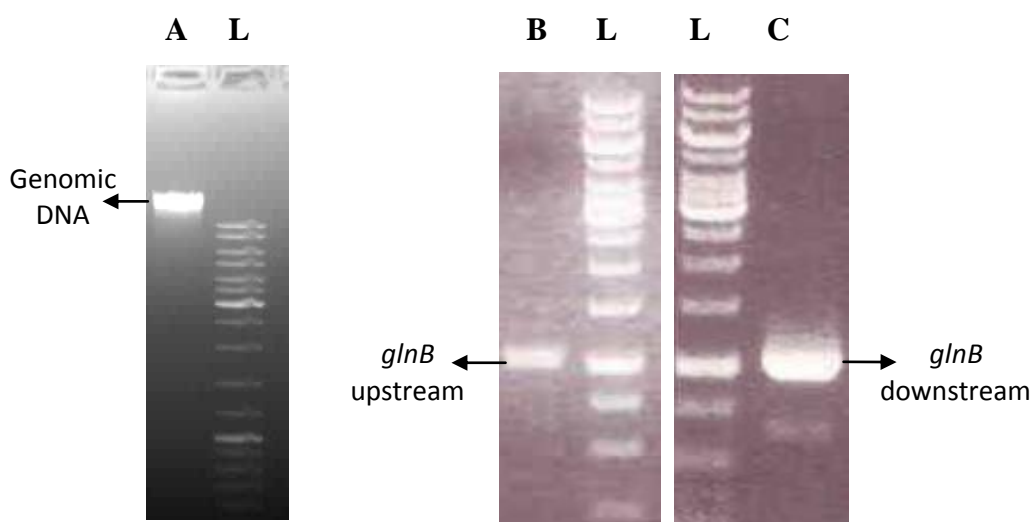


Figure 4. 1 Genomic DNA of *R.capsulatus* (A), agarose gel electrophoresis results of the amplification of *glnB* upstream fragment (~1kb) (B) and *glnB* downstream fragment (~1kb) (C). DNA marker is 1 kb DNA ladder (L).

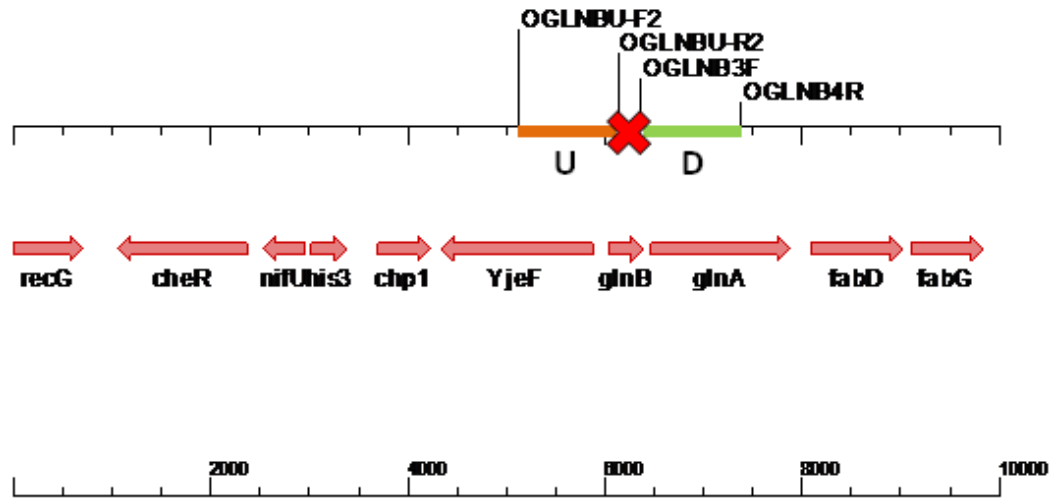


Figure 4. 2 10 kb fragment from *R.capsulatus* The upstream (U) and downstream (D) fragments of *glnB* and the deletion region (X) are indicated.

The components and the cycling conditions of the PCR reaction for amplification of *glnB* upstream and downstream fragments were given in Section 3.6.5. After extracted from the gel, ~1 kb *glnB* upstream fragment was ligated to *HincII* cut dephosphorylated pBtSK and transformed into *E.coli* XL1Blue. The insertion was confirmed by amplification of insert with colony PCR by T3/T7 universal primers (Figure 4.3B) and restriction enzyme digestion. The resulting plasmid was pGBBU (Figure 4.3A)

Similarly, *glnB* downstream fragment was extracted from the gel and used in the ligation with *HincII* cut dephosphorylated pBtSK and transformed into *E.coli* XL1Blue. The resulting plasmid was pGBBD (Figure 4.4A). The insertion was confirmed by colony PCR with T3/T7 universal primers (Figure 4.4B) and restriction enzyme digestion.

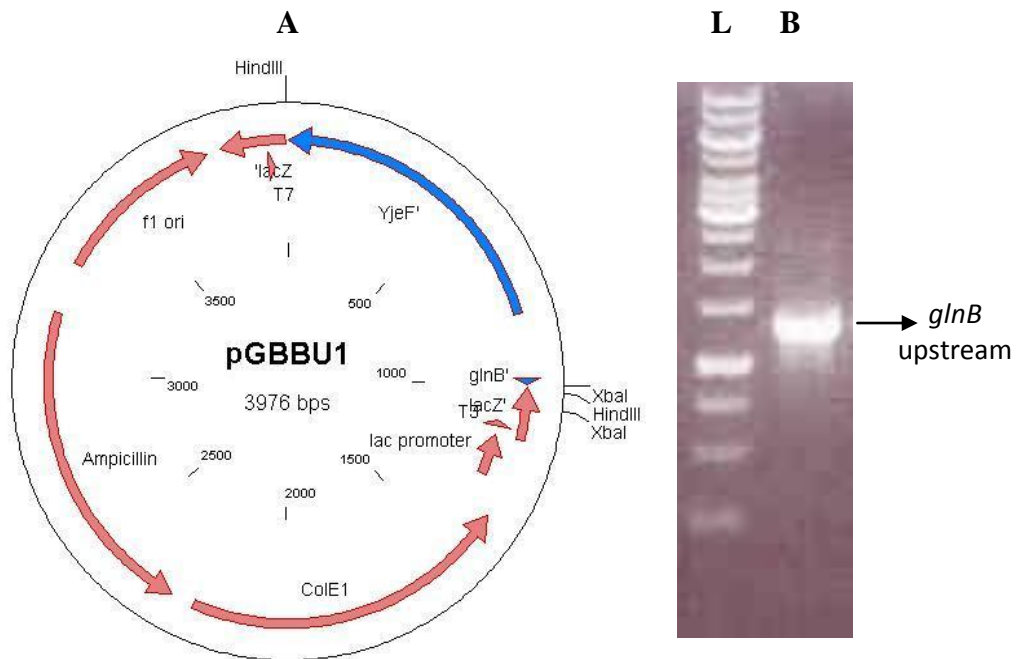


Figure 4. 3 The plasmid containing *glnB* upstream insert (pGBBU1) (A) and agarose gel result of colony PCR for the amplification of the insert (B). DNA marker is 1 kb DNA ladder (L).

For constructing pGBSD, which is the suicide vector (pK18*mobsacB*) containing only the downstream *glnB*, pGBBD was digested with *KpnI*, polished and digested with *BamHI*. So, *glnB* downstream fragment was obtained by insert with one sticky and one blunt end. Suicide vector, pK18*mobsacB*, was first digested with *EcoRI*, then polished and then digested with *BamHI*. The vector and the insert were ligated, giving pGBSD plasmid (Figure 4.5A). In Figure 4.5, the agarose gel electrophoresis results of linearized pK18*mobsacB* (5700 bps) (B) and linearized pGBSD (6700 bps) (C), obtained by single restriction enzyme digestion, are given.

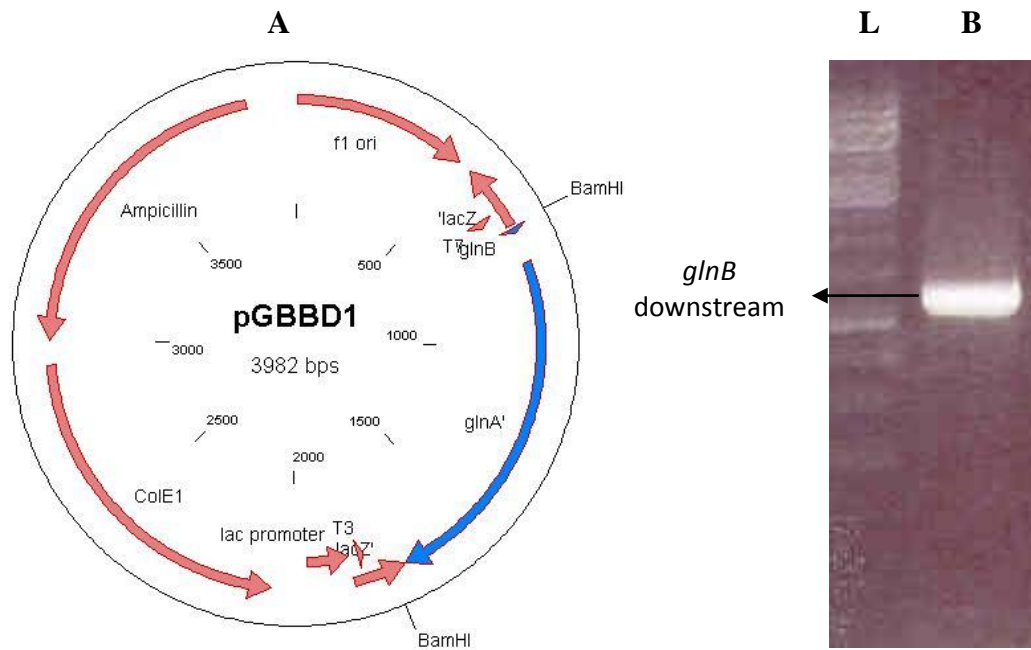


Figure 4. 4 The plasmid containing *glnB* downstream insert (pGBBD1) (A) and agarose gel result of colony PCR for the amplification of the insert (B). DNA marker is 1 kb DNA ladder (L).

The final vector to be delivered to *R.capsulatus* was pGBSUD, which contains *glnB* upstream and downstream fragments side by side. As the final step for construction of the pGBSUD, *glnB* upstream fragment was excised from the pGBBU by *PstI-XbaI* digestion and ligated into *PstI-XbaI* digested pGBSD plasmid. pGBSUD (7700 bps), containing total 2 kb insert of *glnB* upstream and downstream was obtained (Figure 4.6A). Agarose gel electrophoresis results of single digested and double digested pGBSUD are shown in Figure 4.6B-C.

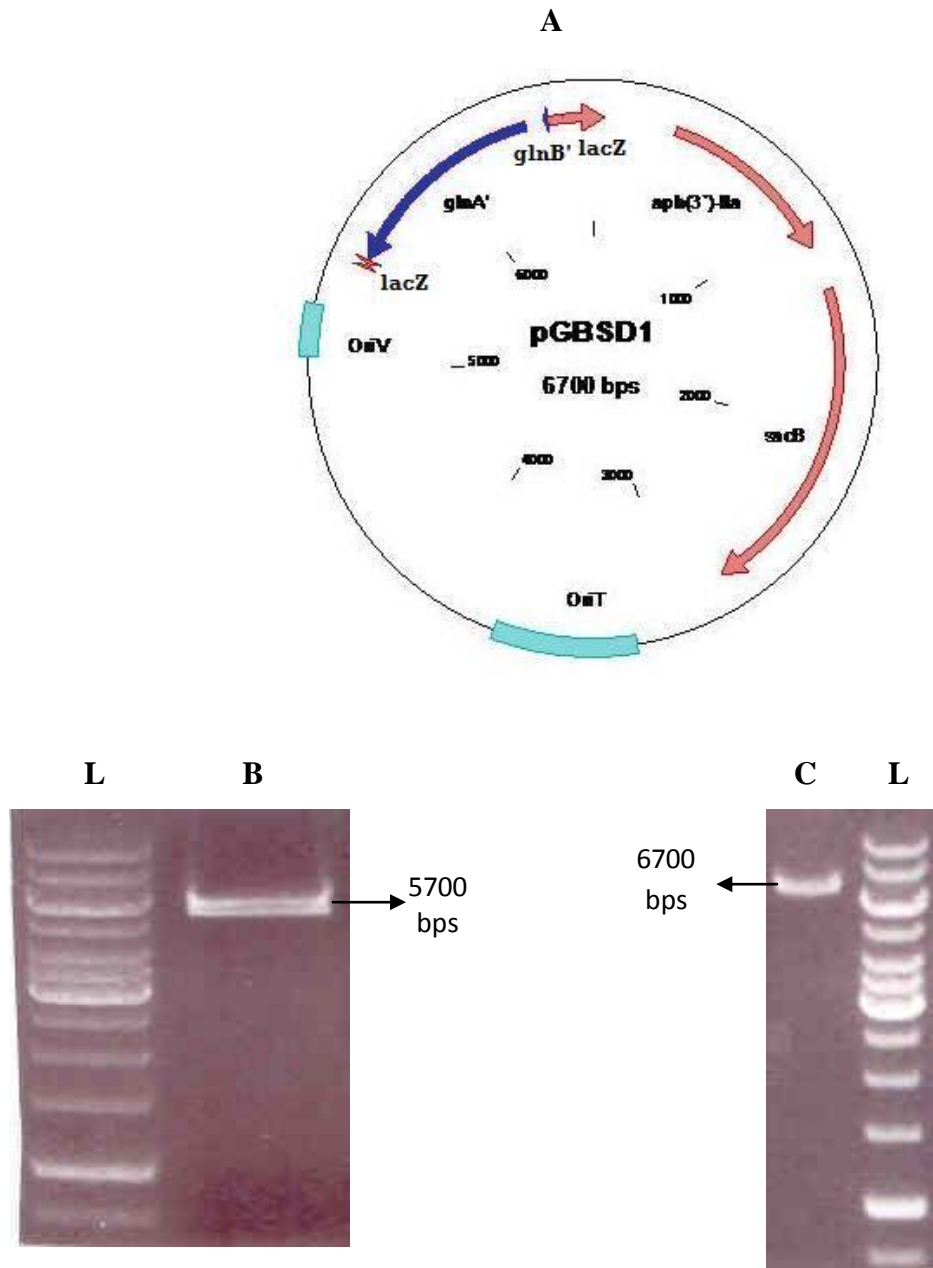


Figure 4. 5 The suicide plasmid (pK18*mobsacB*) containing ~1kb *glnB* downstream insert (pGBSD1) (A). Agarose gel results of linearized pK18*mobsacB* (~5700 bps) (B) and linearized pGBSD (~6700 bps) (C). DNA marker is 1 kb DNA ladder (L).

4.1.2. Delivery of the suicide vector for *glnB* deletion (pGBSUD) to *R.capsulatus* and selection/ screening of the double recombinants

After the final suicide vector containing the deleted *glnB* gene (pGBSUD) was obtained, it was delivered to *E.coli* S17-1 cells by transformation in order to be used in conjugation experiment. In the conjugation experiment, the cell mixture of *E.coli* and *R.capsulatus* was incubated for 6 hours on LB agar plate at a temperature suitable for the growth of both bacteria (31 °C). Then, the cell mixture was collected from the agar surface and suspended in 1 ml of BP medium. From this cell suspension; aliquots with different dilutions were spreaded onto BP agar plates containing 25 µg/ml kanamycin (Km²⁵). *E.coli* S17-1 strain is proline auxotroph and cannot grow in BP minimal medium, so they were easily eliminated. Non-conjugated *R.capsulatus* cells are not resistant to kanamycin and could not grow in the presence of kanamycin, which ensured all the appearing colonies to be conjugated ones. Only the successfully conjugated *R.capsulatus* cells, which received the plasmids from *E.coli* cells, were able to form colonies in BP agar. After 3-4 days of incubation, single recombinant colonies formed on the agar (Figure 4.7).

The single recombinants were selected from the agar surface and inoculated in BP liquid medium and passaged for a few times under no selective pressure. During passaging, the single recombinants undergo second recombination. After passaging, different dilutions (10⁻¹, 10⁻², 10⁻³, and 10⁻⁴) of the final passaged culture were spreaded onto 10 % (w/v) sucrose containing BP agar plates. Sucrose and the selection mechanism of pK18*mobsacB* suicide vector provide a negative selection mechanism for the differentiation of double recombinants from single recombinants. In the suicide vector, *sacB* gene, whose gene product converts sucrose to a toxic compound, is present. Spreading the passaged cells onto sucrose containing BP plates eliminated single recombinants, since they could not survive in the presence of sucrose due to the presence of *sacB* gene in their genomic DNA. Thus, only the double recombinants could form colonies on sucrose containing plates, which were either wild type or the expected mutant strain.

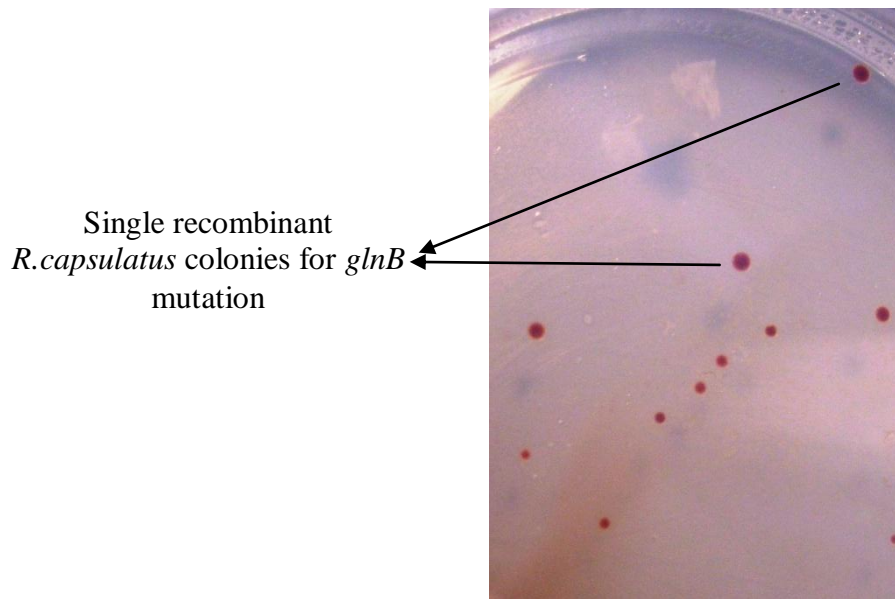


Figure 4. 7 Single recombinant colonies of *R. capsulatus* on BP agar containing kanamycin

Single colonies appeared on the sucrose agar surface were selected and replica plated onto Km²⁵ BP plates. Kanamycin enables further differentiation of single recombinants from double recombinants, since the single recombinants' genomic DNA contain entire plasmid together with kanamycin resistance gene and are able to grow in the presence of kanamycin. Kanamycin sensitive wild type *R. capsulatus* colonies were also inoculated onto kanamycin plates as 'control' of the plates. So, the probable false results, which might have occurred because of inactivation of the kanamycin in the plate, were avoided. The colonies, which were able to grow in the sucrose containing plates but not in kanamycin containing plates, were selected and regarded as 'potential candidates' for *glnB* mutants.

4.1.3. Confirmation of *glnB* mutation by genetic methods

Several potential double recombinant colonies were selected to further analyze. The selected potential candidates may contain either the wild type *glnB* gene or the

deleted *glnB* gene. So, further confirmations were required in order to differentiate the wild type and mutant (*glnB*⁻). By colony PCR method, many of these colonies had been understood to contain wild type *glnB* gene, however one selected colony contained deleted *glnB* gene. The deletion mutation in *glnB* gene was confirmed by observation of the short amplicon (400 bps) obtained from colony PCR (Figure 4.8B), as 626 bps long amplicon was routinely obtained from wild type cells of the same PCR reaction (Figure 4.8A). The final confirmation step was the sequencing the genomic DNA of the mutant candidate. Sequencing of the 400 bps PCR amplicon also confirmed the expected deletion in *glnB* gene. The sequencing result is given in Appendix F.

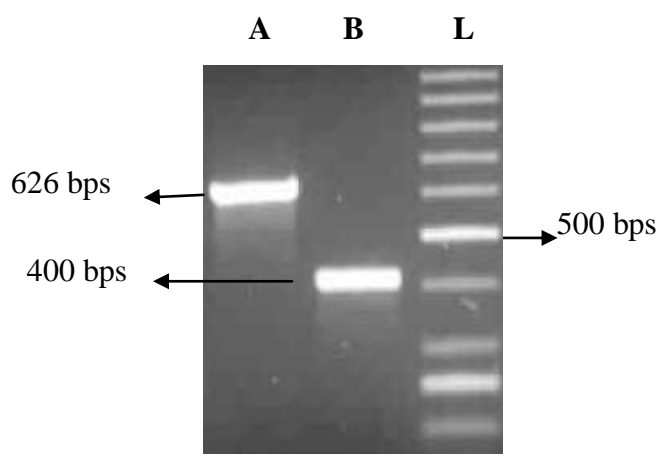


Figure 4. 8 Agarose gel results of the colony PCR of wild type *R.capsulatus* (A), *glnB* mutant *R.capsulatus* (B). The DNA marker is 50 bp DNA ladder (L).

4.2. Mutagenesis studies for *glnK* gene

4.2.1. Construction of the suicide vector for deletion inactivation of *glnK*

For inactivation of *glnK* gene in *R.capsulatus*, the internal part of the gene was deleted again by homologous recombination taking place between the gene to be inactivated and the deleted gene in the designed suicide vector. The construction of the vector for inactivation of *glnK* was very similar with *glnB*. First, genomic DNA of *R.capsulatus* DSM1710 was again used (Figure 4.1A) as DNA template in PCR reaction in order to amplify both upstream and downstream fragments of *glnK* gene, but not the internal deletion part (215 bps). The agarose gel electrophoresis results of amplifications of *glnK* upstream and downstream are given in Figure 4.9A-B. The locations of the *glnK* upstream and downstream fragments together with the deletion site are shown in Figure 4.10.

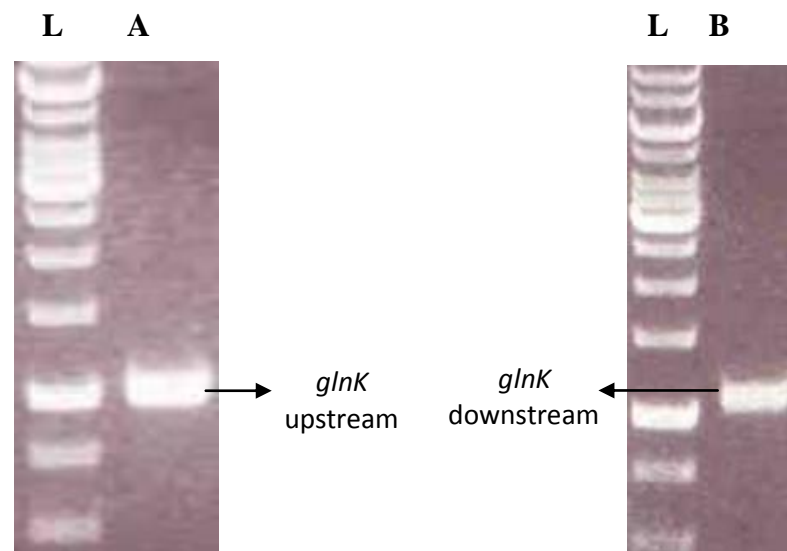


Figure 4. 9 Agarose gel results of the amplification of *glnK* upstream fragment (~1kb) (A) and *glnK* downstream fragment (~1kb) (B). DNA marker is 1 kb DNA ladder (L).

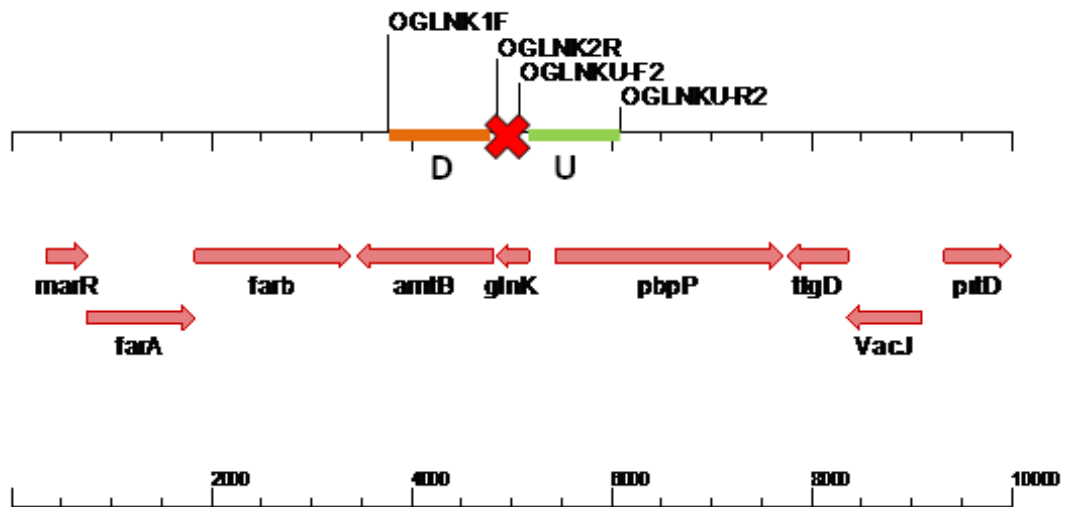


Figure 4. 10 kb fragment from *R. capsulatus*. The upstream (U) and downstream (D) fragments of *glnK* and the deletion region (X) are indicated.

The components and the cycling conditions of the PCR reaction for amplification of *glnK* upstream and downstream fragments were given in Section 3.6.5. After extracted from the gel, ~1 kb *glnK* upstream fragment was ligated to *Hinc*II cut dephosphorylated pBtSK and transformed into *E. coli* XL1Blue. The insertion was confirmed by colony PCR with T3/T7 universal primers (Figure 4.11B) and restriction enzyme digestion. The resulting plasmid was pGKBU (Figure 4.11A)

Similar to upstream, *glnK* downstream fragment was extracted from the gel and used in the ligation with *Hinc*II cut dephosphorylated pBtSK and transformed into *E. coli* XL1Blue. The insertion was confirmed by colony PCR with T3/T7 universal primers (Figure 4.12B) and restriction enzyme digestion. The resulting plasmid was pGKBD (Figure 4.12A).

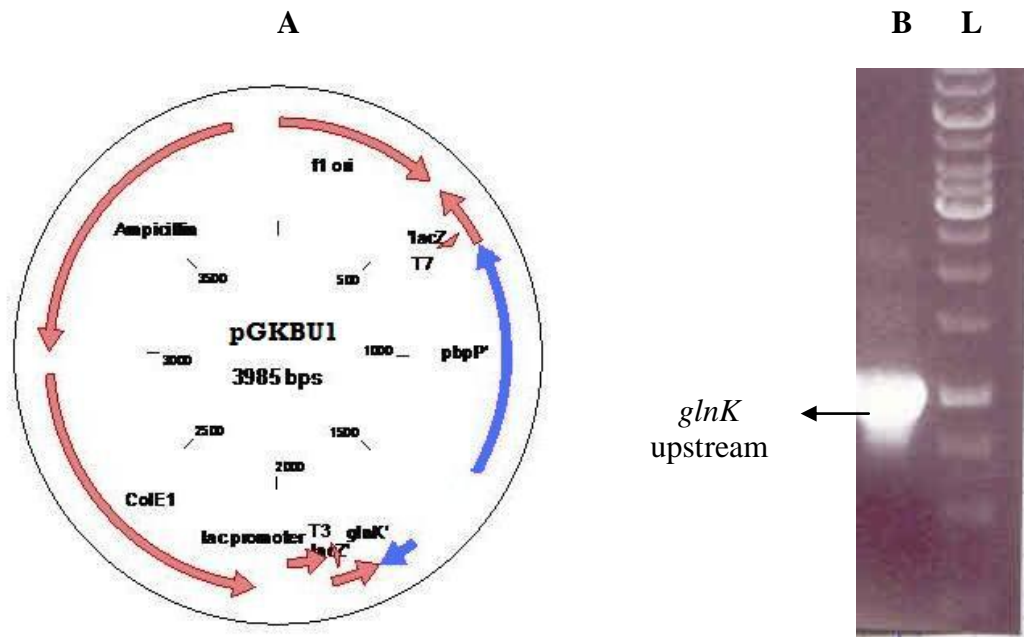


Figure 4. 11 The plasmid containing *glnK* upstream insert (pGKBU1) (A) and agarose gel result of colony PCR for the amplification of the insert (B). DNA marker is 1 kb DNA ladder (L).

In order to construct pGKSD, first, *glnK* downstream is excised from the pGKBD by digestion with PstI and XbaI. Then, excised insert was ligated with PstI-XbaI digested pK18*mobsacB*. The resulting plasmid was pGKSD, 6700 bps (Figure 4.13A). Agarose gel results of the empty plasmid and the linearized pGKSD are given in Figure 4.13B-C, respectively.

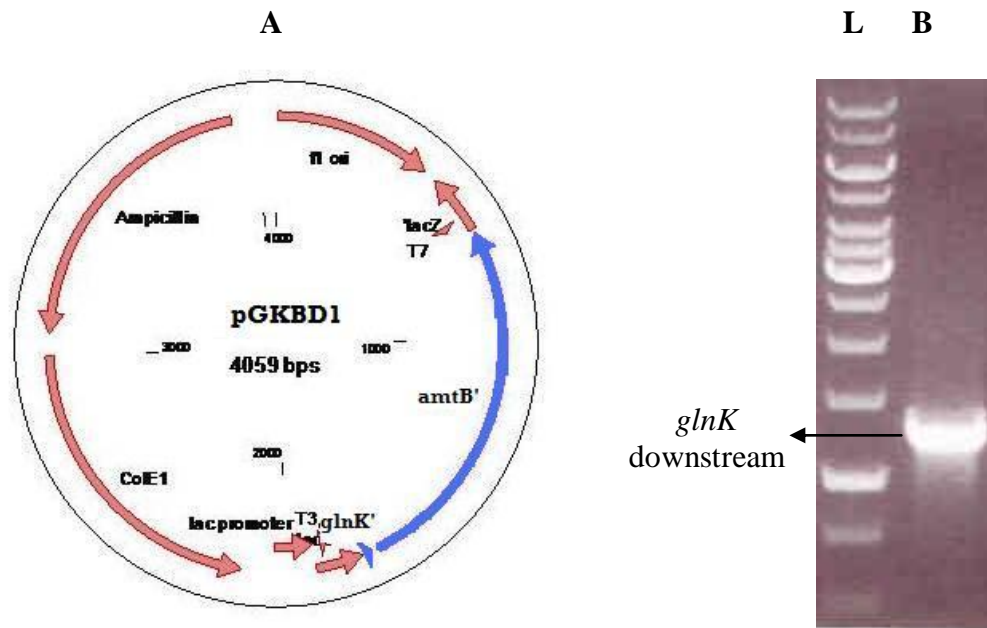


Figure 4. 12 The plasmid containing *glnK* downstream (pGKBD1) (A) and the agarose gel result of colony PCR for the amplification of the insert (B). DNA marker is 1 kb DNA ladder (L).

The final construct of *glnK* (Figure 4.14A) was obtained by ligating BamHI-EcoRI cut pGKSD with *glnK* upstream fragment excised from pGKBU by BamHI-EcoRI digestion. pGKSUD (7700 bps) (Figure 4.14B), containing total 2 kb insert of *glnK* upstream and downstream was obtained. Double digestion of the final construct (pGBSUD) was also performed in order to excise 1 kb insert (Figure 4.14C).

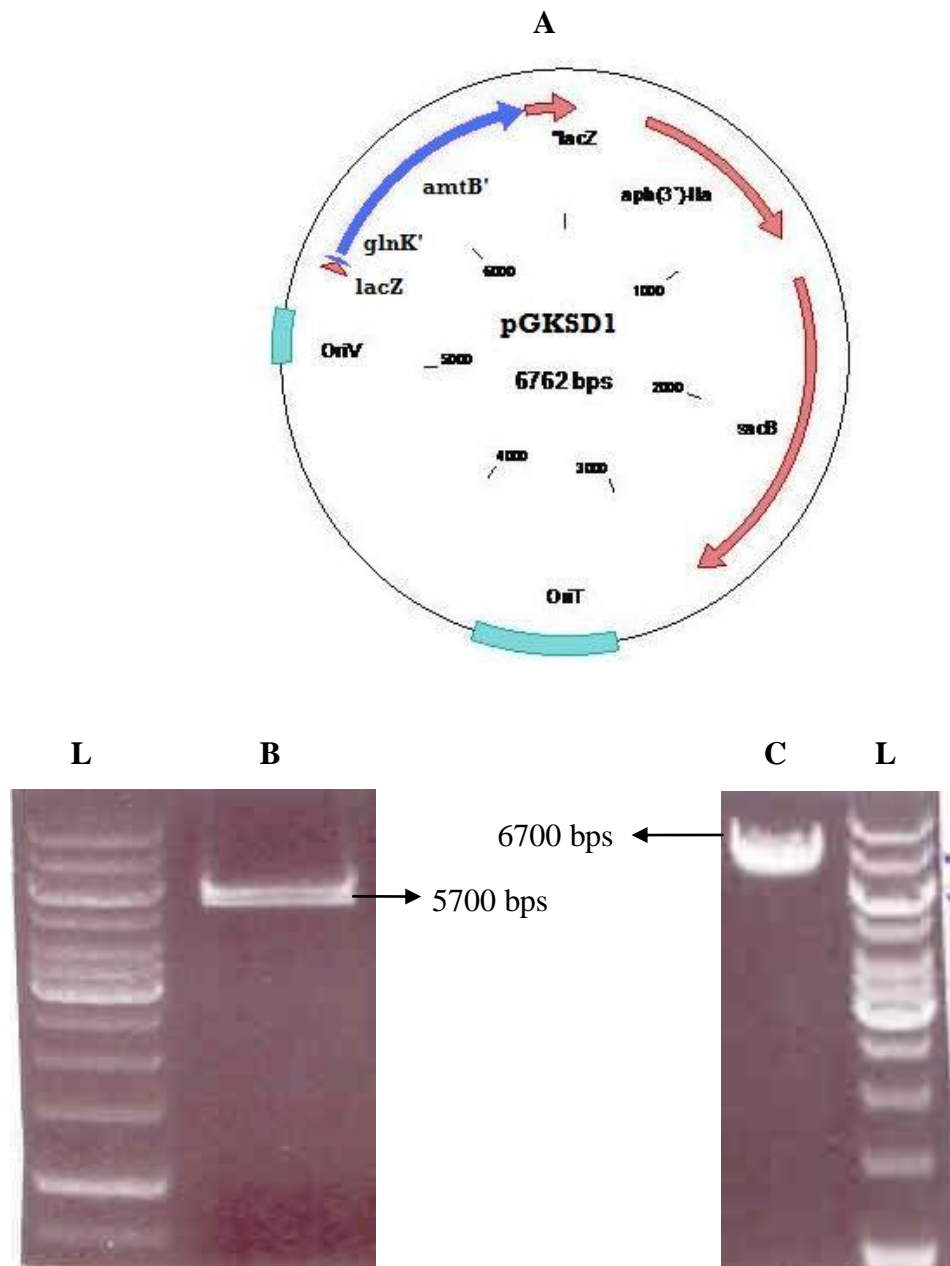


Figure 4. 13 The suicide plasmid (pK18*mobsacB*) containing ~1kb *glnB* downstream insert (pGKSD1) (A). Agarose gel results of linearized pK18*mobsacB* (~5700 bps) (B) and linearized pGKSD (~6700 bps) (C). DNA marker is 1 kb DNA ladder (L).

4.2.2. Delivery of the suicide vector for *glnK* deletion (pGKSUD) to *R.capsulatus* and selection-screening of the double recombinants

The strategy to deliver the final *glnK* deletion vector (pGKSUD) to *R.capsulatus* was exactly same with *glnB* deletion strategy. After pGKSUD, containing the deleted *glnK* gene (pGBSUD) was obtained; transformation into *E.coli* S17-1 cells was performed. In conjugation experiments, this cell strain containing pGKSUD was mixed with wild type and *glnB*⁻ *R.capsulatus* strains, individually. After the experimental procedure, the successful single recombinants were observed in the Km²⁵ BP agar plates (Figure 4.15).

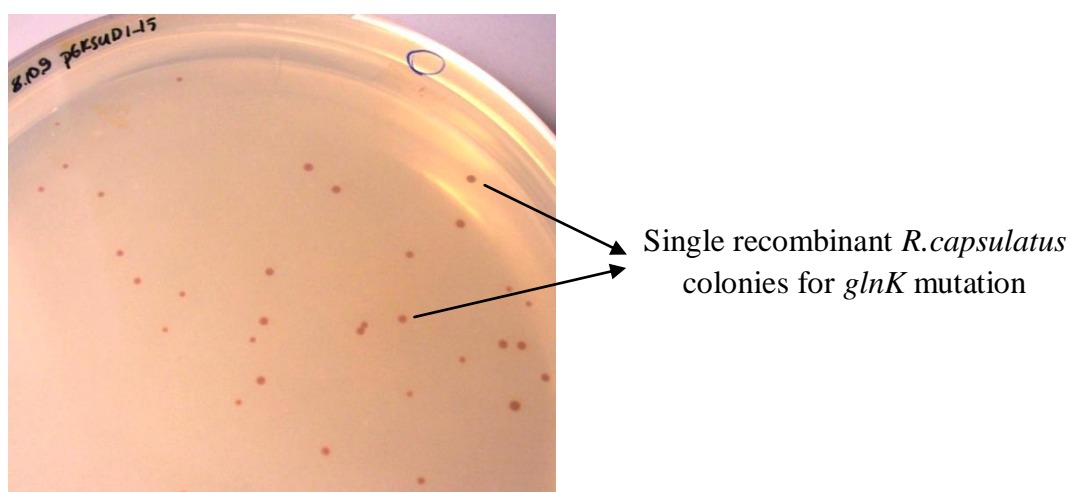


Figure 4. 15 Single recombinant colonies of *R.capsulatus* on BP agar containing kanamycin

Again, the single recombinants were passaged to allow second recombination. After passaging, inoculations were performed with different dilutions (10^{-1} , 10^{-2} , 10^{-3} , and 10^{-4}) onto 10 % sucrose containing BP agar plates. The appearing colonies were selected and replica plated onto kanamycin plates, with wild type *R.capsulatus* as the 'control'. Quite a number of colonies were selected and their growths were

investigated in the presence of kanamycin. All of the colonies, which were selected from sucrose plates, could form colonies on the kanamycin BP plate. Even this observation was not expected for potential mutants, the colonies were checked by colony PCR and the lengths of *glnK* gene products were investigated. A typical agarose gel result of a PCR reaction, which was done for screening of *glnK* deletion mutation, can be seen in Figure 4.16. All of the PCR products, obtained by using the selected colonies as template in colony PCR (Figure 4.16A-G), corresponded to wild type *glnK* gene (860 bps), whereas the expected product size was 645 bps for *glnK* mutant that contains deleted *glnK* gene. Lane H & I in Figure 3.16 were positive controls, which included wild type *R.capsulatus* colony as template. The negative control was the PCR reaction without any template (Figure 4.16J).

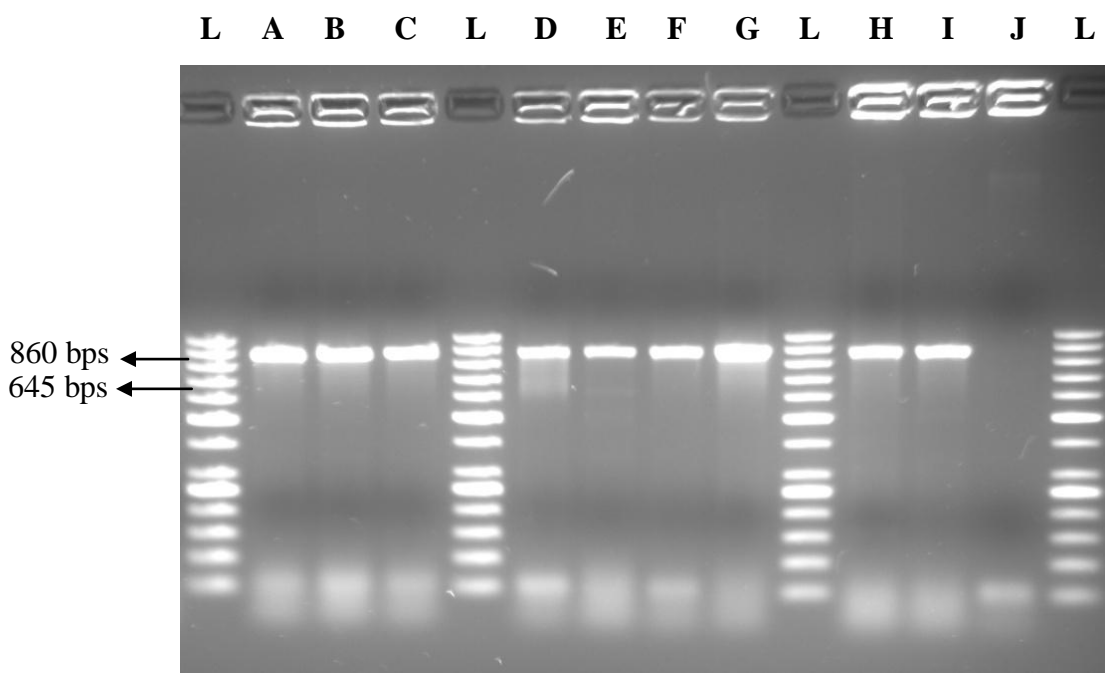


Figure 4. 16 A typical agarose gel result of the PCR reaction for the screening of *glnK* deletion. The expected length of the deleted *glnB* corresponds to 645 bps, however the length of the PCR products for 10 screened colonies (A-J) corresponded to the wild type *glnB* gene (860 bps). DNA marker is 50 bp DNA ladder (L).

In order to obtain *glnK* mutant *R.capsulatus*, containing the deleted *glnK* gene, and *glnB glnK* mutant *R.capsulatus*, containing deleted *glnB* and *glnK* gene, conjugation procedure was repeated for several times with the same construct and with similar constructs obtained by the same strategy from different ligation reactions. After each conjugation experiment, the procedure for selection and screening were repeated. However, double recombinant colonies could not be obtained; even though successful single recombinants were obtained. There was no colony which grew on sucrose and did not grow on kanamycin. Besides, these colonies were screened by colony PCR and has not been observed to contain short PCR product which indicating deletion in *glnK* gene. The attempts to obtain a *glnK* mutant or *glnB glnK* double mutant did not give satisfactory results.

The construction of the suicide vectors and the applied mutagenesis strategy of *glnB* and *glnK* were very similar to each other. Hence, the successful achievement of *glnB* mutation indicates that there was no problem about the experimental procedure of *glnK* mutagenesis.

Since the single recombinants of *glnB* were successfully obtained, the inability to obtain a *glnK* gene deletion might be explained such that; either most of the single recombinants returned to wild type after second recombination event due to a deleterious effect of the mutation or all of the bacterial cells containing inactive *glnK* gene were eliminated. This might have resulted into the domination of cell culture by wild type cells, which prevents appropriate selection of the mutants. On the other hand, the mutation in *glnK* may be lethal.

As described in Section 2.3.4, P_{II} proteins are highly conserved and found in most of the life forms. Proteins of the P_{II} signal transduction superfamily play a major role in coordinating the regulation of central metabolic processes. Signals from the carbon, nitrogen and energy status of the cells are converted into different conformational (and modification) states of the P_{II} proteins. Depending on these states, the P_{II} proteins interact with various target proteins, most of which perform or regulate

crucial reactions in nitrogen assimilatory pathways (Forchhammer, 2008). There is intense research ongoing about P_{II} proteins, in order to reveal their functions completely, to understand how they interact with various target proteins in the cell and to comprehend the whole picture of interactions of P_{II} proteins. P_{II} proteins help to coordinate carbon and nitrogen assimilation by regulating the activity of signal transduction enzymes in response to diverse signals (Ninfa and Atkinson, 2000). Their functions are crucial for the cell. Mutational analysis of P_{II} proteins in various organisms, such as *Cyanobacteria* sp., *Rhodobacter* sp., *Rhizobium* sp., *Rhodospirillum* sp. and so on, have been carried out to understand the functional characteristics of P_{II} proteins and to reveal the nature of interactions (Drepper et al., 2003; Meletzus et al., 1998; Omar et al. 1994; Zhang et al., 2000; Masepohl et al., 2002; de Zamaroczy, 1998; Kim et al., 2008; Zhang et al., 2006; de Zamaroczy et al., 1998; Hanson et al., 1998).

In this study, the effect of mutagenesis on the genes of PII proteins (GlnB and GlnK) and ammonium inhibition on hydrogen production of *R.capsulatus* was investigated. *glnB* mutant *R.capsulatus* was successfully obtained and its hydrogen production was investigated at different ammonium levels. However, *glnK* mutant could not be obtained. It might be suggested that GlnK protein might be an essential protein in *R.capsulatus* DSM1710 and its inactivation led to poor growth or death of the mutant cell.

In some of the studies issuing mutagenesis analyses of P_{II} proteins, the attempts to obtain P_{II} mutants were successful; however in some of them the attempts were unsuccessful. A similar case to ours was observed by Meletzus et al. (1998). They tried to obtain *glnK* mutant, but their attempt was unsuccessful and the mutations that eliminated the P_{II} homologue (*glnK*-like) in *Azotobacter vinelandii* were considered as lethal. They applied gene replacement strategy by double cross over event, similar to the gene inactivation strategy that has been followed in the present study. The wild type *glnK* gene was exchanged with kanamycin cassette inserted 'inactive' *glnK*. After they selected ampicillin sensitive and kanamycin resistant colonies, they

cultured the colonies in selective (kanamycin containing) medium for three times. When they isolated and examined the genomic DNA's of the passaged colonies, they detected the presence of wild type *glnK* genes. Besides, the kanamycin resistances of the colonies were disappeared in nonselective medium, even after ten subcultures in selective medium. The same problem persisted in different media compositions and growth conditions.

In another study by *Rhodobacter rubrum*, growth problems in mutants lacking P_{II} proteins were also observed (Zhang et al., 2001; Zhang et al., 2006). *Azospirillum brasiliense glnB glnZ* (the *glnK* homologue) double mutants showed poor growth in both rich and minimal media (de Zamaroczy et al., 1998). The reason for the poor growth is unknown. The inactivation of *glnB* gene in cyanobacterium *Nostoc punctiforme* (Hanson et al., 1998) led to lethality of the mutants. An *Escherichia coli* strain lacking both *glnB* and *glnK* grows very poorly in nitrogen-rich minimal medium, but well in rich LB medium (Atkinson & Ninfa, 1998).

Zhang et al. (2006) proposed that the growth problem of P_{II} mutants of *Rs. rubrum* is related with glutamine synthetase (GS) activity. They have identified suppressor mutants that were able to restore a normal growth phenotype to *Rs. rubrum* strains lacking P_{II} homologues. When they analyzed suppressor mutations, they found that their common property was revealed to be of decreasing GS activity; strongly indicating that high GS activity is the cause of poor growth in *Rs. rubrum* strains lacking P_{II} homologues. This high GS activity reflects both overexpression of *glnA* as well as the failure of ATase to adenylylate GS. P_{II} interacts with adenylyltransferase (ATase, the product of *glnE*) to control GS activity by reversible adenylylation (Rhee et al., 1985a,b; Jaggi et al., 1997). ATase catalyses both directions of this modification reaction, with P_{II} stimulating GS adenylylation and P_{II}-UMP stimulating the deadenylylation of GS in *E. coli* (Rhee et al., 1985; Stadtman, 2001). Besides, it was shown by van Heeswijk et al. (1996) that P_{II}, encoded by the *glnB* gene, is not always essential for GS regulation; for instance upon ammonia deprivation of a *glnB* deletion strain, glutamine synthetase can be deadenylylated as

effectively as in the wild-type strain. This might indicate that GlnK protein has a role in the regulation of the GS. GlnK mutation might cause an impaired regulation on the GS activity.

It is proposed by Zhang and colleagues (2006) that there is a reason to believe that the absence of P_{II} homologues typically does cause elevated GS levels, but the specific impact of the lack of P_{II} homologues on the phenotype is likely to depend on other factors as well. The impaired regulation of GS might have led to the severe growth problems, since GS is the primary enzyme required for the assimilation of N₂ and ammonia in many prokaryotes, (Magasanik, 1982; Leigh and Dodsworth, 2007), including *R.capsulatus* (Wall and Gest, 1979), and for the control of global carbon/nitrogen balance (Forchhammer, 2004).

Almost all bacteria and archaea encode at least one ammonium transport (Amt) protein, which is encoded by *amtB* gene located on the downstream of *glnK* gene. The *amtB* gene is structurally linked to a *glnK* gene that encodes GlnK (P_{II}) protein (Section 2.3.4) (Javelle et al., 2004; Javelle and Merrick, 2005). In *A.vinelandii*, *glnK* and *amtB* genes are located in the same operon. There are evidences about the cotranscription of these genes. A small intergenic region is located between *glnK* and *amtB* as well as there are no obvious transcriptional terminator- or promoter-like structures, indicating the probable cotranscription of *glnK* and *amtB* from the same operon (Meletzus et al., 1998). The cotranscription of *glnK* and *amtB* have been seen in various organisms; such as *Azorhizobium caulinodans* (Michel-Reydellet et al., 1998) and *E.coli* (Javelle and Merrick, 2005). In the case of *glnB-A* operon, *glnA* is located downstream of *glnB*. Therefore, they are considered to be in the same operon. However, there are evidences of the presence of another promoter in the upstream of the *glnA* (Foster-Hartneyt and Kranz, 1994). They suggested that *glnB* is transcribed from two different promoters. This might be the reason of observing different levels of *glnBA* and *glnA* transcripts in *R.capsulatus*. In the present study, *glnB* mutant was successfully obtained, however *glnK* mutant could not be obtained.

The difference in the structures of *glnK-amtB* operon and *glnBA* operon might have led this result.

The deletion in the *glnB* might not affect the transcription of downstream *glnA* gene drastically, since there is an extra promoter in the upstream of *glnA* for the transcription of *glnA* gene. On the other hand, the deletion of *glnK* might affect the transcription of *amtB* in a negative way. If the deletion mutation would lead some problems in the transcription of *glnK-amtB* operon, the transcript level of *amtB* would be reduced. This is because there is no extra promoter for the transcription of *amtB* gene. Subsequently, deficiency of ammonium transport protein (AmtB) could occur in the cell.

In addition to the lack of AmtB activity in the cell, there might be other unpredictable drawbacks of the absence of AmtB activity, since the coupling of AmtB and GlnK in bacteria and archaea is almost invariable and it seems probable that these two proteins may constitute an ancestral nitrogen- responsive system that has been coupled with a variety of unrelated nitrogen regulatory processes (Javelle and Merrick, 2005).

Drepper et al. (2003) successfully inactivated all of the P_{II} proteins of *R.capsulatus* B10S. In the double mutant that they have obtained, both *glnB* and *glnK* genes were disrupted in order to study ammonium regulation mechanism. However, they had to try the mutagenesis studies several times with various constructs, until they succeed to obtain double mutant of *R.capsulatus*. After many trials for mutagenesis, they could finally obtain a successful double mutant (Hallenbeck P. C., personal communication). After investigation of successful *glnB glnK* mutant, they found out that all three levels of the ammonium regulation of the molybdenum nitrogenase were completely circumvented in the double mutant, resulting in the synthesis of active molybdenum nitrogenase even in the presence of high concentrations of ammonium (see Section 2.3.3 for ammonium regulation) (Masepohl et al., 2002). From this study, it was concluded that both GlnB and GlnK proteins are critical in ammonium regulation on nitrogenase. The successful achievement of the double

mutant might be because of the presence of some residual GlnK activity in the mutant, which they could obtain after several trials. This ‘impaired’ GlnK may not be able to perform regulatory functions. However, it may perform its ‘nonregulatory’ functions, which are essential for the cell. So, the cell does not suffer from the absence of GlnK protein, which leads to fruitful results in the mutagenesis studies.

Moreover, it was revealed that the functions of GlnB and GlnK overlap (van Heeswijk et al., 1996; Leigh and Dodsworth, 2007; Atkinson and Ninfa, 1998). These proteins, having very similar structures and functions, can compensate the absence of another. Ammonium regulation was not revealed in single mutants of *glnB* and *glnK*. This result is in accordance with my observations. In single *glnB* mutant that I obtained, the ammonium regulation was still present, inhibiting hydrogen production by nitrogenase in the presence of ammonium (Section 3.1.3). Therefore, GlnK was able to compensate the function of GlnB protein, when there was no active GlnB protein in the cell. This result was also observed by Kim et al (2008). The related results of the present study will be given further.

The components in the nitrogen regulation are common in various organisms, but also there are great differences between them. Dixon and Kahn (2004) stated that ‘The necessity to respond to the concentrations of fixed nitrogen and external oxygen, and to provide sufficient energy for nitrogen fixation, imposes common regulatory principles among diazotrophs. In the diazotrophic proteobacteria i.e. *R.capsulatus*, this is reflected by common regulatory components and the use of similar regulatory networks. However, there is considerable plasticity in the regulatory networks, which differ among microorganisms and are dependent on host physiology’. The P_{II} proteins exhibit remarkable functional versatility in diverse organisms and control a wide range of processes related to nitrogen metabolism (Forchhammer, 2008). Besides to the variations in different organisms, there might be also differences between the strains of the same organism. This might be also an explanation for the inability to obtain a *glnB glnK* mutant in *R.capsulatus* DSM1710

in the present study whereas the *glnB glnK* mutant of *R.capsulatus* B10S strain could be obtained (Drepper et al, 2001).

4.3. Growth and hydrogen production of wild type and *glnB* mutant *R.capsulatus* on ammonium containing media

The aim of the present study was to determine the effect of mutation on the H₂ production and on the regulation over N₂ase. For this aim, the growth behavior and H₂ production profile of *glnB* mutant *R.capsulatus* was investigated and compared with wild type. The H₂ production media and conditions were described in Section 3.4 and H₂ production setup was described in Section 3.5. In the same incubator, two different H₂ production setup was established and the parallel sets of the experiment were performed. Samplings of the cultures were done with time intervals for 24 hours. Data for pH, optical density, and organic acid analyses were obtained together with H₂ production data. The carbon source of the media was acetate, which was previously determined to be a good carbon source for *R.capsulatus* (Koku et al., 2002), with the concentration determined to be optimum for H₂ production (30 mM) (Özgür et al., 2010). The nitrogen source of the medium was either glutamate (2 mM), which is an excellent nitrogen source for H₂ production (Koku et al., 2002), or ammonium chloride (NH₄Cl) with various concentrations to observe the effect of ammonium ion (NH₄) (Akköse et al., 2009).

4.3.1. The effect of ammonium on the growth of wild type and *glnB* mutant *R.capsulatus*

Cell growth curves of the batch cultures contain well described phases. The lag phase represents the time interval between the inoculation time and the start of growth. In lag phase, the cells try to adapt themselves to the new medium by increasing their metabolic activities and synthesizing necessary proteins and enzymes. The interval of lag phase depends on the history of the culture and the growth conditions. In the case of inoculation of the culture into the same medium with the same growth conditions, the lag phase is very short and cell division immediately starts. The cell division

occurs in the exponential phase, the logarithm of cell number results in a straight line. The cells in exponential phase are in their healthiest states. In batch culture, exponential phase stops due to lack of nutrients and accumulation of waste products. This phase is stationary phase, in which there is no net increase or decrease in cell number, because some cells die and some cells divide at the same time. Death phase follows lag phase, the cells starts to die and cell concentration decreases (Madigan and Martinko, 2006).

The growth curves of wild type and the *glnB* mutant *R.capsulatus* in media containing different ammonium chloride (NH_4Cl) concentrations (See Table 3.3) are given in Figure 4.17 and 4.18, respectively

From Figure 4.17 and 4.18, it is seen that the cell growth basically follow a similar pattern. From the figures, it is observable that the lag phases of the cultures were either very narrow or did not present, indicating that the cells started directly to divide after inoculation. This is not an unexpected observation, since the inoculation was into the same medium with optimum growth conditions. The mother culture was also in exponential phase, which also led to the continuous cell division of the cells.

Since *R.capsulatus* cells are photosynthetic, they are able to survive under continuous illumination. The biomass reaches the maximum value in the exponential phase. After nutrients are exhausted, the cells adapt themselves to the new environment and biomass stabilizes to a modest value with small oscillations.

Nitrogen concentration has an important role in growth since it is the second most abundant element found in the cell. The biomass increased as the ammonium concentration increased, due to the availability of the nitrogen source. The highest biomass concentration was observed in 8 mM NH_4Cl containing medium both for the wild type and mutant bacteria, with the maximum dry cell weight approaching 1.0. Then, the next highest growth was observed for 5 mM and 3 mM, in order. 2 mM glutamate control medium and 2 mM NH_4Cl medium showed similar growth curves,

due to the similar nitrogen sources in these media. The lowest growth was for 1 mM NH_4Cl containing medium, resulting in limited growth due to the lack of nitrogen source.

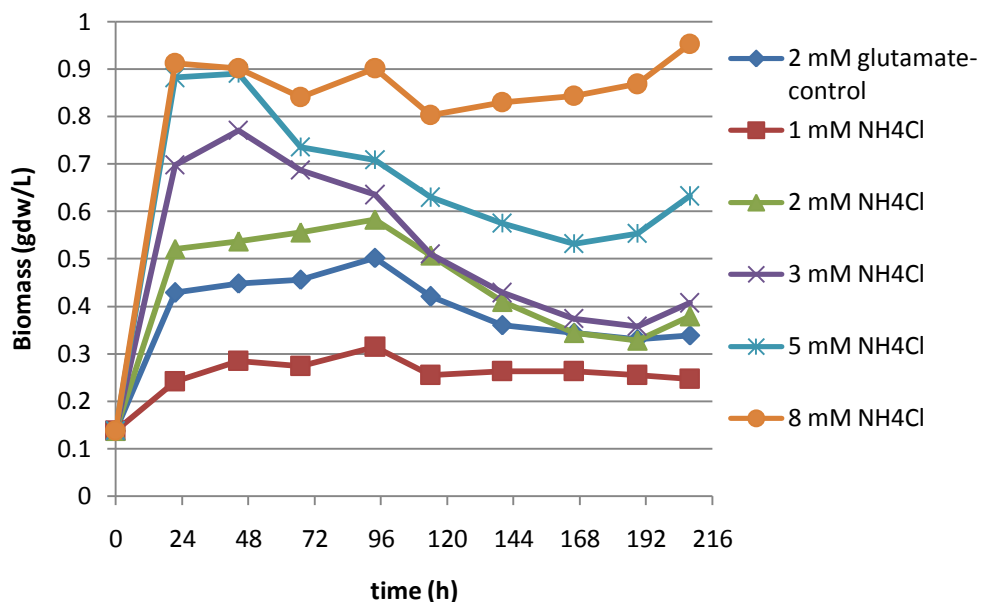


Figure 4. 17 Biomass of wild type *R. capsulatus* in different ammonium levels

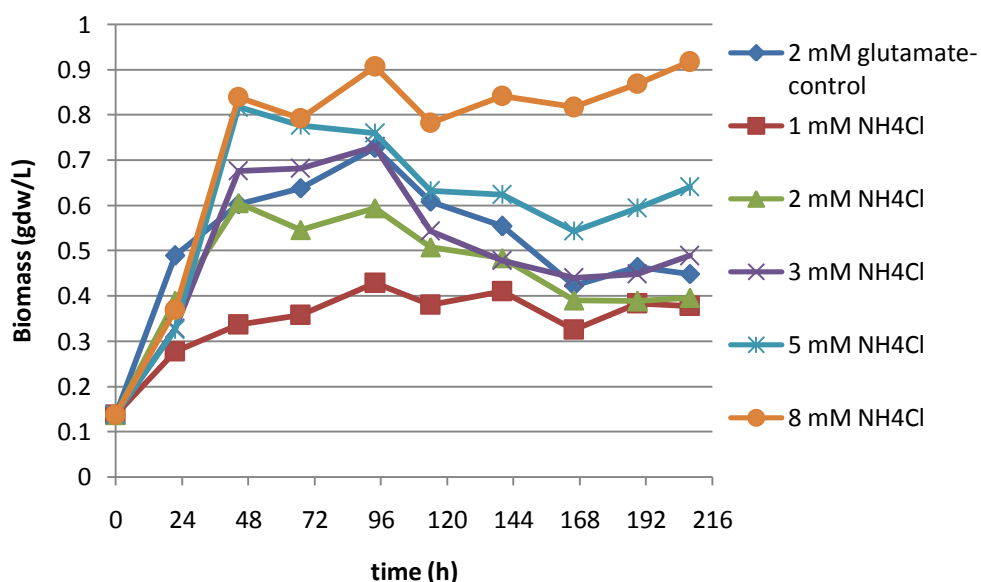


Figure 4. 18 Biomass of *glnB* mutant *R. capsulatus* in different ammonium levels

From the comparison of the growth of wild type cells with the mutant cells, it can be concluded that the mutation did not cause any significant decrease in the growth of mutant cells. It might indicate that the effect of mutation in the cell was tolerated in terms of growth.

4.3.1.1. Modeling of cell growth

In the exponential phase, rate of growth is expressed by the equation

$$\frac{dX}{dt} = \mu.X \quad (4.1)$$

where X is the bacterial concentration, t is the time, and μ is the specific growth rate. Integrating this equation gives

$$X = X_o .e^{-\mu.t} \quad (4.2)$$

As Equation (4.2) is rearranged, the experimental specific growth rate for a definite interval becomes:

$$\mu = \frac{\ln\left(\frac{X_2}{X_1}\right)}{(t_2 - t_1)} \quad (4.3)$$

Cell growth takes place with a fast rate in the exponential phase. Then, approaches to an asymptotic value before death phase. When the death phase is excluded, the shape of the growth curve look like 'S'. So, it might be called as 'sigmoidal curves'. There are mathematical equations calculated for sigmoidal curves. These equations, which include lag, exponential and stationary phases but exclude death phase, are used for analysis of cell growth curves. One such model is the 'Logistic Model', which is

developed by Verhulst (1838), and is substantially used for bacterial cell growth in food and growth media (Fujikama, 2004; Gibson et al., 1987; Nath et al., 2008; Eroğlu et al., 2004; Uyar, 2008; Eroğlu et al., 2008; Androga, 2009; Koku et al., 2003). In the previous studies, *R. capsulatus* DSM1710 (Androga, 2009; Sevinç, 2010) and *R.sphaeroides* (Uyar, 2008; Eroğlu, 2008; Nath et al., 2008) cell growth were reported to fit to logistic model. So, this model is used in the present study.

In the logistic model, the growth rate is expressed as

$$\frac{dX}{dt} = k_c X \left(1 - \frac{X}{X_{\max}} \right) \quad (4.4)$$

where k_c is the apparent specific growth rate (h^{-1}), X is the dry cell weight (gdw/L) and X_{\max} is the maximum dry cell weight (gdw/L). The difference between Equation 4.1 and 4.4 is the presence of the term $\left(1 - \frac{X}{X_{\max}} \right)$ in the Equation 4.4. When Equation 4.4 is integrated, Equation 4.5 is obtained:

$$X = \frac{X_{\max}}{\left[1 + \exp \left(-k_c \cdot t \right) \left(\frac{X_{\max}}{X_o} - 1 \right) \right]} \quad (4.5)$$

where X_o is the initial bacterial concentration (g/L).

The experimental data for cell growth was given in Figures 4.17 and 4.18. The data from start of the experiment to the start of the death phase were fitted to logistic model by using Curve Expert 1.3. The curves fitted to logistic model for wild type and mutant *R.capsulatus* in different ammonium concentrations are given in Appendix I. An example of these is given in Figure 4.19

From the experimental data, maximum specific growth rate (μ_{\max}) was calculated by using Equation 4.3 together with initial and maximum experimental bacteria concentrations ($X_{0,e}$ and $X_{\max,e}$). From the model, initial bacterial concentration ($X_{0,m}$), maximum bacterial concentration ($X_{\max,m}$) specific growth rate constant (k_c) and the extent of the fit (r) was obtained. These parameters of wild type and *glnB* mutant *R.capsulatus* are all given in Tables 4.1 and 4.2, respectively.

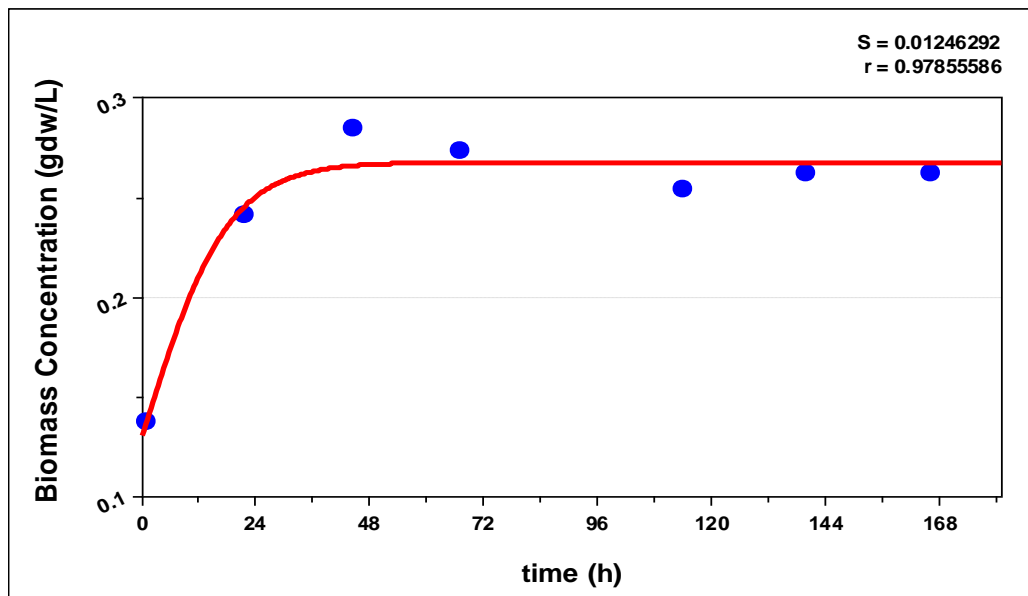


Figure 4. 19 The logistic growth model of wild type *R.capsulatus* for 1 mM NH_4Cl containing medium

Table 4. 1 Comparison of experimental and logistic model constants of wild type *R.capsulatus* for different ammonium concentrations (subscript ‘e’ represents experimental values; subscript ‘m’ represents model values).

	2 mM glutamate (control)	1 mM NH₄Cl	2 mM NH₄Cl	3 mM NH₄Cl	5 mM NH₄Cl	8 mM NH₄Cl
R	0.980	0.979	0.996	0.982	0.963	0.981
X _{o,e} (gdw/L)	0.138	0.138	0.138	0.138	0.138	0.138
X _{o,m} (gdw/L)	0.122	0.130	0.120	0.089	0.054	0.039
X _{max,e} (gdw/L)	0.502	0.285	0.584	0.771	0.890	0.953
X _{max,m} (gdw/L)	0.456	0.268	0.560	0.698	0.804	0.873
μ _{max} (L/h)	0.049	0.027	0.065	0.079	0.090	0.092
k _c (L/h)	0.173	0.114	0.180	0.530	1.067	1.397

Table 4. 2 Comparison of experimental and logistic model constants of *glnB* mutant *R.capsulatus* for different ammonium concentrations (subscript ‘e’ represents experimental values; subscript ‘m’ represents model values).

	2 mM glutamate (control)	1 mM NH₄Cl	2 mM NH₄Cl	3 mM NH₄Cl	5 mM NH₄Cl	8 mM NH₄Cl
r	0.989	0.974	0.973	0.991	0.979	0.981
X _{o,e} (gdw/L)	0.137	0.137	0.137	0.137	0.137	0.137
X _{o,m} (gdw/L)	0.123	0.139	0.139	0.100	0.049	0.072
X _{max,e} (gdw/L)	0.638	0.429	0.605	0.730	0.817	0.907
X _{max,m} (gdw/L)	0.602	0.391	0.565	0.727	0.799	0.844
μ _{max} (L/h)	0.062	0.021	0.034	0.037	0.041	0.042
k _c (L/h)	0.132	0.060	0.107	0.085	0.12	0.107

The following conclusions can be drawn from Tables 4.1 and 4.2:

- i. The experimental data well fitted to the model, with r values very close to 1.
- ii. Experimental (initial and the maximum) cell concentrations are quite close to the model values.
- iii. The maximum cell concentration increases with initial ammonium concentration. That indicates the significance of ammonium concentration on biomass.
- iv. The maximum cell concentration obtained with 2 mM glutamate is 0.456 gdw/L. This concentration can be obtained if the ammonium concentration in the medium is close to 2 mM.
- v. *glnB* mutant *R.capsulatus* has the same growth behavior with the wild type in the case of glutamate.
- vi. Specific growth rate (k_c) or μ are less in *glnB* mutant compared to the wild type *R.capsulatus*. This shows that the mutation decreased the ammonium assimilation for growth.

4.3.2. pH variations in wild type and *glnB* mutant *R.capsulatus* at different ammonium levels

Sasikala et al. (1991) demonstrated that *R.sphaeroides* can grow at pH values ranging from 6 to 9. However, the optimum pH value was determined to be 6.8-7.0. Moreover, the optimum pH for H₂ production was found to be 7.0. The pH variations of wild and *glnB* mutant *R.capsulatus* in different NH₄Cl concentrations are shown in Figure 4.19 and 4.20. The pH values range between 6.8 and 8, which can be considered as a tolerable pH range, since KH₂PO₄ buffer was present in the media.

Akköse (2008) and Sasikala (1991) showed that the growth and the pH variations were correlated with each other; the pH was highest at the point to the maximum growth. This result was also observed in our case; as the growth increased, pH

increased. In the first 48 hours of the experiment, which corresponded to the exponential growth of the culture, there were rapid increases in pH of the cultures. Similarly, when the cell concentrations started to decrease, the pH values also decreased. Moreover, when pH values of the cultures having different NH_4Cl levels were compared, it can be concluded that pH was higher in the media with elevated NH_4Cl levels, which is due to the occurrence of the increased growth in more NH_4Cl containing media.

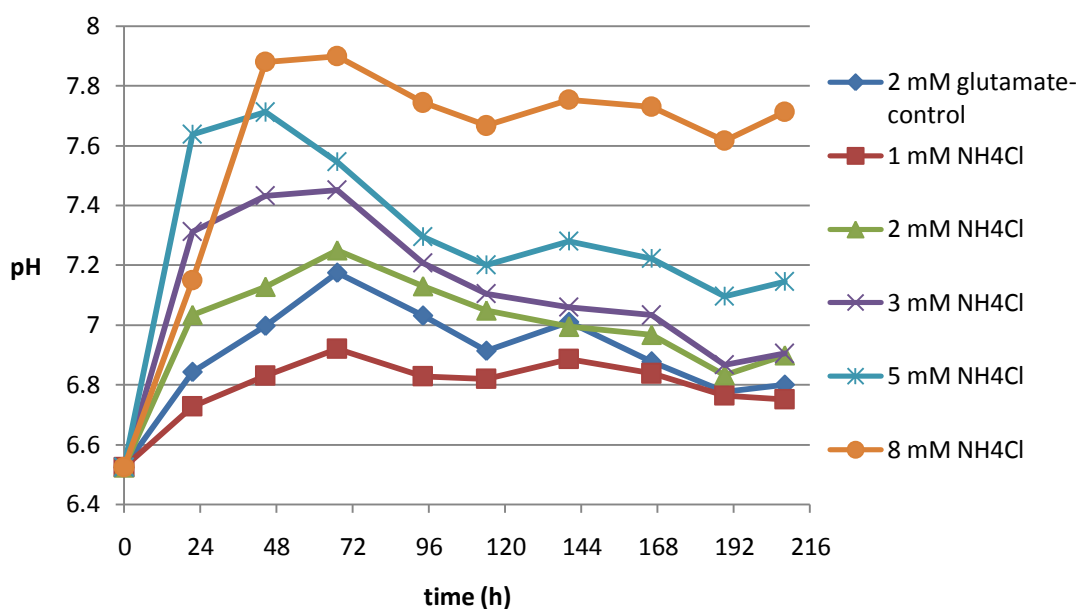


Figure 4. 20 pH measurements of wild type *R. capsulatus* in different ammonium levels

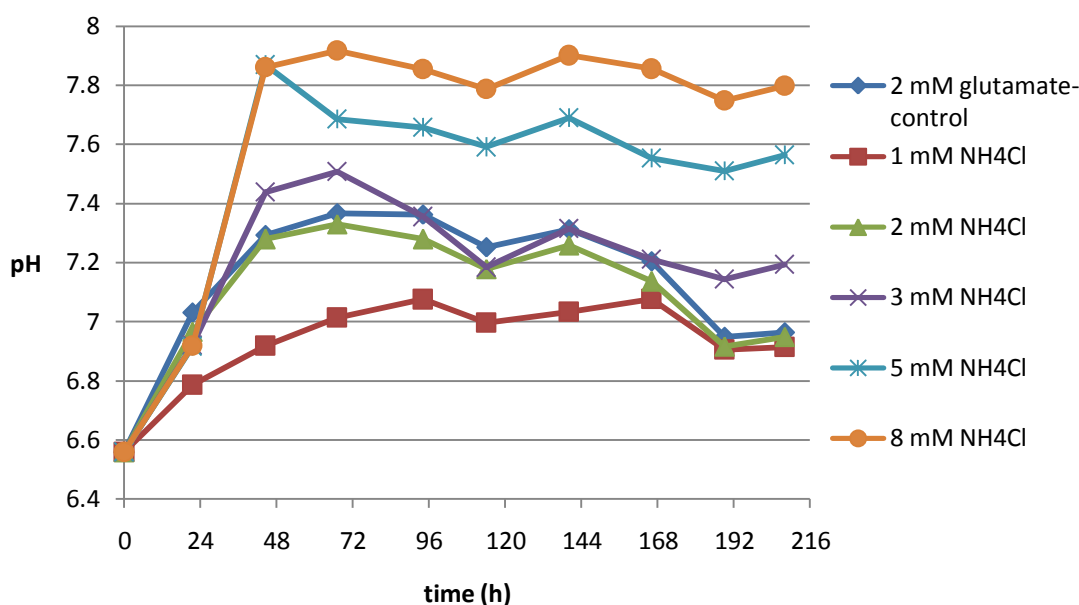


Figure 4. 21 pH measurements of *glnB* mutant *R. capsulatus* in different ammonium levels

4.3.3. Hydrogen production profiles of wild type and *glnB* mutant *R. capsulatus* at different ammonium levels

H₂ production depends on various factors; such as light, oxygen, temperature, growth phase of bacteria and substrates (Sasikala et al., 1991 and 1995; Koku et al, 2002; Akköse, 2008; Sevinç, 2010). The type and the concentration of nitrogen and carbon sources are important factors affecting H₂ production. Although the cells can grow in a variety of nitrogen and carbon sources, they cannot produce H₂ in all of these nutrients (Koku et al., 2002). It is also stated that NH₄ is a very good nitrogen source for the growth of bacteria. However, it significantly inhibits H₂ production (Waligórska et al., 2006), as mentioned before in Section 2.3.5. I observed similar results about the effect of nitrogen source (Figure 4.21 and Figure 4.22). For both wild type and *glnB* mutant *R. capsulatus* bacteria, as the concentration of NH₄Cl in the medium increased, H₂ production decreased. The highest H₂ production was observed in the control medium, including 2 mM glutamate instead of NH₄Cl. The maximum H₂ production values (ml_{H₂}/ ml_{culture}) were 1.13 and 0.63 for wild type and

mutant bacteria. The H₂ production profiles in 3 mM, 2 mM and 1 mM NH₄Cl media were lower than the control's and followed similar pattern within each other. There was no observation of H₂ production in 8 mM NH₄Cl medium; H₂ production was totally inhibited by ammonium ions.

It is observable that there was a reverse relation between pH and H₂ production. In the cultures reaching high pH values, H₂ production was lower compared with the low pH cultures. The pH of the 8 mM NH₄Cl medium was around to 8.0 and H₂ production was not observed. Similarly, the pH of 5 mM NH₄Cl medium, which is the second lowest H₂ producer, approached 7.8. However, the difference in H₂ production between 5 mM and 8 mM could be also contributed to the dramatic effect of ammonium levels. Similar results were observed by Akköse (2008).

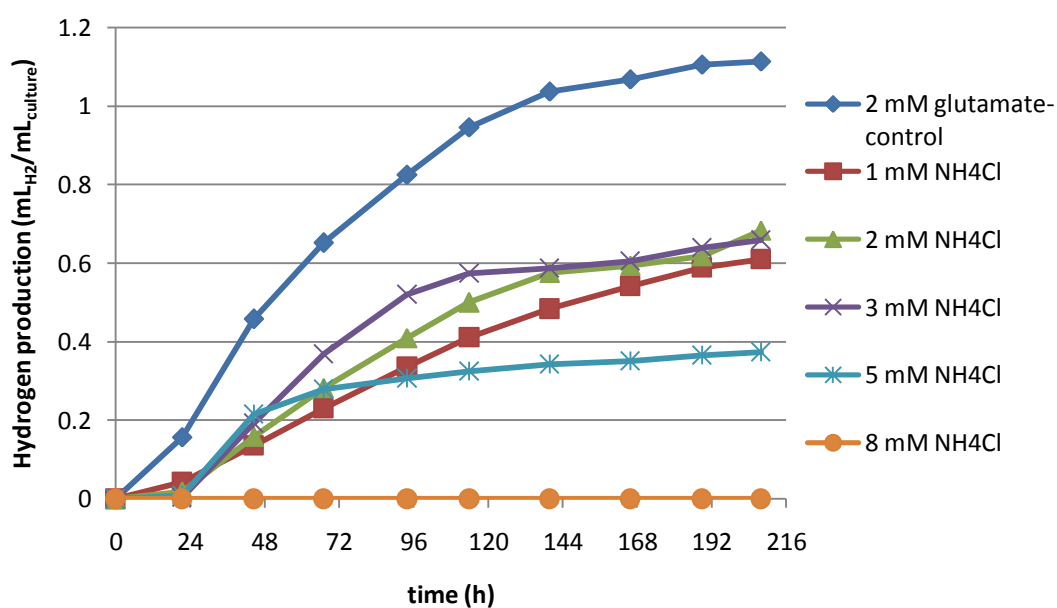


Figure 4. 22 Hydrogen production profile of wild type *R. capsulatus* in different ammonium levels

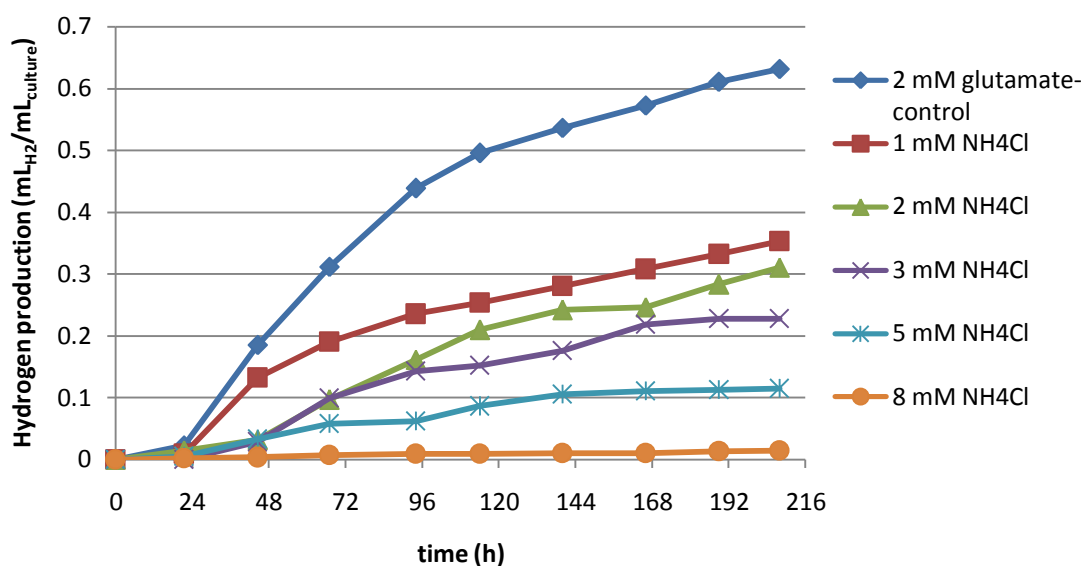


Figure 4. 23 Hydrogen production profile of *glnB* mutant *R.capsulatus* in different ammonium levels

When the H₂ production of wild type and mutant bacteria in control medium (2 mM glutamate) were compared, it was observed that the maximum H₂ production by mutant bacteria was approximately 1.8 times less than the maximum H₂ production of the wild type bacteria. The wild type's maximum H₂ production was around 1.10 mL_{H2}/ mL_{culture}, whereas the maximum H₂ production of mutant bacteria was 0.65 mL_{H2}/ mL_{culture}. This indicated that *glnB* mutation affected H₂ production in a way that is independent of NH₄ effect; suggested that the mutation might have result some changes in the mutant cells and lowered H₂ production in general. Carbon utilization of both wild type and mutant bacteria was efficient; both the wild type and the mutant bacteria could consume almost all the acetate present in the medium (Figure 4.23 and 4.24). This observation disproved the suggestion that the mutation might have led to impaired carbon utilization, which might be proposed to be the reason of low H₂ production.

The efficient carbon utilization and inefficient H₂ production might be due to the byproduct production by the mutant cells, since byproduct formation means the channeling of the reducing equivalents to byproduct formation instead of H₂ production. PHB (polyhydroxybutyrate) is a bacterial storage material and a significant by product of PNS bacteria (for detail, see Section 2.3.6). PHB production depends on carbon and nitrogen sources; it is efficiently produced when acetate is the sole carbon source and ammonium is the nitrogen source (Khatipov et al., 1998; Hustede et al., 1993). PHB production was observed in many H₂ production processes (Eroglu et al., 2008; Melnicki et al., 2009). There is competition between H₂ production and PHB production for reducing equivalents since the release of H₂ and the PHB accumulation can be considered as two alternatives for expending reducing power. Moreover, it was reported that PHB production was enhanced in stress conditions in the presence of light and organic substrates, resulting in substantial amounts of PHB accumulation (Melnicki et al., 2009). If the mutation in the *glnB* gene has resulted stress conditions in the mutant cells, the cells might have produced substantial amount of PHB rather than H₂. The significant decrease in H₂ production of the *glnB* mutant bacteria might be because of PHB accumulation. Although, it was not possible to measure the amount of PHB accumulation in this work, white PHB precipitates were extensively observed in the photobioreactors during H₂ production experiment, especially in the mutant cultures.

The effect of NH₄ on H₂ production of wild and mutant bacteria were similar; as NH₄Cl increased in the medium, there was decrease in H₂ production. As it is seen in Figure 4.21 and 4.22, the maximum H₂ production of wild and mutant strains was 0.61 and 0.35 in 1 mM NH₄Cl; 0.69 and 0.31 in 2 mM NH₄Cl; 0.66 and 0.23 in 3 mM NH₄Cl; 0.37 and 0.12 in 5 mM NH₄Cl media, respectively. It might be concluded that NH₄ inhibition on N₂ase enzyme was not removed in the *glnB* mutant bacteria. GlnB and GlnK proteins have overlapping functions and one active P_{II} protein may compensate the absence of another. Therefore, the result obtained in relation of NH₄ inhibition in *glnB* mutant may be considered as expected. In the literature, it is commonly stated that the disabling of the ammonium regulation of

N₂ase was possible with only double mutation in *glnB* and *glnK*, but not with the single mutations. This is because single active P_{II} protein in single mutants (*glnB* or *glnK*) may compensate the absence of another by accomplishing the function of inactive one. Kim et al. (2008) showed that the single mutants of *glnB* and *glnK* were not enough for the removal of the ammonium regulation of N₂ase.

4.3.3.1. Modeling of hydrogen production

In the Figures 4.22 and 4.23, hydrogen production curves are given. From start of the experiment to a certain time, hydrogen production increase slowly. Then, the increase is rapid with almost a constant rate and finally approaches to an asymptotic value without any further increase. The kinetic model, Modified Gompertz, is widely applied for such data, including the hydrogen production (Mu et al., 2007; Nath et al., 2008; Wang and Wan, 2009).

The equation for the Modified Gompertz Model is:

$$H = H_{\max} \exp \left\{ -\exp \left[\frac{R_{\max} e}{H_{\max}} (\lambda - 1) + 1 \right] \right\} \quad (4.7)$$

H and H_{max} are the instantaneous and the maximum cumulative hydrogen values in millimole per liter culture, respectively. R_{max} is the maximum hydrogen production rate (slope of the straight line cutting the time axis at λ, which is the lag time in hours) in millimole per liter culture per hour.

In the present study, Curve Expert 1.3 was used to fit the experimental hydrogen production data to Modified Gompertz Model. The curves fitted to this model for wild type and *glnB* mutant *R.capsulatus* in different ammonium concentrations are given in Appendix J. An example of these is given in Figure 4.24.

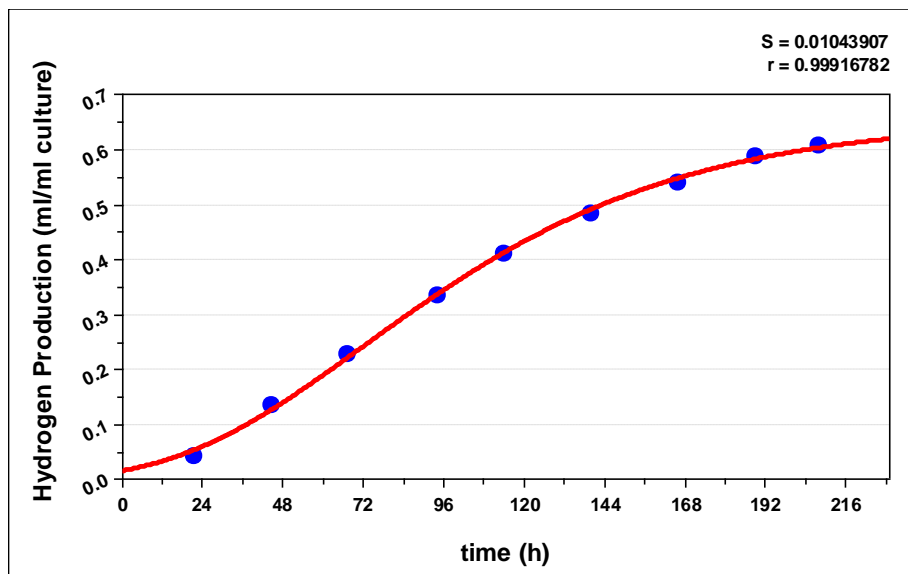


Figure 4. 24 The Modified Gombertz Model of wild type *R.capsulatus* for 1 mM NH_4Cl containing medium

From the experimental data in Figures 4.22 and 4.23, maximum cumulative hydrogen ($H_{\text{max},e}$), maximum rate of hydrogen production ($R_{\text{max},e}$) and the lag time (λ_e) were calculated. From the model, maximum cumulative hydrogen ($H_{\text{max},m}$), maximum rate of hydrogen production ($R_{\text{max},m}$) and the lag time (λ_m) were obtained. In addition to these values, the extent to the fit (r) values, that indicates the similarity between experimental results and model, are given. As the r value increases to 1, better fit achieved. These quantities of wild type and *glnB* mutant *R.capsulatus* are all given in Table 4.3 and 4.4, respectively.

Table 4. 3 Comparison of experimental values and Modified Gobertz Model constants of wild type *R.capsulatus* for different ammonium concentrations (subscript ‘e’ represents experimental values; subscript ‘m’ represents model values).

	2 mM glutamate (control)	1 mM NH₄Cl	2 mM NH₄Cl	3 mM NH₄Cl	5 mM NH₄Cl
r	0.998	0.999	0.992	0.997	0.991
H _{max,e} (mmol/L)	1.113	0.610	0.683	0.658	0.375
H _{max,m} (mmol/L)	1.116	0.656	0.642	0.632	0.346
R _{max,e} (mmol/L.h)	0.011	0.004	0.008	0.008	0.006
R _{max,m} (mmol/L.h)	0.011	0.004	0.008	0.009	0.008
λ _e (h)	5.541	10.756	38.628	20.700	16.000
λ _m (h)	7.194	16.819	37.698	24.131	19.785

Table 4. 4 Comparison of experimental values and Modified Gobertz Model constants of *glnB* mutant *R.capsulatus* for different ammonium concentrations (subscript ‘e’ represents experimental values; subscript ‘m’ represents model values).

	2 mM glutamate (control)	1 mM NH₄Cl	2 mM NH₄Cl	3 mM NH₄Cl	5 mM NH₄Cl
r	0.997	0.986	0.996	0.993	0.992
H _{max,e} (mmol/L)	0.631	0.353	0.311	0.228	0.115
H _{max,m} (mmol/L)	0.618	0.335	0.31	0.236	0.121
R _{max,e} (mmol/L.h)	0.006	0.004	0.002	0.002	0.001
R _{max,m} (mmol/L.h)	0.006	0.003	0.002	0.002	0.001
λ _e (h)	17.142	16.625	21.000	24.682	16.250
λ _m (h)	17.309	10.024	30.101	26.453	14.981

The following conclusions can be drawn from Tables 4.3 and 4.4:

- i. The experimental data fit well to the model with r values very close to 1.
- ii. Experimental maximum cumulative hydrogen production values are quite close to the model values.
- iii. Experimental maximum hydrogen production rate values are quite close to the model values.
- vii. Maximum cumulative hydrogen production values decrease with initial ammonium concentration. That indicates the significance of ammonium concentration on hydrogen production.
- iv. Maximum hydrogen production obtained with 2 mM glutamate is 0.011 mmol/L for wild type and 0.006 for mutant strain.
- v. Experimental lag time values are similar to the lag time values obtained from the model.

4.3.4. Calculation of Substrate Conversion Efficiency, Yield, Molar Productivity, Light Conversion Efficiency and Product Yield Factor

Substrate conversion efficiency, yield, molar productivity, light conversion efficiency and product yield factor are important parameters in hydrogen production analyses. In this section, these parameters are individually described and calculated.

Substrate conversion efficiency is:

$$\frac{\text{number of moles of hydrogen produced}}{\text{stoichiometric number of moles of hydrogen that would be produced from full use of the initial substrates}} \times 100 \quad (4.8)$$

The substrate was acetic acid (30 mM). Theoretically, 4 moles of H₂ is produced from 1 mole of acetate as in Equation 1.2. Both moles of H₂ produced in the experiment and theoretical moles of H₂ that would be produced from complete utilization of 30 mM acetate were calculated. With these values obtained, substrate conversion efficiencies were calculated.

The calculated substrate conversion efficiencies of wild type and *glnB* mutant *R.capsulatus* were given in Figure 4.25 for different ammonium concentrations.

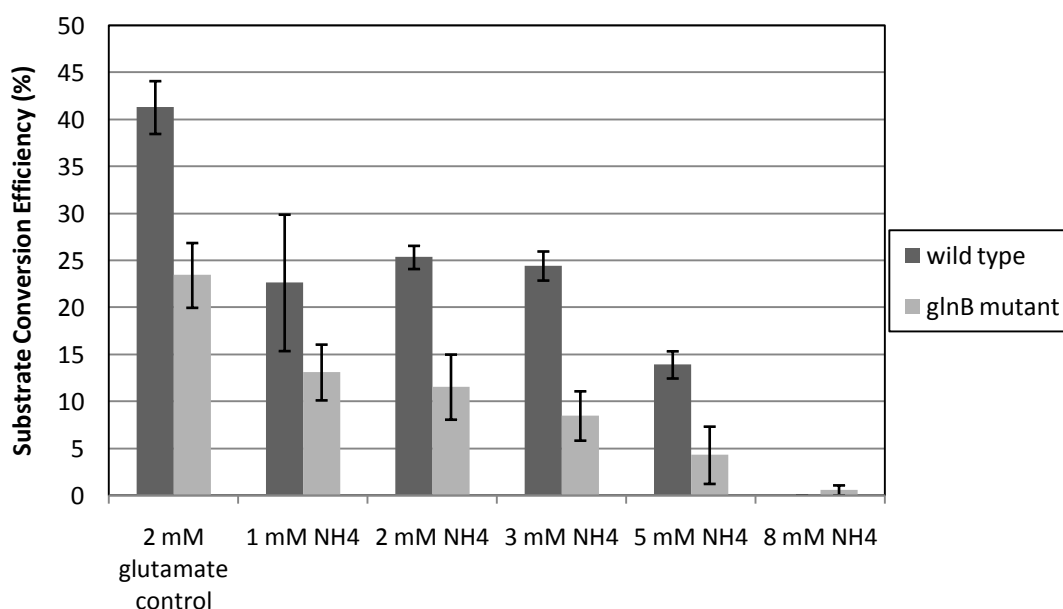


Figure 4. 25 Substrate conversion efficiency values for wild type and *glnB* mutant *R.capsulatus* for different ammonium concentrations

Molar productivity is:

$$\frac{\text{cumulative millimoles of hydrogen produced}}{\text{volume of culture (L) * t(hour)}} \quad (4.9)$$

In this equation, t is the duration of hydrogen production time from the end of the lag phase (λ) to the end of the hydrogen production. Molar productivity can be also considered as the ‘molar rate of production of hydrogen’. Molar productivity values calculated for wild type and *glnB* mutant *R.capsulatus* in different ammonium concentrations are given in Figure 4.26.

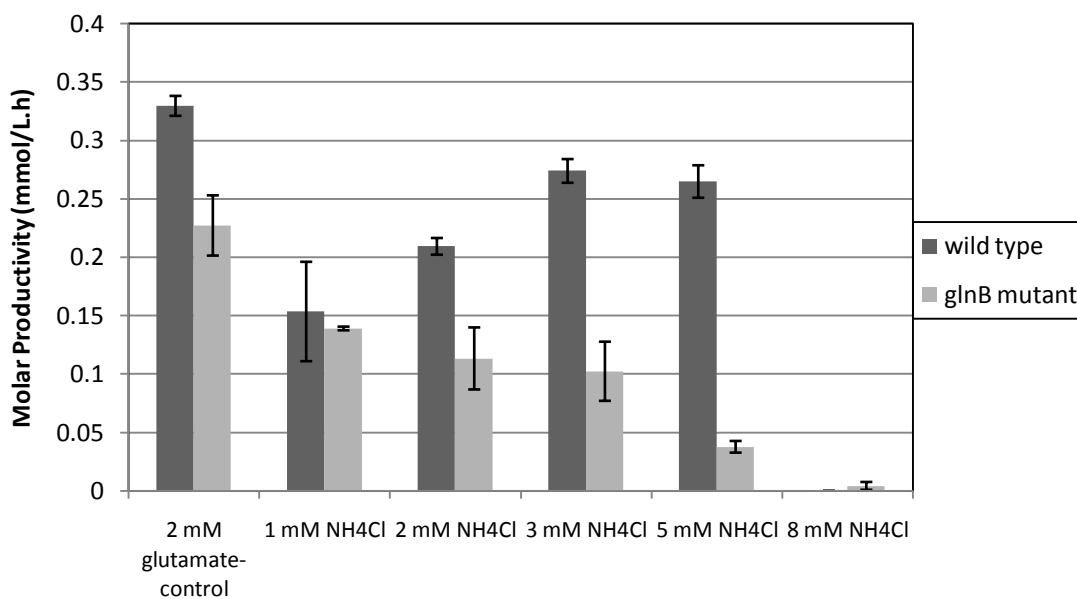


Figure 4. 26 Molar productivity values for wild type and *glnB* mutant *R.capsulatus* for different ammonium concentrations

Yield is:

$$\text{Yield} = \frac{\text{mass of hydrogen produced (g)}}{\text{total mass of substrates (acetate) utilized}} \quad (4.10)$$

Yield values for wild type and *glnB* mutant *R.capsulatus* for different ammonium concentrations are given in Figure 4.27.

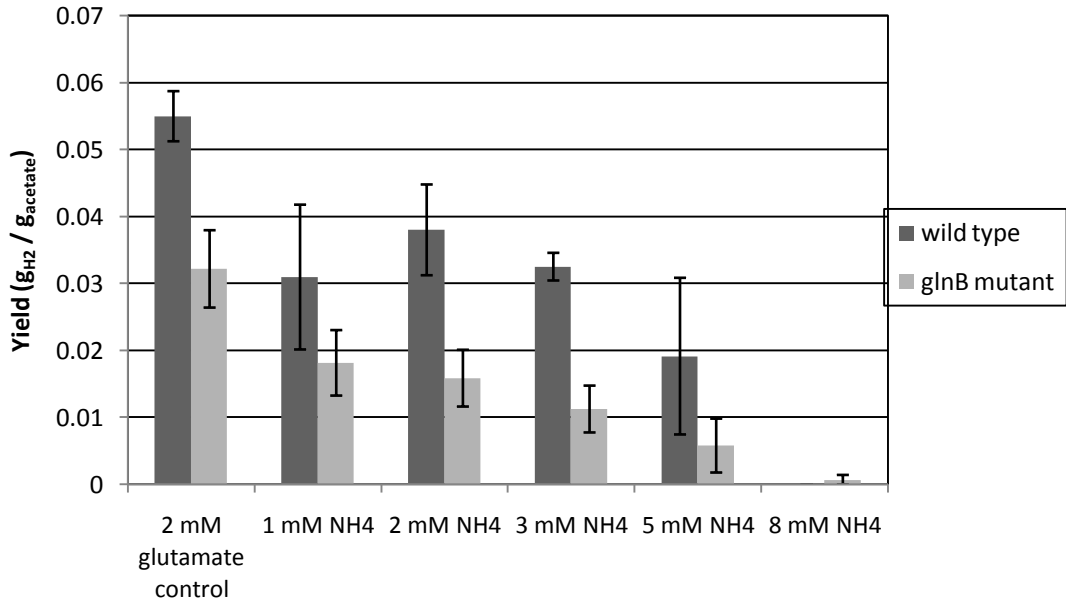


Figure 4. 27 Yield values for wild type and *glnB* mutant *R.capsulatus* for different ammonium concentrations

Light conversion efficiency is:

$$\eta(\%) = \frac{33.6 \times \rho_{H_2} \times V_{H_2}}{I \times A \times t} \times 100 \quad (4.11)$$

Light conversion efficiency (η) is defined as the ratio of the total energy value (heat of combustion) of the hydrogen that has been produced to the total energy input to the photobioreactor by light radiation. In the equation, V_{H_2} is the volume (L) of produced H_2 ; ρ_{H_2} is the density (g/L) of the produced hydrogen gas; I is the light

intensity (W/m^2), A is the irradiated area (m^2) and t is the duration of hydrogen production from the end of the lag phase (λ) to the end of the experiment.

The experiments were carried out in batch mode where the cell concentrations and the absorbed light intensities vary throughout the process. So, incident light intensity was used in the calculation of light conversion efficiency instead of the actual absorbed light intensity (Uyar et. al., 2007). Light conversion efficiencies for wild type and *glnB* mutant *R.capsulatus* for different ammonium concentrations are given in Figure 4.28.

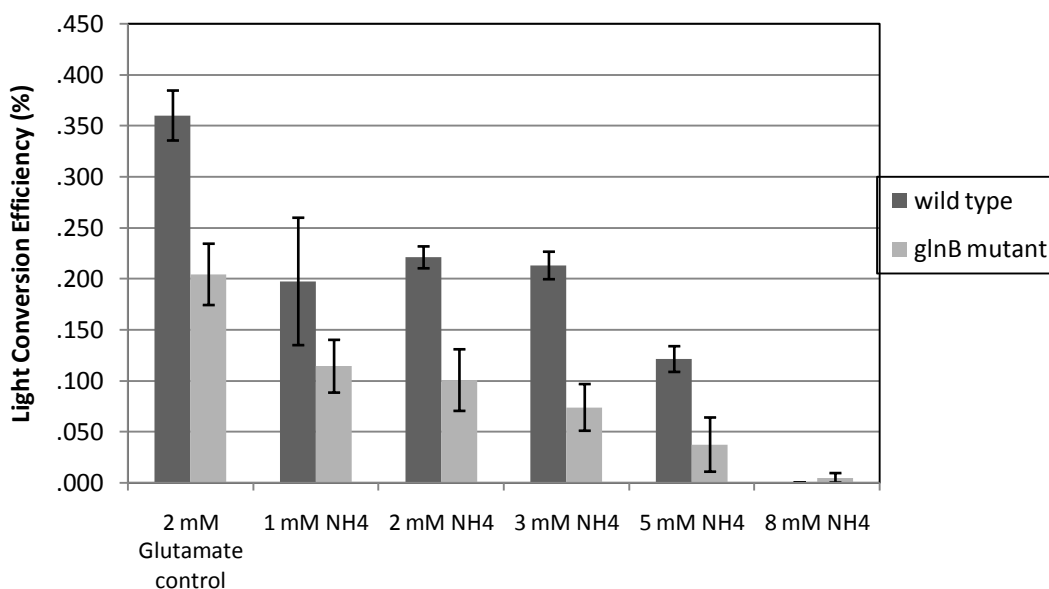


Figure 4. 28 Light conversion values for wild type and *glnB* mutant *R.capsulatus* for different ammonium concentrations

Final important parameter for the analysis of hydrogen production is the product yield factor, which is defined as the ratio of cumulative hydrogen produced in millimoles to the maximum dry cell weight in grams. The calculated values for wild

type and *glnB* mutant *R.capsulatus* in different ammonium concentrations are given in Figure 4.29.

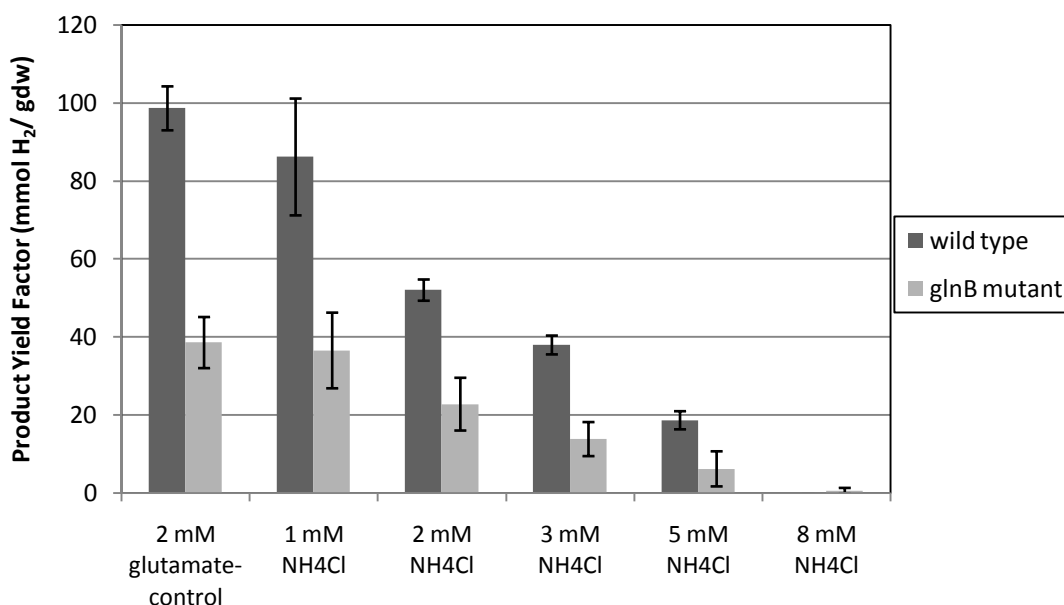


Figure 4. 29 Product yield factor values for wild type and *glnB* mutant *R.capsulatus* for different ammonium concentrations

From Figures 4.25-4.29, the effect of ammonium concentration on H₂ production was observed. As the ammonium concentration in the medium increased from 1 mM to 8 mM, the general trend was decrease in the values of substrate conversion efficiencies, molar productivities, yields, light conversion efficiencies and product yield factors. It might also be concluded that the H₂ production parameters of wild type *R.capsulatus* was higher than those of *glnB* mutant *R.capsulatus*.

4.3.5. Organic acid analysis of wild type and *glnB* mutant *R.capsulatus*

Acetic acid was the only organic acid found in the H₂ production medium. Throughout H₂ production experiment, the concentration of acetic acid decreases due

to the consumption by bacteria. On the other hand, the concentrations of some other organic acids, such as lactic acid, formic acid and propionic acid were determined to be slightly produced during process. The concentrations of these organic acids together with acetic acid concentration were determined for ~24 hour intervals by HPLC analyses (Section 3.5.1). The effect of different ammonium levels on the organic acid utilization and formation are illustrated in the following figures. A sample HPLC chromatogram and a sample calibration curve are given in AppendixE.

4.3.5.1. Acetate utilization

In Figure 4.23 and 4.24, the variations in the concentrations of acetic acid with respect to different ammonium levels in the wild type and *glnB* mutant *R.capsulatus* are given, respectively. For both wild type and *glnB* mutant *R.capsulatus*, most of the acetic acid present in the media was completely consumed. However, the decrease in acetic acid concentration was much more rapid in the media containing higher NH₄ concentrations. In the 8 mM NH₄Cl containing medium, most of the acetic acid was consumed in the first day and the rest of the acetic acid in the medium was consumed in the second day. As the NH₄Cl concentration of the medium decreased, the acetic acid was utilized with a moderate rate.

When the acetic acid utilization of wild type and *glnB* mutant *R.capsulatus* was compared, it is observed that there is no significant difference between them. The acetate could be successfully utilized by both strains. Moreover, the effect of ammonium on acetic acid consumption were similar both for *wild* and *glnB* strains.

Similar acetic acid utilization and growth pattern were observed for both wild and *glnB* strain. However, the H₂ production in the mutant strain was lower than the wild type. These observations strongly indicate that the excess PHB production by the mutant strain has the main responsibility for the low H₂ production.

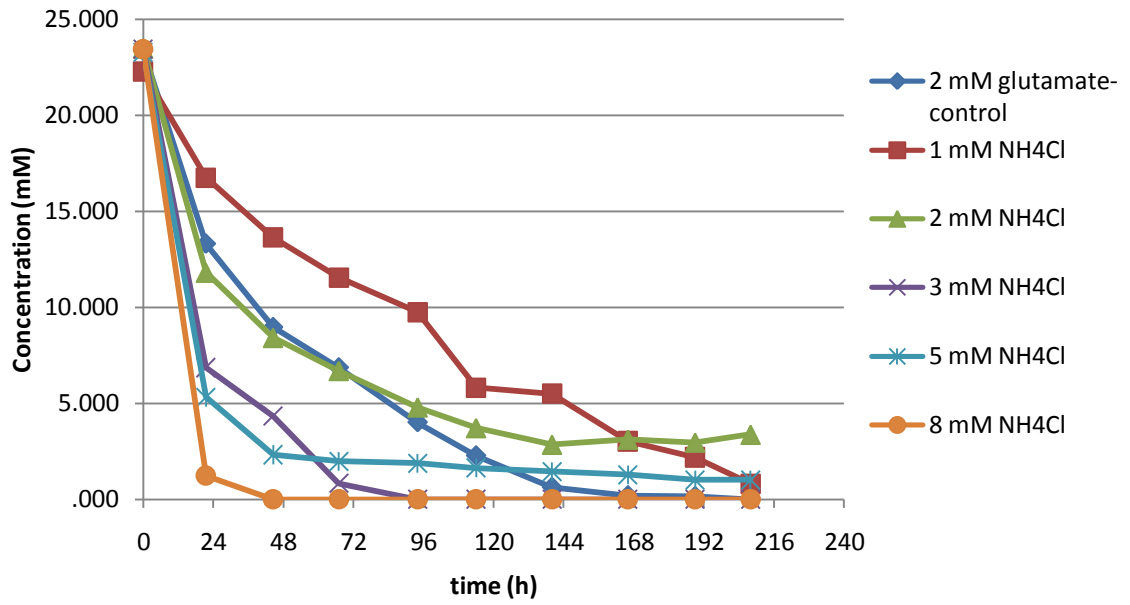


Figure 4. 30 Acetic acid consumption by wild type *R.capsulatus* in different ammonium levels

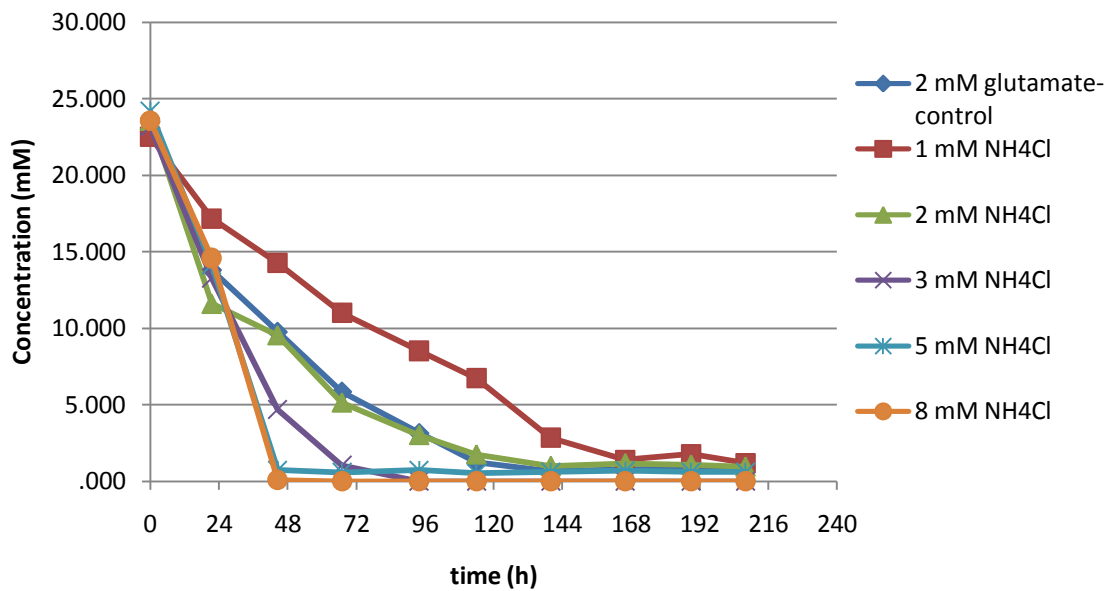


Figure 4. 31 Acetic acid consumption by *glnB* mutant *R.capsulatus* in different ammonium levels

4.3.5.2. Lactic acid, formic acid and propionic acid formation

Together with the consumption of the acetic acid as the carbon source, formation of lactic acid, formic acid and propionic acid were also observed. For both wild and *glnB* mutant *R.capsulatus*, the variations in the lactic acid, formic acid and propionic acid concentrations in different ammonium levels are given in Figure 4.25-4.26, Figure 4.27-4.28 and Figure 4.29-4.30, respectively.

As it is seen in Figure 4.25-4.26 and Figure 4.29-4.30, the concentrations of lactic acid and propionic acid are lower than 1mM, which are quite low values. So, the evaluation and interpretation of the variations of these results might not be meaningful. However, it can be deduced that organic acids started to accumulate after 3-4 days from the start of the experiment and consumed at the late days of the experiment.

Different from others, formic acid was accumulated to significant concentrations, up to 5 mM in the wild type bacteria with gradual increase in time. On the other hand, there was also considerable formic acid formation in the mutant strain; however the trend of *glnB* mutant was not gradual like wild type. There were rapid increases and decreases in the concentration of formic acid in the mutant strain. Formic acid formation during H₂ production was also observed by Sevinç (2010) and Androga (2009).

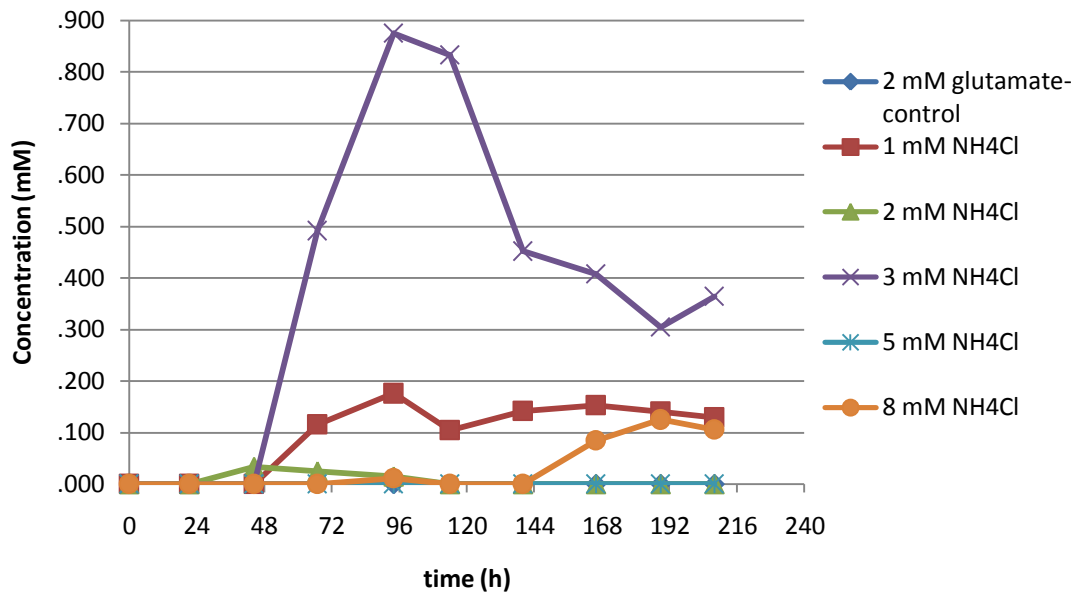


Figure 4. 32 Lactic acid formation by wild type *R. capsulatus* in different ammonium levels

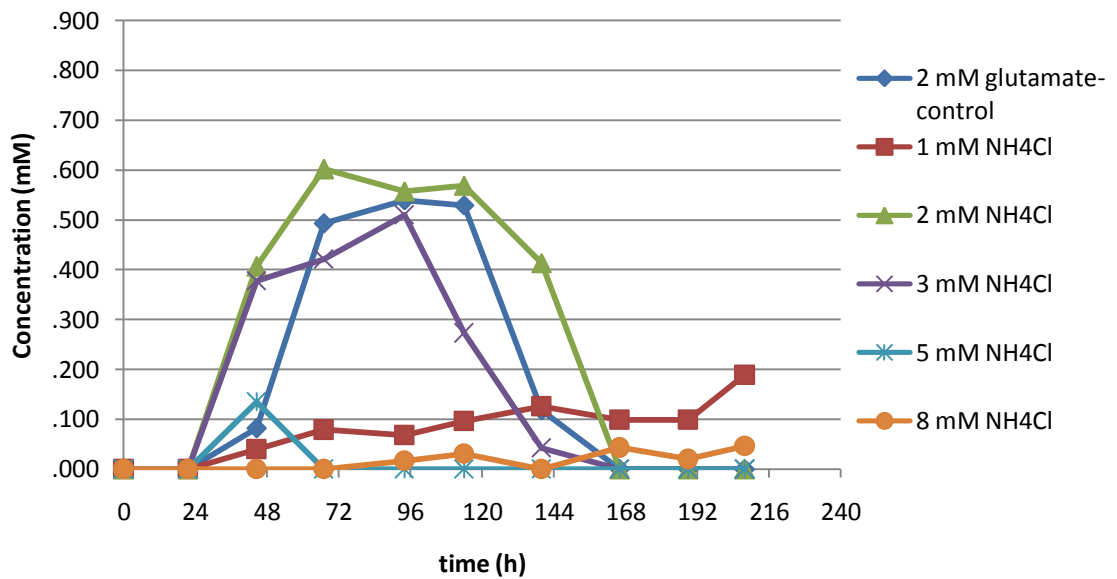


Figure 4. 33 Lactic acid formation by *glnB* mutant *R. capsulatus* in different ammonium levels

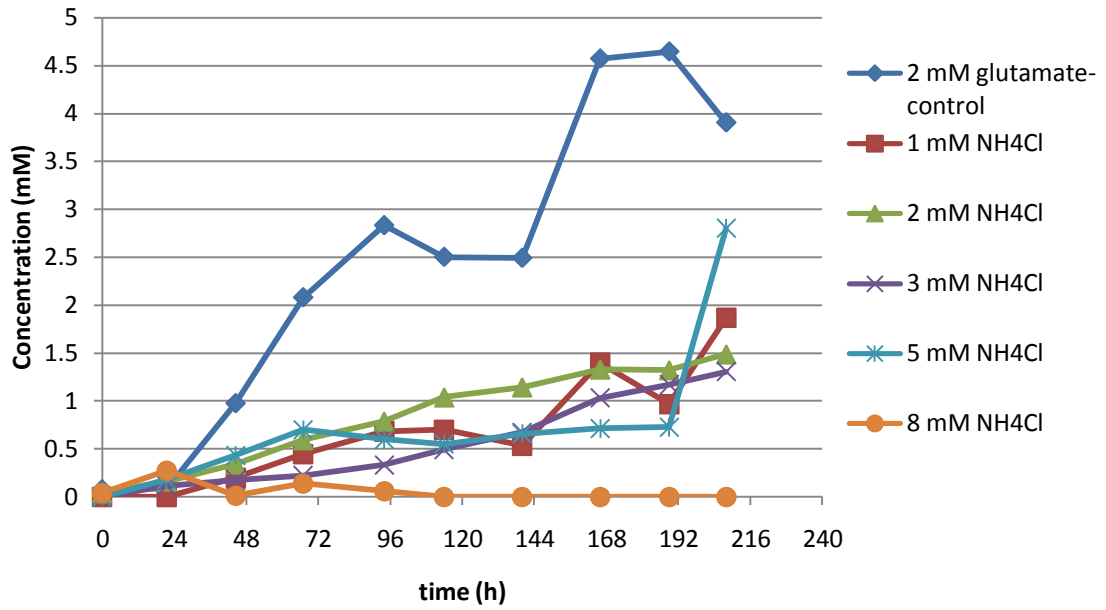


Figure 4. 34 Formic acid formation by wild type *R.capsulatus* in different ammonium levels

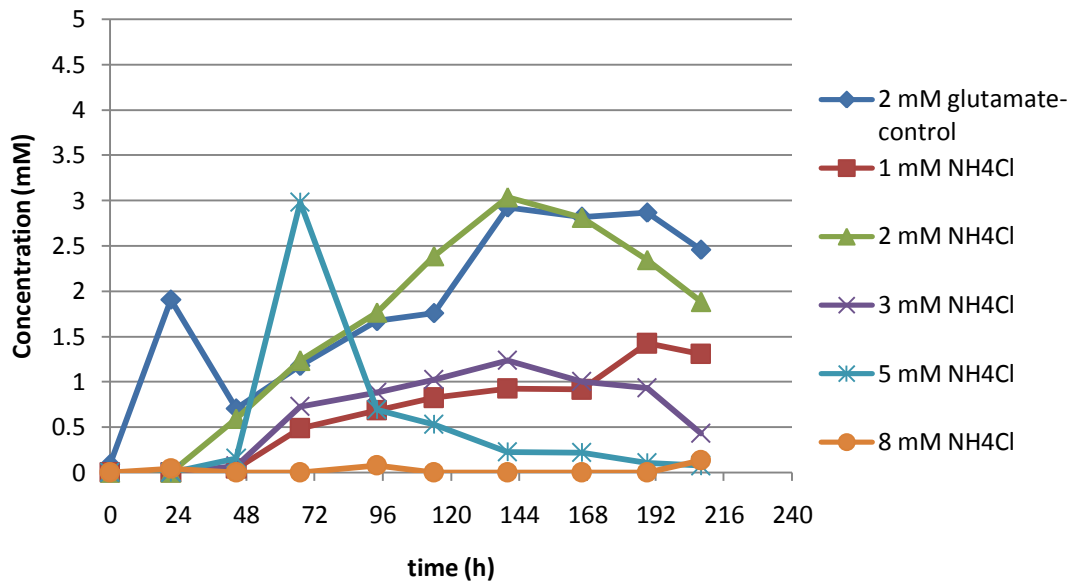


Figure 4. 35 Formic acid formation by *glnB* mutant *R.capsulatus* in different ammonium levels

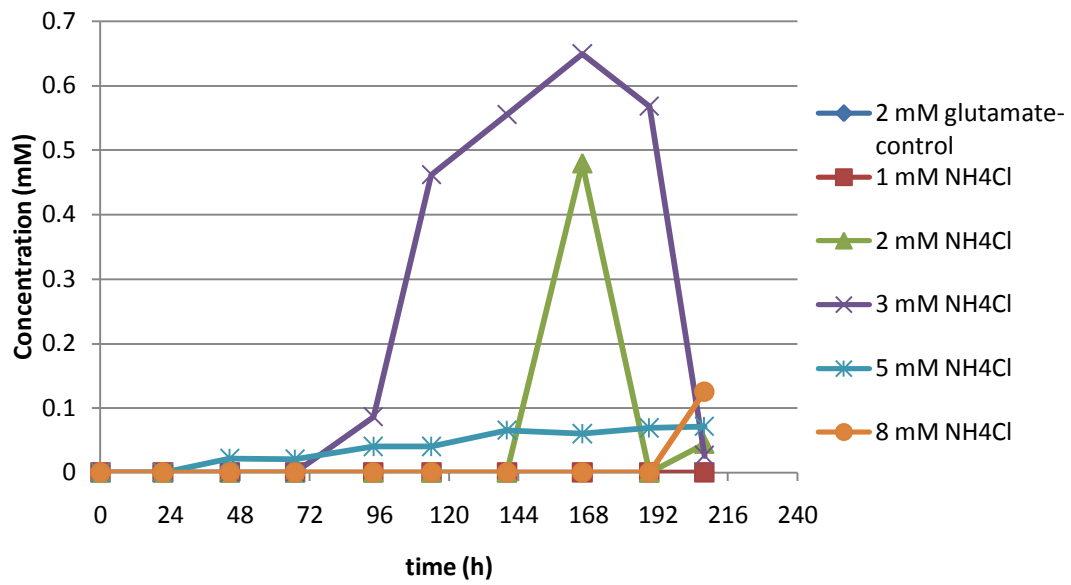


Figure 4. 36 Propionic acid formation by wild type *R. capsulatus* in different ammonium levels

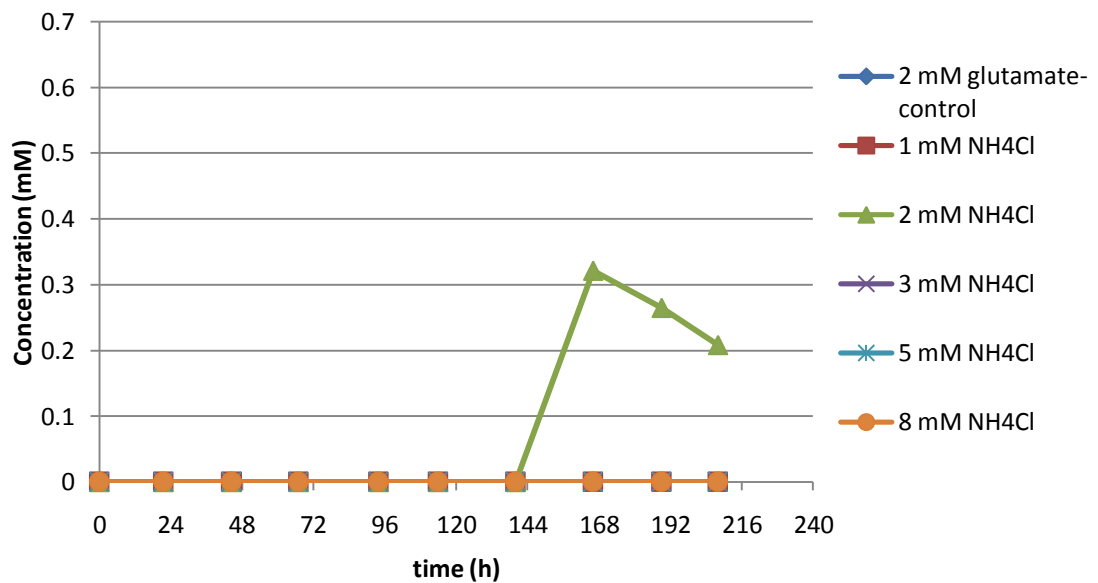


Figure 4. 37 Propionic acid formation by *glnB* mutant *R. capsulatus* in different ammonium levels

CHAPTER 5

CONCLUSION

In the present study, GlnB and GlnK (P_{II} signal transduction proteins), which have important roles in ammonium regulation of nitrogenase enzyme, were targeted to be inactivated. For this purpose, deletion mutations were introduced into *glnB* and *glnK* genes. *glnB* gene was successfully disrupted, however *glnK* mutant could not be selected. In order to distinguish the effect of *glnB* mutation on growth, pH and hydrogen production, *glnB* mutant *Rhodobacter capsulatus* was compared with the wild type strain. Moreover, the concentrations of acetic acid, lactic acid, formic acid and propionic acid in the cultures were determined periodically. Experimental data for the growth fitted well to Logistic Model and experimental data for hydrogen production fitted well to Modified Gompertz Model both for *glnB* mutant and the wild type strains

Based on the results obtained and discussion of these results, the followings were deduced:

- i. *glnB* mutant was successfully obtained. In this mutant, active GlnK protein might have compensated the absence of GlnB protein. So, ammonium still inhibited hydrogen production in the mutant strain.
- ii. In the case of *glnK* mutation, active GlnB protein might not compensate the absence of GlnK protein. Hence, *glnK* mutant might not be selected due to growth problems which might have arisen from the absence of GlnK activity in the cell.
- iii. P_{II} signal transduction protein - GlnK- would be an essential protein for the cell, since its mutant could not be selected.

- iv. Both *glnB* mutant and the wild type strains could grow efficiently on acetate as the sole carbon source in the medium. Moreover, moderate levels of lactic acid, formic acid and propionic acids were produced and utilized throughout the experiment.
- v. Specific growth rate of the *glnB* mutant *R.capsulatus* was less than wild type *R.capsulatus*.
- vi. The maximum biomass concentration increased with increasing ammonium concentration.
- vii. The pH of the cultures varied both for *glnB* mutant and the wild type strains, mainly due to the variations of organic acids in the medium. However, range of pH variations were in tolerable range.
- viii. The hydrogen production of both *glnB* mutant and the wild type strains were negatively affected from ammonium levels in the media. As the ammonium level increased in the medium, hydrogen production decreased due to the inhibition of nitrogenase by ammonium.
- ix. Hydrogen productivity of wild type *R.capsulatus* was greater than that of the *glnB* mutant *R.capsulatus*.
- x. Inactivation of only GlnB protein couldn't reveal the ammonium regulation on nitrogenase, since the hydrogen production of the *glnB* mutant was still affected from ammonium. This might be due to the presence of active GlnK protein in the cell, which still functions in the ammonium regulation. Complete inactivation of P_{II} proteins might be necessary for complete release of the regulation.

REFERENCES

Afşar N; Özgür E; Gügan M; De Vrije T; Yücel M; Gündüz U; Eroğlu I (2009). “Hydrogen production by *R.capsulatus* on dark fermenter effluent of potato steam peel hydrolysate”. Chemical Engineering Transactions, 18: 385-390.

Akkerman I; Janssen, M; Rocha, J; Wijffels, H R (2002). “Photobiological hydrogen production: photochemical efficiency and bioreactor design”. International Journal of Hydrogen Energy 27: 1195-1208.

Akköse S (2008). “Expression analysis of nitrogenase genes in *Rhodobacter sphaeroides* O.U.001 grown under different physiological conditions” M.sc. Thesis in Biology Department, Middle East Technical University, Ankara, Turkey

Akköse S; Gündüz U; Yücel M, Eroğlu I (2009). “Effects of ammonium ion, acetate and aerobic conditions on hydrogen production and expression levels of nitrogenase genes in *Rhodobacter sphaeroides* O.U.001”. International Journal of Hydrogen Energy 34: 8818-8827.

Aldor I S; Keasling J D (2003). “Process design for microbial plastic factories: metabolic engineering of polyhydroxyalkanoates”. Current Opinion in Biotechnology, 14:475–483

Amar M; Patriarca E J; Manco G; Bernard P; Riccio A; Lamberti A; Defez R; Iaccarino M (1994). “Regulation of nitrogen metabolism is altered in a *glnB* mutant strain of *Rhizobium leguminosarum*”. Molecular Microbiology 11: 685–693.

Androga D D (2009). "Biological hydrogen production on acetate in continuous panel photobioreactors using *Rhodobacter capsulatus*", M.sc. Thesis in Chemical Engineering Department, Middle East Technical University, Ankara, Turkey

Arcondeguy T; Jack R; Merrick M (2001). "P_{II} signal transduction proteins, pivotal players in microbial nitrogen control". *Microbiology and Molecular Biology Reviews* 65, no. 1: 80-105.

Asada Y; Miyake J (1999). "Photobiological hydrogen reduction". *Journal of Bioscience and Bioengineering* 88, no. 1: 1-6.

Atkinson M R; Ninfa A J (1998). "Role of the GlnK signal transduction protein in the regulation of nitrogen assimilation in *Escherichia coli*". *Molecular Microbiology* 29, no. 2: 431-447.

Ayub N D; Pettinari M J; Ruiz J A; López N I (2004). "A polyhydroxybutyrate-producing *Pseudomonas* sp. isolated from Antarctic environments with high stress resistance". *Current Microbiology*, Sep;49(3):170-4.

Basak N; Das D (2007). "The prospect of purple non-sulfur (PNS) photosynthetic bacteria for hydrogen production: the present state of the art". *Journal of Microbiology*, no. 23: 31-42.

Benemann J R (1997). "Feasibility analysis of photobiological hydrogen production". *International Journal of Hydrogen Energy* 22, no. 10/11: 979-987.

Benemann J R; Weare N M (1974). "Nitrogen fixation by *Anabaena cylindrica*. III. hydrogen-supported nitrogenase activity". *Archives of Microbiology* 101: 401-408.

Benemann J R; Weare N M (1974). "Hydrogen evolution by nitrogen-fixing *Anabaena cylindrica* cultures". *Science* 184, no. 4133: 174-175.

Biebl H; Pfennig N (1981). "Isolation of members of the family Rhodosprillaceae In: the prokaryotes" Editors: Starr, M P; Stolp H; Trüper H G; Balows A; Schlegel H G. New York: Springer-Verlag, 267-273

Blauwkamp T; Ninfa A J (2002). "Physiological role of the GlnK signal transduction protein of *Escherichia coli*: survival of nitrogen starvation". *Molecular Microbiology* 46, no. 1: 203-214.

Brandl H; Gross R A; Lenz R W; Lloyd R; Fuller R C (1991). "The accumulation of poly(3-hydroxyalkanoates) in *Rhodobacter sphaeroides*". *Archives of Microbiology* 155: 337-340.

Brandl H; Knee E J; Fuller R C; Gross R A; Lenz R W (1989). "The ability of the phototrophic bacterium *Rhodospirillum rubrum* to produce various poly(β -hydroxyalkanoates); potential sources for biodegradable polyesters". *International Journal of Biological Macromolecules* 11:49-55

Burris R H (1991). "Nitrogenases". *The journal of Biological Chemistry* 266, no. 15: 9339-9342.

Chatelet C; Meyer J (2001). "Mapping the interaction of the [2Fe-2S] *Clostridium pasteurianum* ferredoxin with nitrogenase MoFe protein". *Biochimica et Biophysica Acta* 1549:32–36.

Chen J S; Blanchard D K (1978). "Isolation and properties of a unidirectional H₂-oxidizing hydrogenase from the strictly anaerobic N₂-fixing bacterium *Clostridium pasteurianum* W5". *Biochemical and Biophysical Research Communications*; 84(4):1144–50.

Claassen P A M; De Vrije T (2006). "Non-thermal production of pure hydrogen from biomass: HYVOLUTION". *International Journal of Hydrogen Energy*, 31:1416-1423

Claassen P A M; De Vrije T (2005). "Integrated bioprocess for hydrogen production from biomass: Hyvolution". Proceedings International Hydrogen Energy Congress and Exhibition IHEC 2005 Istanbul, Turkey, 13-15 July 2005

Das D; Veziroglu N (2001). "Hydrogen production by biological processes: a survey of literature". International Journal of Hydrogen Energy 26: 13-28.

Dixon R; Kahn D (2004). "Genetic regulation of biological nitrogen fixation". Nature Reviews, Microbiology 2, no. August.

Donohue J T, Kaplan S (1991). "Genetic techniques in Rhodospirillaceae". Methods In Enzymology 24:459-485.

Drepper T; Groß S; Yakunin A F; Hallenbeck P C; Masepohl B; Klipp W (2003). "Role of GlnB and GlnK in ammonium control of both nitrogenase systems in the phototrophic bacterium *Rhodobacter capsulatus*". Microbiology 149: 2203-2212.

Eady R R (1996). "Structure- Function Relationships of Alternative Nitrogenases". Chemistry reviews 96: 3013-3030.

Erb J T; Re˘tey J, Fuchs G, Alber E B (2008). "Ethylmalonyl-CoA mutase from *Rhodobacter sphaeroides* defines a new subclade of coenzyme B12-dependent acyl-CoA mutases". Journal of Biological Chemistry 283:32283-93.

Erođlu E; Erođlu İ; Gündüz U; Turker L; Yucel M (2006). "Biological hydrogen production from olive mill wastewater with two-stage processes". International Journal of Hydrogen Energy 31: 1527-1535.

Erođlu İ; Tabanođlu A; Gündüz U; Erođlu E; Yücel M (2008). "Hydrogen production by *Rhodobacter sphaeroides* O.U.001 in a flat plate solar bioreactor". International Journal of Hydrogen Energy, 33:531-541

Fascetti E; Daddario E; Todini O; Robertiello A (1998). "Photosynthetic hydrogen evolution with volatile organic acids derived from the fermentation of source selected municipal solid wastes". *International Journal of Hydrogen Energy* 23, no. 9: 753-760.

Fedorov A S; Tsygankov A A; Rao K K; Hall D O (1998). "Hydrogen photoproduction by *Rhodobacter sphaeroides* immobilised on polyurethane foam". *Biotechnology Letters* 20: 1007.

Forchhammer K (2004). "Global carbon/nitrogen control by PII signal transduction in cyanobacteria: from signals to targets". *FEMS Microbiology Reviews* 28: 319-333.

Forchhammer K (2008). "PII signal transducers: novel functional and structural insights". *Trends in Microbiology*, no. January: 65-72.

Foster-Hartney D; Kranz R G (1994). "The *Rhodobacter capsulatus glnB* Gene is regulated by NtrC at tandem rpoN-independent promoters". *Journal of Bacteriology* 176, no. 16: 5171-5176.

Fuller R C (1995). "Polyesters and photosynthetic bacteria. From lipid cellular inclusions to microbial thermoplastics". In: *Anoxygenic Photosynthetic Bacteria* (Blankenship R; Madigan M; Bauer C; Editors), pp. 973-990. Kluwer, Dordrecht.

Gest H, Kamen M D (1949). "Photoproduction of molecular hydrogen by *Rhodospirillum rubrum*". *Science*; 109:558-9.

Ghirardi M L; Togasaki R K; Seibert M (1997). "Oxygen sensitivity of algal H₂-production". *Applied Biochemistry and Biotechnology* 63-65: 141-51.

Gross A R; Ulmer H W; Lenz R W; Tshudy J D; Udon C P; Brandt H; Füller R C (1992). “Biodeuteration of poly (β -hydroxybutyrate)”. *International Journal of Biological Macromolecules* 14: 33–40.

Gussin G N; Ronson C W; Ausubel F M (1986). “Regulation of nitrogen fixation genes”. *Annual Review of Genetics*. 20: 567-591.

Hall, D O; Markov S A; Watanabe Y; Rao K K (1995). “The potential applications of cyanobacterial photosynthesis for clean technologies”, *Photosynthesis Research* 46, 159–167

Hallenbeck P C; Gennaro G (1998). “Stopped-flow kinetic studies of low potential electron carriers of the photosynthetic bacterium, *Rhodobacter capsulatus*: Ferredoxin I and *NifF*”. *Biochimica et Biophysica Acta* 1365:435–442.

Hallenbeck P C; Ghosh D (1987). “Molecular aspects of nitrogen fixation by photosynthetic prokaryotes”. *Critical Reviews in Microbiology* 14, no. 1: 1-48.

Hallenbeck P C; Benemann J R. (2002). “Biological hydrogen production; fundamentals and limiting processes”. *International Journal of Hydrogen Energy* 27: 1185-1193.

Hallenbeck P C. Personal communication, 18th World Hydrogen Energy Conference (WHEC) in Essen, Germany. May 16-21, 2010.

Hanson T E; Forchhammer K; De Marsac N T; Meeks J C (1998). “Characterization of the *glnB* gene product of *Nostoc punctiforme* strain ATCC 29133: *glnB* or the PII protein may be essential”. *Microbiology* 144: 1537-47.

Hawkes F; Dinsdale R; Hawkes D L; Hussy I (2002). "Sustainable fermentative hydrogen production: challenges for process optimization". *International Journal of Hydrogen Energy* 27, no. 11-12: 1339-1347.

Henson B J; Watson L E; Barnum S R (2004). "The evolutionary history of nitrogen fixation, as assessed by *NifD*". *The Journal of Molecular Evolution*, 58:390–399

Herrero M; Lorenzo V; Timmis K N (1990). "Transposon vectors containing non-antibiotic resistance selection markers for cloning and stable chromosomal insertion of foreign genes in gram-negative bacteria". *Journal of Bacteriology* 172:6557–6567.

Hustede E; Steinbuchel A; Schlegel H G (1993). "Relationship between the photoproduction of hydrogen and the accumulation of PHB in non-sulphur purple bacteria". *Applied Microbiology and Biotechnology* 39: 87-93.

Igarashi R Y; Seefeldt L C (2003). "Nitrogen fixation: The mechanism of the Mo-dependent nitrogenase". *Critical Reviews in Biochemistry and Molecular Biology* 38: 351-384.

Imhoff J. F; Truper H G; Pfennig N (1984). "Rearrangement of the species and genera of the phototrophic purple nonsulfur bacteria". *International Journal of Systematic Bacteriology* 34, no. 3: 340-343.

Imhoff F J (1995). "Taxonomy and physiology of phototropic purple bacteria and green sulfur bacteria". *Anoxygenic Photosynthetic Bacteria* 2: 1-15

Javelle A; Merrick M (2005). "Complex formation between AmtB and GlnK: an ancestral role in prokaryotic nitrogen control". *Biochemical Society transactions* 33, no. part 1: 170-2.

Javelle A; Severi E; Thornton J; Merrick M (2004). “Ammonium sensing in *Escherichia coli*. Role of the ammonium transporter AmtB and AmtB-GlnK complex formation”. *The Journal of Biological Chemistry* 279, no. 10: 8530-8538.

Jiang P; Peliska J A; Ninfa A J (1998). “Enzymological characterization of the signal-transducing uridylyltransferase/uridylyl-removing enzyme (EC 2.7.7.59) of *Escherichia coli* and its interaction with the PII protein”. *Biochemistry* 37: 12782-12794.

Kadar Z; Vrije T; van Noorden G E; Budde M A W; Szengyel Z; Reczy K; Claassen P A M (2004). “Yields from glucose, xylose, and paper sludge hydrolysate during hydrogen production by the extreme thermophile *Caldicellulosiruptor saccharolyticus*”, *Biotechnology and Applied Biochemistry* 113–116:497–508.

Kapdan I; Kargi F (2006). “Biohydrogen production from waste materials”. *Enzyme and Microbial Technology* 38: 569-582.

Kars G; Gündüz U; Yücel M; Rakhely G; Kovacs K L; Eroğlu I (2009). “Evaluation of hydrogen production by *Rhodobacter sphaeroides* O.U.001 and its *hupSL* deficient mutant using acetate and malate as carbon sources”. *International Journal of Hydrogen Energy* 34: 2184-2190.

Kars G; Gündüz U (2010). “Towards a super H₂ producer: Improvements in photofermentative biohydrogen production by genetic manipulations”. *International Journal of Hydrogen Energy* 35: 6646-6656.

Khatipov, E, M Miyake, J Miyake, and Y Asada (1998). “Accumulation of poly- β -hydroxybutyrate by *Rhodobacter sphaeroides* on various carbon and nitrogen substrates”. *FEMS Microbiology Letters* 162: 39-45.

Kim E; Lee M; Kim M; Lee J (2008). “Molecular hydrogen production by nitrogenase of *Rhodobacter sphaeroides* and by Fe-only hydrogenase of *Rhodospirillum rubrum*. International Journal of Hydrogen Energy 33: 1516-1521.

Kim M; Baek J; Lee J K (2006). “Comparison of H₂ accumulation by *Rhodobacter sphaeroides* KD131 and its uptake hydrogenase and PHB synthase deficient mutant”. International Journal of Hydrogen Energy 31: 121-127.

Klemme J H (1993). “Photoproduction of hydrogen by purple bacteria: a critical evaluation of the rate limiting steps”. Z Naturf; 48c:482–7.

Koku H; Eroğlu I; Gündüz U; Yücel M; Türker L (2002). “Aspects of the metabolism of hydrogen production by *Rhodobacter sphaeroides*”. International Journal of Hydrogen Energy 27: 1315-1329.

Koku H, Eroğlu I; Gündüz U; Yücel M; Türker L (2003). “Kinetics of biological hydrogen production by the photosynthetic bacterium *Rhodobacter sphaeroides* O.U. 001”, International Journal of Hydrogen Energy, 28: 381-388

Kovacs K L; Bagyinka C; Bodrossy L; Csaki R; Fodor B; Györfi K; Hanczar T; Kalman M; Osz J; Perel K; Polyak B; Rakhely G; Takacs M; Toth A; Tusz J (2000). “Recent advances in biohydrogen research”. European Journal of Physiology 439: 81-83.

Kovacs K L; Kovacs A T; Maroti G; Bagi Z; Csanadi G, Perei K; Balint B (2004). “Improvement of biohydrogen production and intensification of biogas formation”. Reviews in Environmental Science and Bio/Technology 3: 321-330.

Leigh J A; Dodsworth J A (2007). “Nitrogen regulation in bacteria and archaea”. Annual Review of Microbiology 61: 349-377.

Levin D B; Pitt L; Love M (2004). “Biohydrogen production: prospects and limitations to practical application”. *International Journal of Hydrogen Energy* 29: 173 - 185.

Liebergessell M; Hustede E; Timm A; Steinbtichel A; Fuller R C; Lenz R W; Schlegel H G (1991). “Formation of poly(3-hydroxyalkanoates) by phototrophic and chemolithotrophic bacteria”. *Archives of Microbiology* 155 : 415-421

Little R; Reyes-Ramirez F; Zhang Y; van Heeswijk W C; Dixon R (2000). “Signal transduction to the *Azotobacter vinelandii* NifL-NifA regulatory system is influenced directly by interaction with 2-oxoglutarate and the PII regulatory protein”. *EMBO J* 19, 6041–6050.

Magasanik B (1982). “Genetic control of nitrogen assimilation in bacteria”. *Annual Review of Genetics* 16: 135-168.

Masepohl B; Drepper T; Paschen A; Groß S; Pawlowski A; Raabe K; Riedel K; Klipp W (2002). “Regulation of nitrogen fixation in the phototrophic purple bacterium *Rhodobacter capsulatus*”. *Journal of Molecular Microbiology and Biotechnology* 4, no. 3: 243-248.

Masepohl B; Klipp W; Puhler A (1988). “Genetic characterization and sequence analysis of the duplicated *nifA/nifB* gene region of *Rhodobacter capsulatus*”. *Molecular and General Genetics*. 212: 27–37.

Masepohl B; Drepper T; Klipp W (2004). “Genetics and regulation of nitrogen fixation in free-living bacteria” (Klipp W; Masepohl B; Gallon J R and Newton W E; editors.), pp. 141-173, Kluwer Academic Publishers, Netherlands.

Meherkotay S; Das D (2008). “Biohydrogen as a renewable energy resource-Prospects and potentials”. *International Journal of Hydrogen Energy* 33: 258-263.

Meletzus D; Rudnick P; Doetsch N; Green A; Kennedy C (1998). "Characterization of the *glnK-amtB* operon of *Azotobacter vinelandii*". *Journal of Bacteriology* 180, no. 12: 3260-3264.

Melis A (2002). "Green alga hydrogen production: progress, challenges and prospects". *International Journal of Hydrogen Energy* 27: 1217-1228.

Meyer J; Kelley B; Vignais P M (1978). "Nitrogen fixation and hydrogen metabolism in photosynthetic bacteria". *Biochimie* 60, 245-260.

Michel-Reydellet N; Kaminski P A (1999). "*Azorhizobium caulinodans* PII and GlnK proteins control nitrogen fixation and ammonia assimilation". *Journal of bacteriology* 181, no. 8: 2655-8.

Michel-Reydellet N; Desnoues N; De Zamaroczy M; Elmerich C; Kaminski P A (1998). "Characterisation of the *glnK-amtB* operon and the involvement of AmtB in methylammonium uptake in *Azorhizobium caulinodans*. *Molecular and General Genetics* 258: 671-677.

Miyake J (1990). "Application of photosynthetic systems for energy conversion". In: Veziroglu T N, Takashashi P K (editors). *Hydrogen energy progress VIII. Proceedings 8th WHEC held in Hawaii*. New York, Elsevier Science Pub Co., pp 755-764.

Miyake J; Mao X Y; Kawamura S (1984). "Photoproduction of hydrogen from glucose by a co-culture of a photosynthetic bacterium and *Clostridium butyricum*. *Journal of Fermentation Technology* , 62, 531-535.

Miyamoto K (1997). "Renewable biological systems for alternative sustainable energy production" FAO Agricultural Services Bulletin (edited by Miyamoto K), Food and Agriculture Organization of the United Nation, pp:1-5

Momirlan M; Veziroğlu T N (2002). "Current status of hydrogen energy". Renewable and Sustainable Energy Reviews 6: 141-179

Momirlan M; Veziroglu T (1999). "Recent directions of world hydrogen production". Renewable and Sustainable Energy Reviews 3: 219-231.

Nath K; Das D (2004). "Improvement of fermentative hydrogen production: various approaches". Applied microbiology and biotechnology 65: 520-9.

Nath K; Das D (2006). "Amelioration of biohydrogen production by a two-stage fermentation process". Industrial Biotechnology; 2:44-7.

Niel E W J V, Budde M A W; De Haas G G; Van Der Wal F J; Claassen P A M; Stams A J M (2002). "Distinctive properties of high hydrogen producing extreme thermophiles, *Caldicellulosiruptor saccharolyticus* and *Thermotoga elfii*". International Journal of Hydrogen Energy 27: 1391-1398.

Ninfa A J; Atkinson M R (2000). "PII signal transduction proteins". Trends in Microbiology 8, no. 4: 172-179.

Oh Y K; Seol E H; Kim M S; Park S (2004). "Photoproduction of hydrogen from acetate by a chemoheterotrophic bacterium *Rhodospseudomonas palustris* P4". International Journal of Hydrogen Energy 29: 1115 - 1121.

Omar M; Patriarca E J; Manco G; Bernard P; Riccio A; Lamberti A; Defez R; Laccarino M (1994). "Regulation of nitrogen metabolism is altered in a *glnB* mutant strain of *Rhizobium leguminosarum*". Molecular Microbiology 11, no. 4: 685-693.

Paschen A; Drepper T; Masepohl B; Klipp W (2001). “*Rhodobacter capsulatus nifA* mutants mediating *nif* gene expression in the presence of ammonium”. FEMS Microbiology Letters 200: 207-213.

Pellerin N B; Gest H (1983). “Diagnostic features of the photosynthetic bacterium *Rhodospseudomonas sphaeroides*”, Current Microbiology, 9: 339-344.

Rees D C; Howard J B (2000). “Nitrogenase: standing at the crossroads”. Current Opinion in Chemical Biology 4: 559-566.

Reith J H; Wijffels R H; Barten H (2003). “Bio-methane and bio-hydrogen: Status and perspectives of biological methane and hydrogen production”. The Hague: Smiet offset; p. 103–23.

Ribbe M; Gadkari D; Meyer O (1997). “N₂ fixation by *Streptomyces thermoautotrophicus* involves a molybdenum-dinitrogenase and a manganese-superoxide oxidoreductase that couple N₂ reduction to the oxidation of superoxide produced from O₂ by a molybdenum-CO dehydrogenase”. Journal of Biological Chemistry 272:26627-26633.

Rhee S G, Park S C; Koo J H (1985). “The role of adenylyltransferase and uridylyltransferase in the regulation of glutamine synthetase in *Escherichia coli*”. Current Topics In Cellular Regulation 27: 221-232.

Robson R L; Eady R R; Richardson T H; Miller R W; Hawkins M; Postgate J R (1986). “The alternative nitrogenase of *Azotobacter chroococcum* is a vanadium enzyme”, Nature (London). 322, 388-390.

Rocha J S; Barbosa M J; Wijffels R H (2001). “Hydrogen production by photosynthetic bacteria: Culture media, yields and efficiencies”, In: Miyake J,

Matsunaga T; San Pietro A (Editors), Biohydrogen II - An Approach to Environmentally Acceptable Technology, Elsevier Science Ltd., UK, 3-32.

Ozgür E; Mars A E; Peksel Ö; Louwerse A; Yücel M; Gündüz U; P A M Claassen; Eroğlu I (2010). "Biohydrogen production from beet molasses by sequential dark and photofermentation". International Journal of Hydrogen Energy 35: 511-517.

Ozgür E; Uyar B; Öztürk Y; Yücel M; Gündüz U; Eroğlu I (2010). "Biohydrogen production by *Rhodobacter capsulatus* on acetate at fluctuating temperatures". Resources, Conservation and Recycling 54: 310-314.

Rosen M A; Scott D S (1992). Hydrogen energy progress IX, Proceedings of the Ninth World Hydrogen Energy Conference. Paris (France), 1992: 457.

Rudnick P; Meletzus D; Green A; He L; Kennedy C (1997). "Regulation of nitrogen fixation by ammonium in diazotrophic species of proteobacteria". Soil Biology and Biochemistry 29, no. 5-6: 831-841.

Sambrook J; Fritsch E F; Maniatis T (1989). "Molecular cloning: A laboratory manual". Cold Spring Harbor, NY: Cold Spring Harbor Laboratory Press

Sasikala K; Ramana C V; Rao P R; Kovacs K L (1993). "Anoxygenic phototrophic bacteria: physiology and advances in hydrogen technology". Advances in Applied Microbiology 10:211-215

Sasikala K; Ramana C H V; Rao P R; Subrahmanyam M (1990). "Effect of gas phase on the photoproduction of hydrogen and substrate conversion efficiency in the photosynthetic bacterium *Rhodobacter sphaeroides* O.U.001", International Journal of Hydrogen Energy, 15: 795-797.

Sasikala K; Ramana C H V; Rao P R (1991). “Environmental regulation for optimal biomass yield and photoproduction of hydrogen by *Rhodobacter sphaeroides* O.U.001”, International Journal of Hydrogen Energy, 16: 597-601

Sasikal K; Ramana C H V; Rao P R (1995). “Regulation of simultaneous hydrogen photoproduction during growth by pH and glutamate in *Rhodobacter sphaeroides* O.U.001”, International Journal of Hydrogen Energy, 20: 123-126.

Seibert M; Flynn T Y; Ghirardi M L (2001). “Strategies for improving oxygen tolerance of algal hydrogen production”. In: Miyake J, Matsunaga T, San Pietro A, editors. Biohydrogen II. Amsterdam: Pergamon, Elsevier Science, 2001. p. 67–77.

Senior P J (1975). “Regulation of nitrogen metabolism in *Escherichia coli* and *Klebsiella aerogenes*: studies with the continuous-culture technique”. Journal of Bacteriology. 123, 407–418

Sevinç P (2010). “Kinetic analyses of the effects of temperature and light intensity on growth, hydrogen production and organic acid utilization by *Rhodobacter capsulatus*”, M.sc. thesis in Biotechnology Engineering Department, Middle East Technical University, Ankara, Turkey

Schafer A; Tauch A; Jager W; Kalinowski J; Thierbach G; Pühler A (1994). “Small mobilizable multi-purpose cloning vectors derived from the *Escherichia coli* plasmids pK18 and pK19: selection of defined deletions in the chromosome of *Corynebacterium glutamicum*. Gene. 1994:145;69-73.

Siemann S; Schneider K; Dröttboom M; Müller A (2002). “The Fe-only nitrogenase and Mo nitrogenase from *Rhodobacter capsulatus*. A comparative study on the redox properties of the metal clusters present in the dinitrogenase components”. European Journal of Biochemistry 269, 1650–1661.

Stadtman E R (2001). “The story of glutamine synthetase regulation”. *The Journal of Biological Chemistry* 276, no. 48: 44357-44364.

Steinbuechel A (1991). “Polyhydroxyalkanoic acid”. In: *Biomaterials* (Byrom, D., Editor.), pp. 125-213. Stockton Press, New York.

Türkarıslan S; Yiđit D O; Aslan K; Erođlu I, Gündüz U (1998). “Photobiological hydrogen production by *Rhodobacter sphaeroides* O.U. 001 by utilization of waste water from milk industry”. In: Zaborsky OR; Benemann J R; Matsunaga T; Miyake J; Pietro A S; editors. *Biohydrogen*. New York: Plenum Press; p. 151–6.

Tsygankov A A (2007). “Biological generation of hydrogen”. *Russian Journal of General Chemistry* 77, no. 4: 685-693.

Uyar B (2008). “Hydrogen production by microorganisms in solar bioreactor”, Ph.D. Thesis in Biotechnology Engineering Department, Middle East Technical University, Ankara, Turkey

Valdez-Vazquez I; Poggi-Varaldo H M (2009). “Hydrogen production by fermentative consortia”. *Renewable and Sustainable Energy Reviews* 13: 1000-1013.

Vignais P M; Billoud B; Meyer J (2001). “Classification and phylogeny of hydrogenases”. *FEMS Microbiology Reviews* 25: 455-501.

Vignais P M; Colbeau A; Willison J C; Jouanneau Y (1985). “Hydrogenase, nitrogenase, and hydrogen metabolism in the photosynthetic bacteria”. *Advances in Microbial Physiology*. 26, 155-234.

Waligórska M; Seifert K; Szymańska K; Łaniecki M (2006). “Optimization of activation conditions of *Rhodobacter sphaeroides* in hydrogen generation process”. *Journal of Applied Microbiology* 101: 775-84.

Wall J D; Gest H (1979). “Derepression of nitrogenase activity in glutamine auxotrophs of *Rhodopseudomonas capsulate*”. Journal of Bacteriology 137, no. 3: 1459-1463.

Westby C A; Enderlin C S; Steinberg N A; Joseph C M; Meeks J C (1987). “Assimilation of NH₄ *spirillum brasiliense* grown under nitrogen limitation and excess”. Journal of Bacteriology 169: 4211–4214

Woodward J; Orr M; Corday K; Greenbaum E (2000). “Enzymatic production of biohydrogen”. Nature 405:1014–1015

Wray L; Atkinson M; Fisher S (1994). “The nitrogen-regulated *Bacillus subtilis* nrgAB operon encodes a membrane protein and a protein highly similar to the *Escherichia coli* glnB-encoded PII”. Journal of Bacteriology 176:108–114.

Yetiş M; Gündüz U; Eroğlu I; Yücel M; Türker L (2000). “Photoproduction of hydrogen from sugar refinery wastewater by *Rhodobacter sphaeroides* O.U. 001. International Journal of Hydrogen Energy 25:1035–41.

Yiğit D Ö; Gündüz U; Eroğlu I; Türker L; Yücel M (1999) “Identification of by-products in hydrogen producing bacteria; *Rhodobacter sphaeroides* O.U. 001 grown in the waste water of a sugar refinery” Journal of Biotechnology 70 125–131

Zhang Y; Pohlmann E L; Ludden P W; Roberts G P (2001). “Functional characterization of three GlnB homologs in the photosynthetic bacterium *Rhodospirillum rubrum*: Roles in sensing ammonium and energy status”. Journal of Bacteriology 183, no. 21: 6159-6168.

Zhang Y; Pohlmann E L; Conrad M C; Roberts G P (2006). “The poor growth of *Rhodospirillum rubrum* mutants lacking PII proteins is due to an excess of glutamine synthetase activity”. Molecular Microbiology 61, no. 2: 497-510.

Zhang Y; Pohlmann E L; Ludden P W; Roberts G P (2000). "Mutagenesis and functional characterization of the *glnB*, *glnA*, and *nifA* genes from the photosynthetic bacterium *Rhodospirillum rubrum*". *Journal of Bacteriology* 182, no. 4: 983-992.

de Zamaroczy M (1998). "Structural homologues P(II) and P(Z) of *Azospirillum brasilense* provide intracellular signalling for selective regulation of various nitrogen-dependent functions. *Molecular Microbiology* 29, no. 2: 449-463.

van Heeswijk W C; Hoving S; Molenaar D; Stegeman B; Kahn D; Westerhoff H V (1996). "An alternative PII protein in the regulation of glutamine synthetase in *Escherichia coli*". *Molecular Microbiology* 21, no. 1: 133-146.

Yamagishi K (1995). "Interim evaluation report of development of environmentally friendly technology for the production of hydrogen". New Energy and Industrial Technology Development Organization, Japan.

APPENDIX A

GROWTH MEDIA

COMPOSITION OF GROWTH MEDIUM FOR E.COLI

LB medium is used for proliferation of *E.coli*. 20 g of LB is dissolved in 1 liter of distilled water.

COMPOSITION OF GROWTH AND HYDROGEN PRODUCTION MEDIA FOR R.CAPSULATUS

Ferric citrate solution (50x):

5 g Fe-citrate was dissolved in 100 ml distilled water and autoclaving for sterilization.

Table A. 1 The compositions of the BP media containing acetate and malate as sole carbon sources. The growth media are 20/10 acetate/glutamate (A/G) and 7.5/10 malate/glutamate (M/G) containing media. The H₂ production medium is 30/2 acetate/glutamate (A/G) medium

Medium Composition (1000 ml)	Growth Medium (20/10 A/G)	Hydrogen Production Medium (30/2 A/G)	Growth Medium (7.5/10 M/G)
KH ₂ PO ₄	3 g	3 g	0.5 g
MgSO ₄ .7H ₂ O	0.5 g	0.5 g	0.2 g
CaCl ₂ .2H ₂ O	0.05 g	0.05 g	0.05 g
Na-Glutamate	1.85 g	0.36 g	1.85 g
NaCl	-	-	0.4 g
Acetate	1.15 ml	2.29 ml	-
L-Malic acid	-	-	1 g
Vitamin Solution (10x)	0.1 ml	0.1 ml	0.1 ml
Fe-Citrate (50x)	0.5 ml	0.5 ml	0.5 ml
Trace Element Solution (10x)	0.1 ml	0.1 ml	0.1 ml

Table A. 2 The composition of 10 x Vitamin solution for 100 ml

Composition	Amount
Thiamin chloride hydrochloride	0.5 g
Niacin (Nicotinic acid)	0.5 g
D+ Biotin	15 mg

Table A. 3 The composition of 10 x trace element solution for 100 ml

Composition	Amount
ZnCl ₂	700 mg
MnCl ₂ .4H ₂ O	1000 mg
H ₃ BO ₃	600 mg
CoCl ₂ .6H ₂ O	2000 mg
CuCl ₂ .2H ₂ O	200 mg
NiCl ₂ .6H ₂ O	200 mg
Na ₂ MoO ₄ . 2H ₂ O	400 mg
HCl (25 % v/v)	10 ml

APPENDIX B

SOLUTIONS AND BUFFERS

TAE

40 mM Tris base (Buffer grade)

1mM EDTA disodium dihydrate

Glacial acetic acid

EtBr

10mg ethidium bromide is dissolved in 1 ml distilled water

CaCl₂

11.1 g of CaCl₂ (anhydrous) is dissolved in 100 ml of distilled water

Ampicillin

100 µg ampicillin is dissolved in 1 ml sterile water

Kanamycin

25 µg kanamycin is dissolved in 1 ml sterile water

Streptomycin

25 µg streptomycin is dissolved in 1 ml sterile water

Tetracycline

25 µg tetracycline is dissolved in 1 ml sterile water.

IPTG (Isopropyl β -D-1-thiogalactopyranoside)

25 μ g IPTG is dissolved in 1 ml sterile water

X-GAL (bromo-chloro-indolyl-galactopyranoside)

25 μ g X-GAL is dissolved in 1 ml sterile water

APPENDIX C

OPTICAL DENSITY-DRY WEIGHT CALIBRATION CURVE

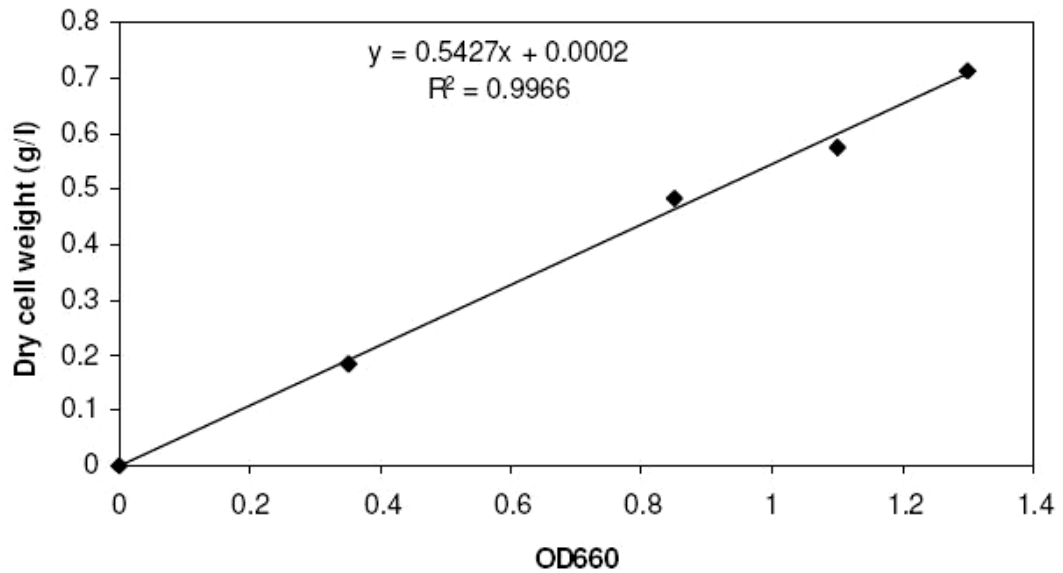


Figure C. 1 Calibration curve and the regression trend line for *Rhodobacter capsulatus* (DSM 1710) dry weight versus OD660 (Uyar, 2008).

APPENDIX D

SAMPLE GAS CHROMATOGRAM

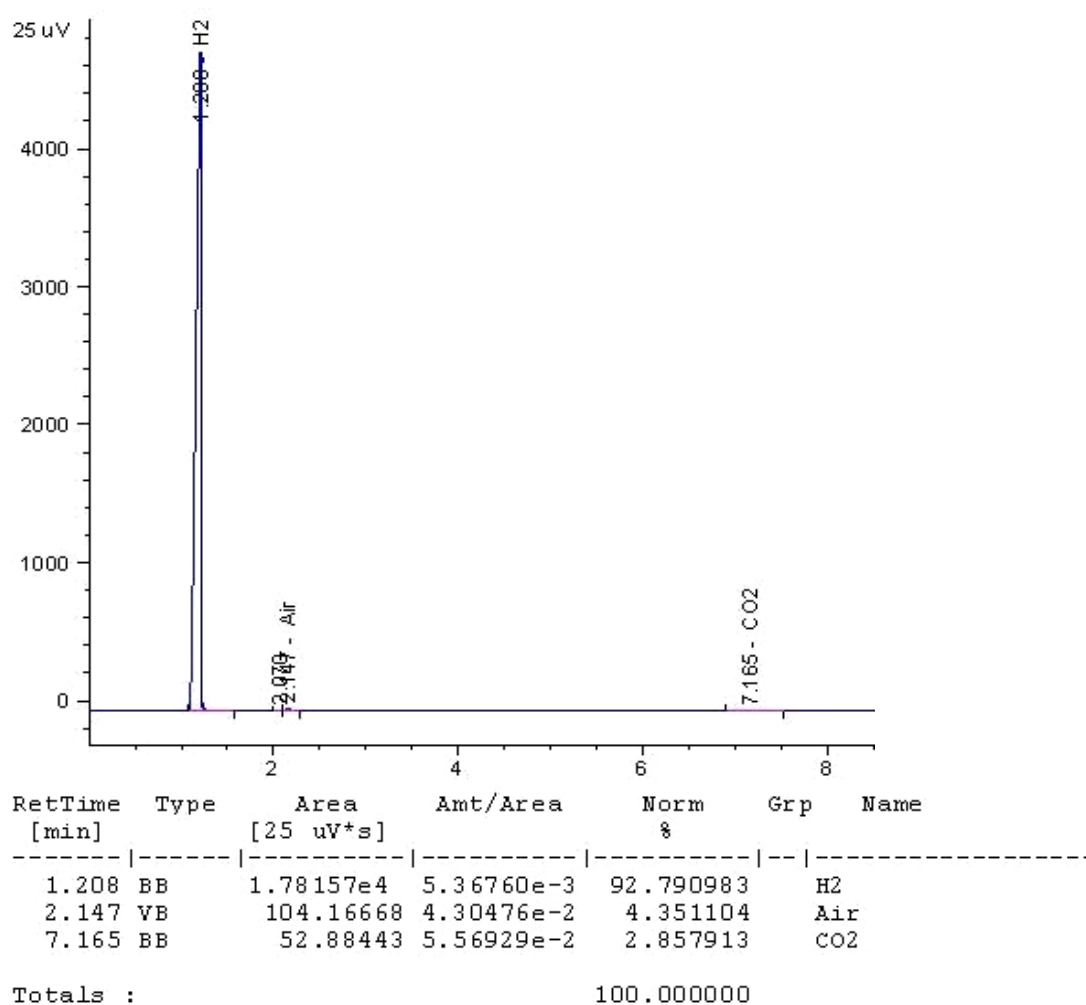
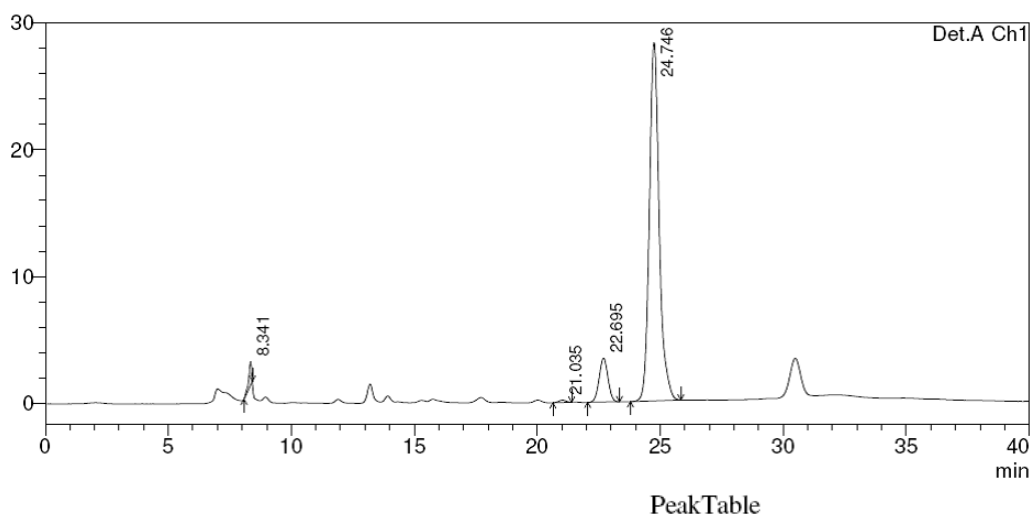


Figure D. 1 A sample chromatogram for GC analysis of the collected gas

APPENDIX E

SAMPLE HPLC CHROMATOGRAM AND CALIBRATION CURVES



Peak#	Ret. Time	Area	Height	Area %	Height %
1	8.341	14689	1859	1.654	5.516
2	21.035	3735	182	0.420	0.542
3	22.695	86422	3453	9.730	10.248
4	24.746	783359	28200	88.196	83.694
Total		888205	33695	100.000	100.000

Figure E. 1 A Sample HPLC analysis chromatogram. Peak 1 (mobile phase- H₂SO₄), Peak 2 (lactic acid), Peak 3 (formic acid) and Peak 4 (acetic acid).

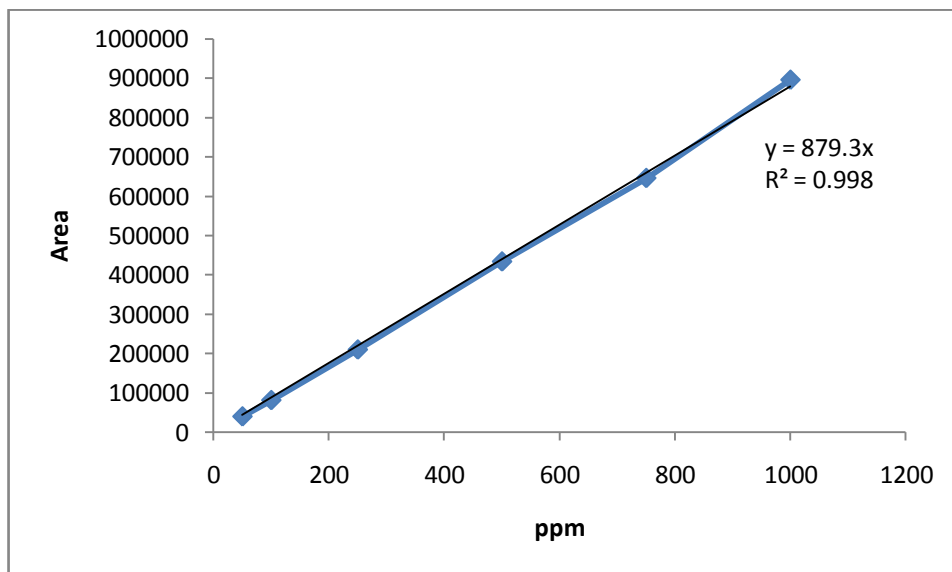


Figure E. 2 The acetic acid calibration curve

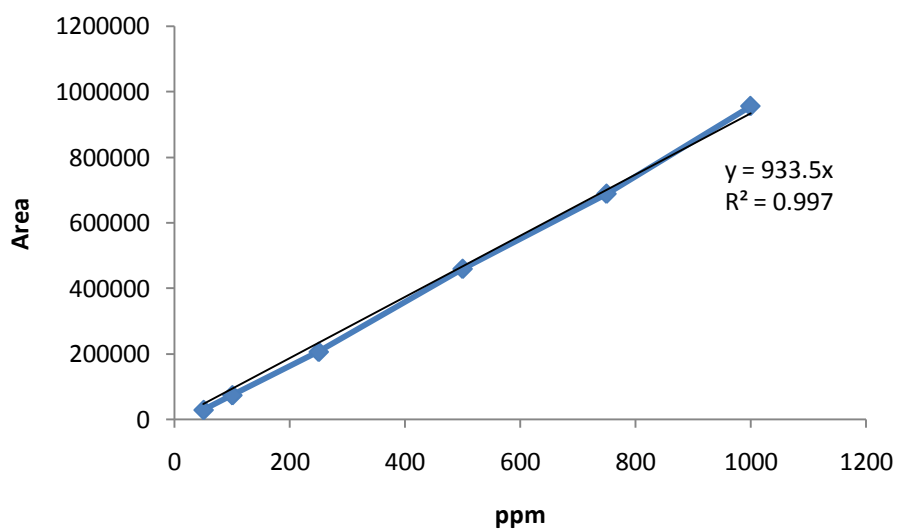


Figure E. 3 The lactic acid calibration curve

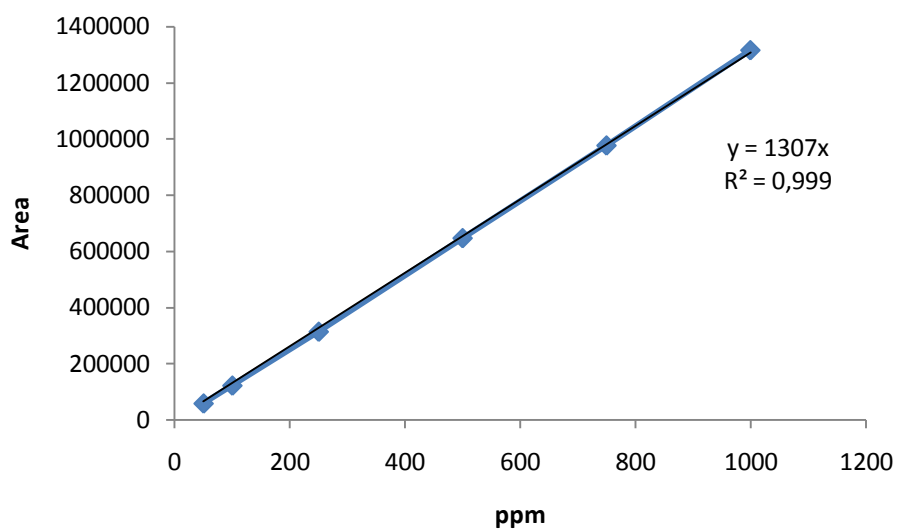


Figure E. 4 Formic acid calibration curve

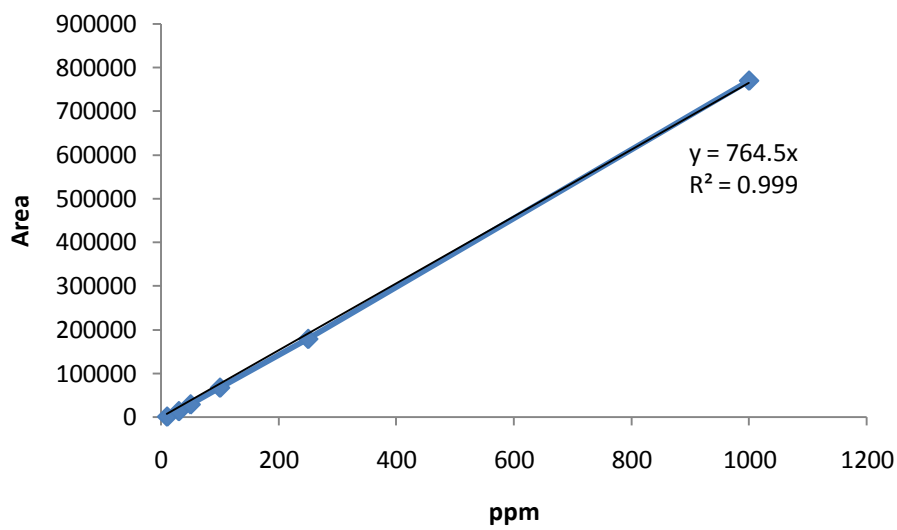


Figure E. 5 Propionic acid calibration curve

APPENDIX F

SAMPLE DNA SEQUENCE ANALYSIS

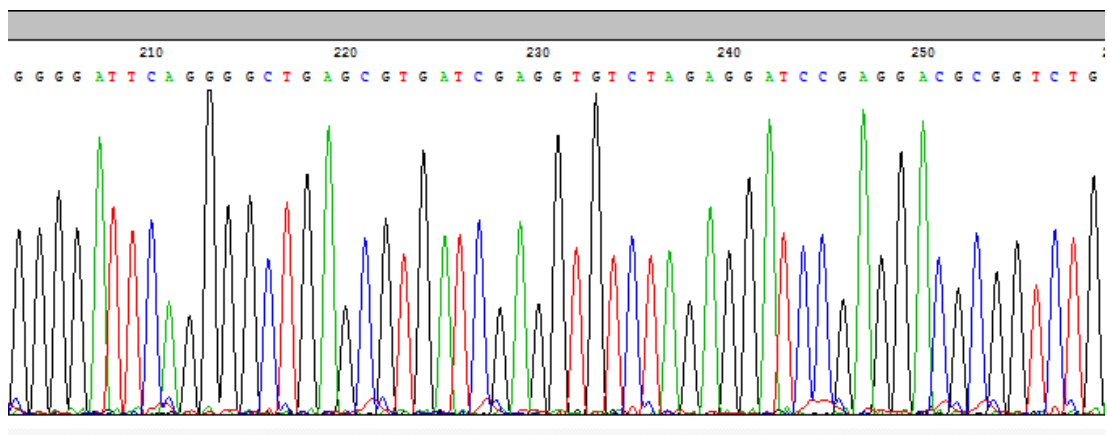


Figure F. 1 A sample sequence analysis

APPENDIX G

PRIMERS AND SEQUENCES

Table G. 1 Complete list of primers and their sequences

Primer Name	Sequence
OGLNBU-F2	<i>CTGCAG-AACGCATCTCCTCGGTCAAG</i>
OGLNBU-R2	<i>TCTAGA- CACCTCGATCACGCTCAGCC</i>
OGLNB3F	<i>GGATCC-GAGGACGCGGTCTGAGACTT</i>
OGLNB4R	<i>TCGCGTGTTTCAGGATACCG</i>
OGLNKH-F2	<i>GGATCC-GAAGCCCTTGATTTCCGTCAC</i>
OGLNKH-R2	<i>GAATTC-GCGGCAGTCGGTCTCGTAATC</i>
OGLNK1F	<i>CTGCAG-CCTTGGTGACGAAGAAGTAG</i>
OGLNK2R	<i>TCTAGAGACGAAGCGCTGTAAGAACC</i>
T3	<i>AATAACCCTCACTAAAG</i>
T7	<i>AATACGACTCACTATAG</i>

Table G1. Complete list of primers and their sequences continued

M13fw	CGCCAGGGTTTTCCCAGTCACGAC
M13rev	AGCGGATAACAATTTACACAGGA
OGNB5F	GCCGCCCAAACAGTTTACAC
OGLNB6R	CGCCTTCATCAGATCGAGAG
OGLNK5F	TCAGCACGGAGAGCATGTTC
OGLNK6R	TTCCGCCGCGCAACTTACAC

The sequence of *glnB* gene:

“ATGAAGAAGGTCGAGGCGATCATCAAGCCGTTCAAGCTCGATGAAGTG
AAGGAAGCGCTTCAGGAAGCGGGGATTCAAGGGCTGAGCGTGATCGAGG
TGAAAGGCTTCGGGCGGCAAAAGGGCCATACCGAGCTGTATCGCGGGGC
CGAATATGTCGTCGACTTCCTGCCAAGGTGAAGATCGAGATGGTTCTGC
CCGACGAGATGGTCGATATCGCCATCGAGGCCATCGTCGGCGCCGCCCG
CACCGAAAAGATCGGCGACGGGAAGATCTTCGTCTCCTCCATCGAACAG
GCGATCCGCATCCGCACCGGCGAGACCGGCGAGGACGCGGTCTGA”

The sequence of *glnK* genes:

“TTACAGCGCTTCGTGCGCCAGCTTCGCCGGTGCGCACCCGCACGGCCTGA
TTCACGTCGAGCACGAAGATCTTGCCGTCGCCGATCTTGTCGGTCTTGGC
CGCTTTCAGGATCGTCTCGACCACCTCGTCGGCCAGATTGTCGGCCACGA
CGATTTCAAGCTTCACCTTCGGCACGAAATTCACCGCATATTCGGCGCCG
CGATAAATTTCCGTATGCCCCGACTGCGCGCCGAAGCCCTTGATTTCCGT
CACCATCATCCCGCGCACGCCGATGCCGGTCAGCGCCTCGCGGACCTCCT
CGAGCTTGAACGGTTTGATCGCTGCAATGATGAGTTTAC”

APPENDIX H

RESTRICTION ENDONUCLEASES AND DNA/RNA MODIFYING ENZYMES

*Bam*HI (Fermentas, cat. # ER0054)

*Eco*RI (Fermentas cat. # ER0274)

*Eco*RV (Eco32I) (Fermentas, cat. # ER0301)

*Hinc*II (HindII) (Fermentas, cat. # ER0494)

*Hind*III (MBI Fermentas cat. # ER0501)

*Kpn*I (Fermentas cat. # ER0524)

*Xba*I (Fermentas cat. # ER0684)

*Pst*I (Fermentas cat. # ER0614)

Pfu DNA polymerase (Fermentas, cat. # EP0501)

Taq DNA polymerase (Fermentas, cat. # EP0401)

Phusion high fidelity DNA polymerase (Finnzymes, cat. # F-530S)

DyNAzyme II DNA polymerase (Finnzymes, cat. # F-501S)

Klenow Fragment (Fermentas, cat. #EP0051)

T4 DNA polymerase (Fermentas, cat. #EP0061)

T4 DNA Ligase (Fermentas, cat. #EL0014)

T4 Polynucleotide Kinase (T4 PNK) (Fermentas, cat. # EK0031)

Calf Intestine Alkaline Phosphatase (CIAP) (Fermentas, cat. #EF0341)

APPENDIX I

LOGISTIC MODEL

I1-I11. Curves fitted to the Logistic Model for growth of *Rhodobacter capsulatus* wild type in different concentrations of ammonium

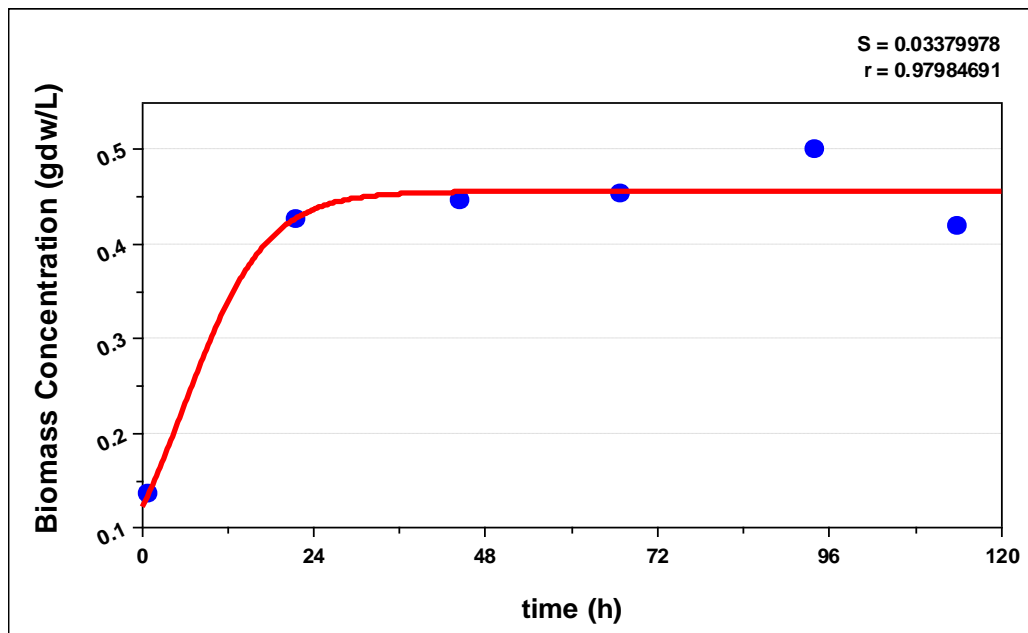


Figure I. 1 The logistic growth model of *R. capsulatus* wild type in 2 mM glutamate (control) containing medium

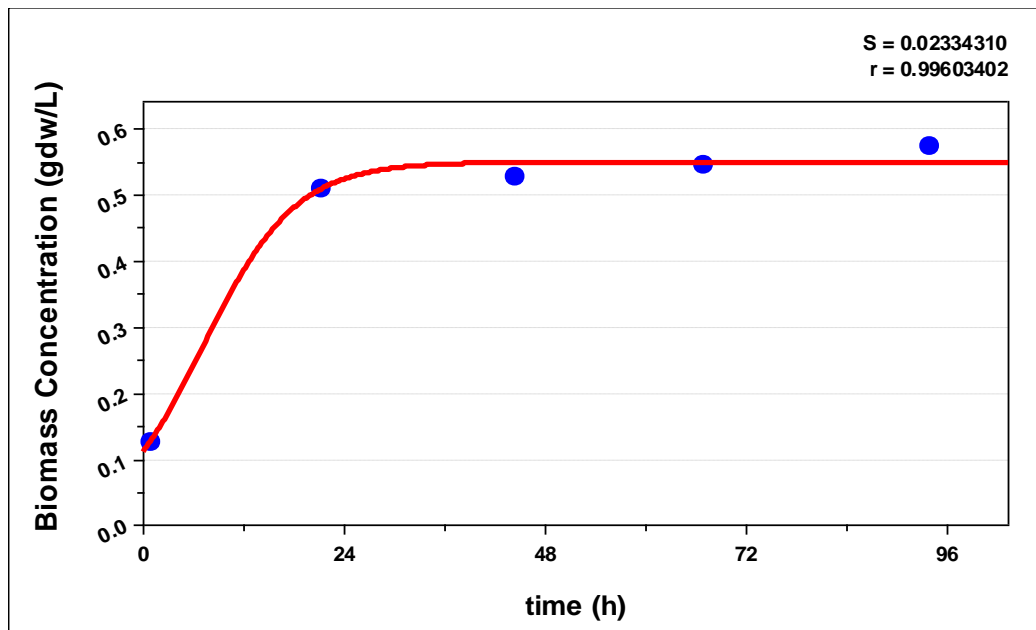


Figure I. 2 The logistic growth model of *R.capsulatus* wild type in 2 mM NH_4Cl containing medium

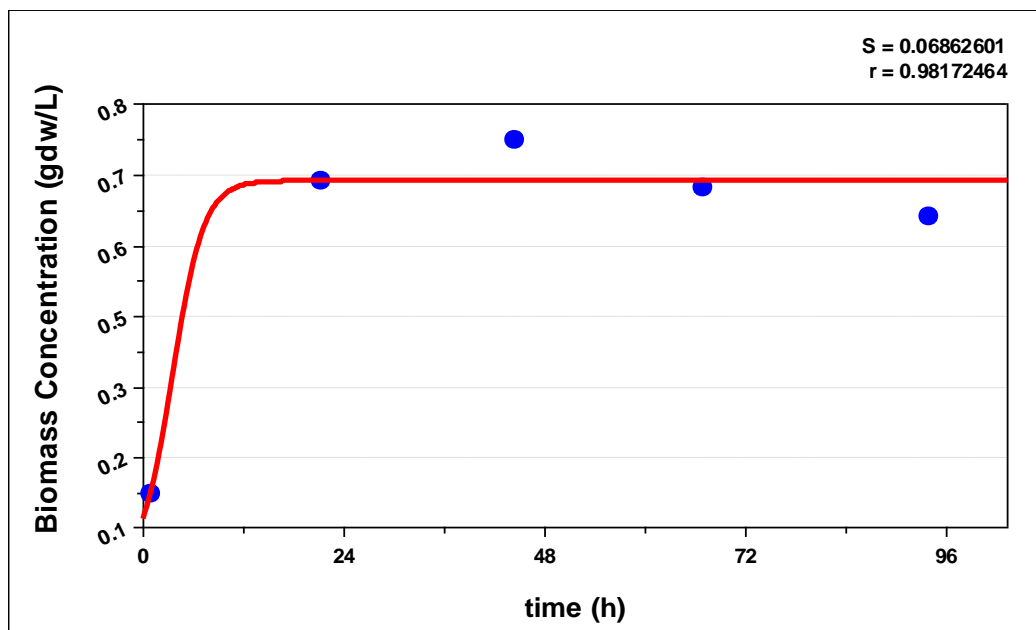


Figure I. 3 The logistic growth model of *R.capsulatus* wild type in 3 mM NH_4Cl containing medium

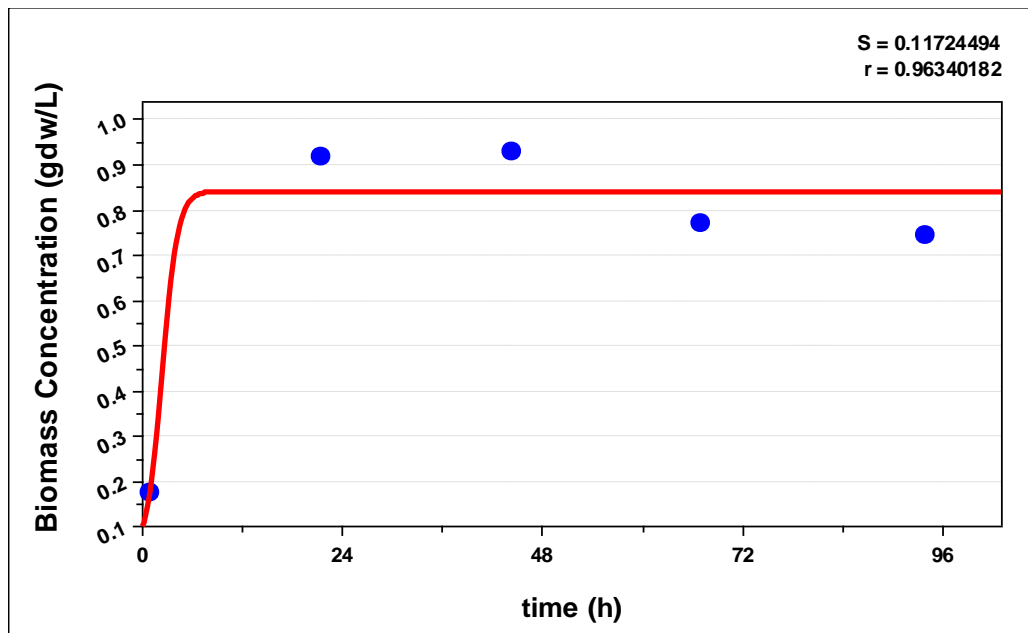


Figure I. 4 The logistic growth model of *R. capsulatus* wild type in 5 mM NH_4Cl containing medium

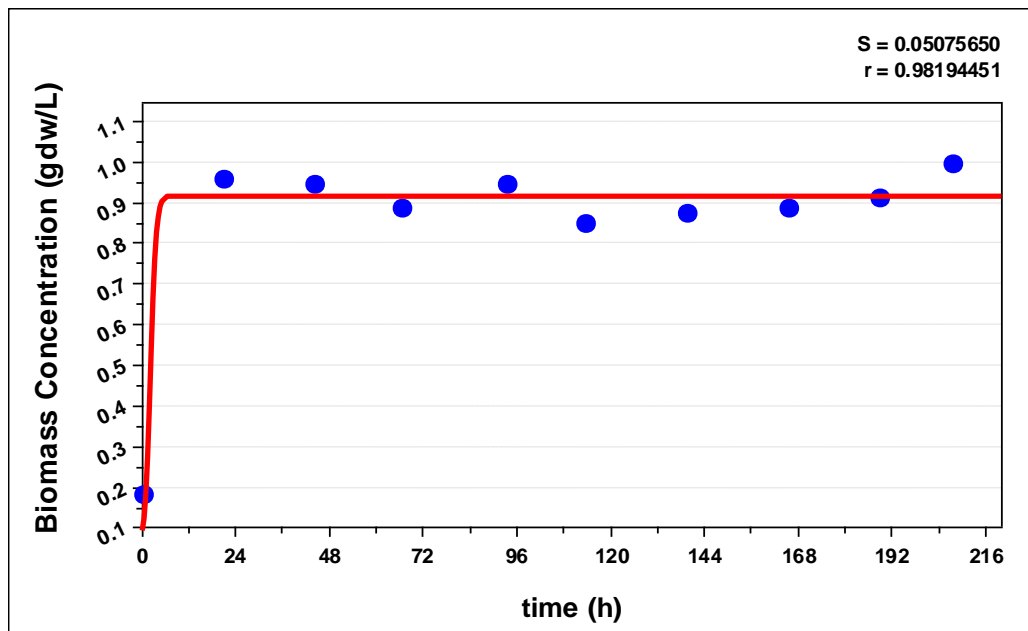


Figure I. 5 The logistic growth model of *R. capsulatus* wild type in 8 mM NH_4Cl containing medium

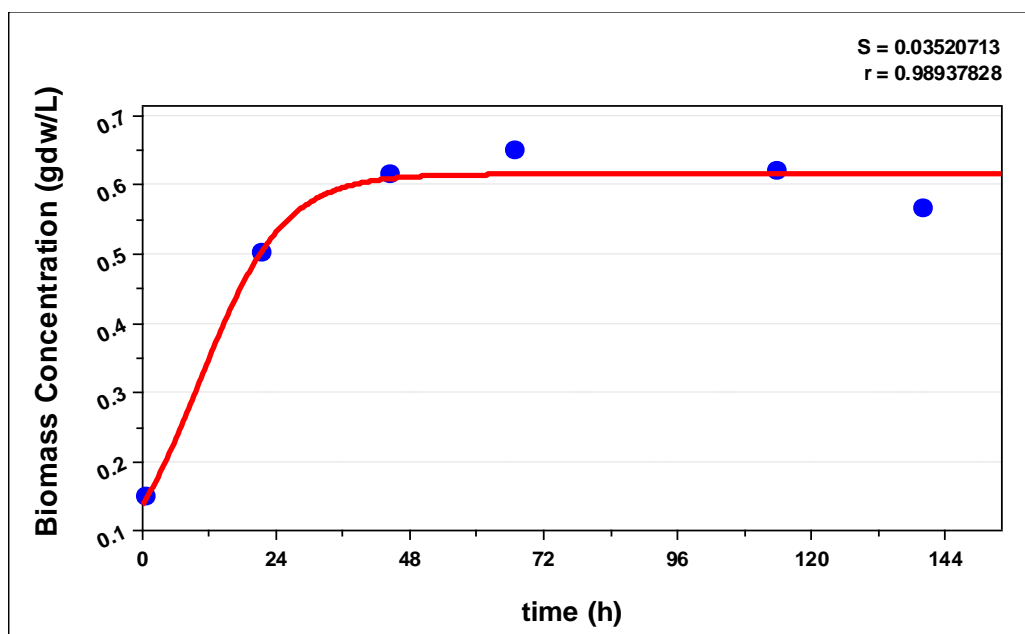


Figure I. 6 The logistic growth model of *R.capsulatus glnB* mutant in 2 mM glutamate (control) containing medium

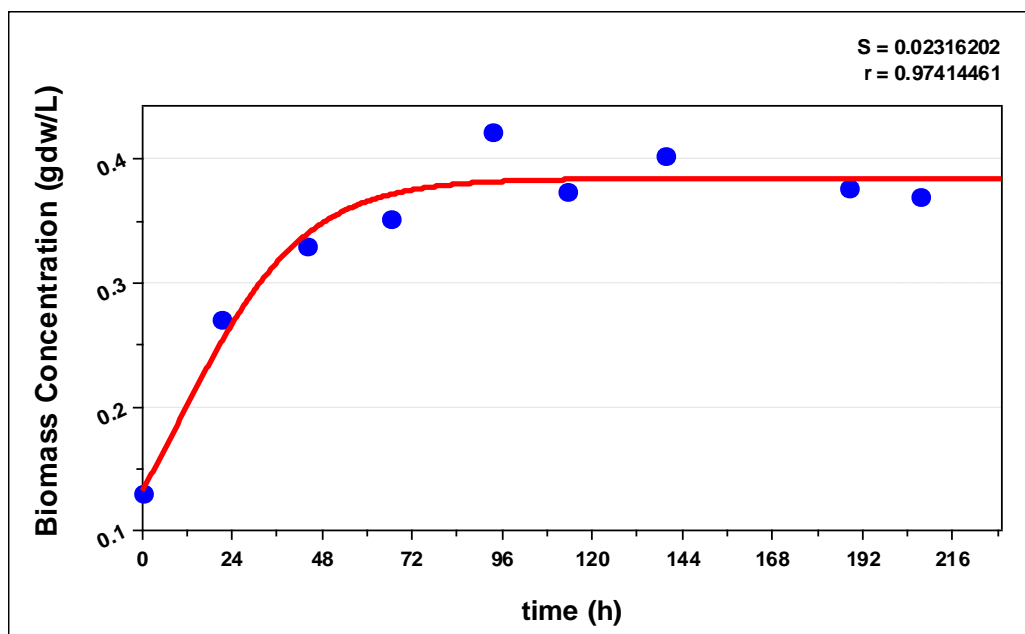


Figure I. 7 The logistic growth model of *R.capsulatus glnB* mutant in 1 mM NH_4Cl containing medium

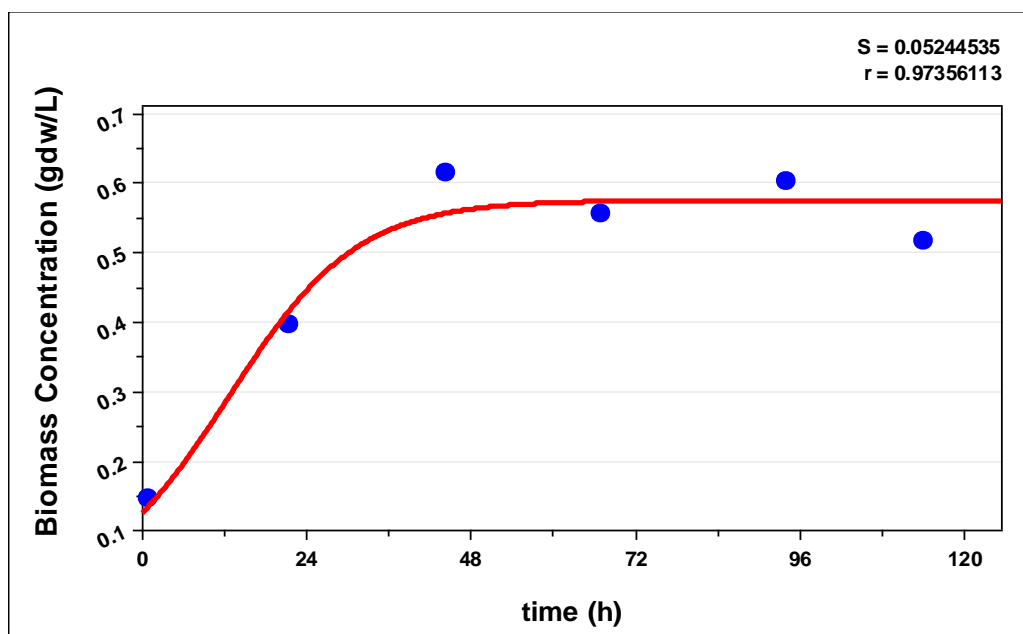


Figure I. 8 The logistic growth model of *R. capsulatus glnB* mutant in 2 mM NH_4Cl containing medium

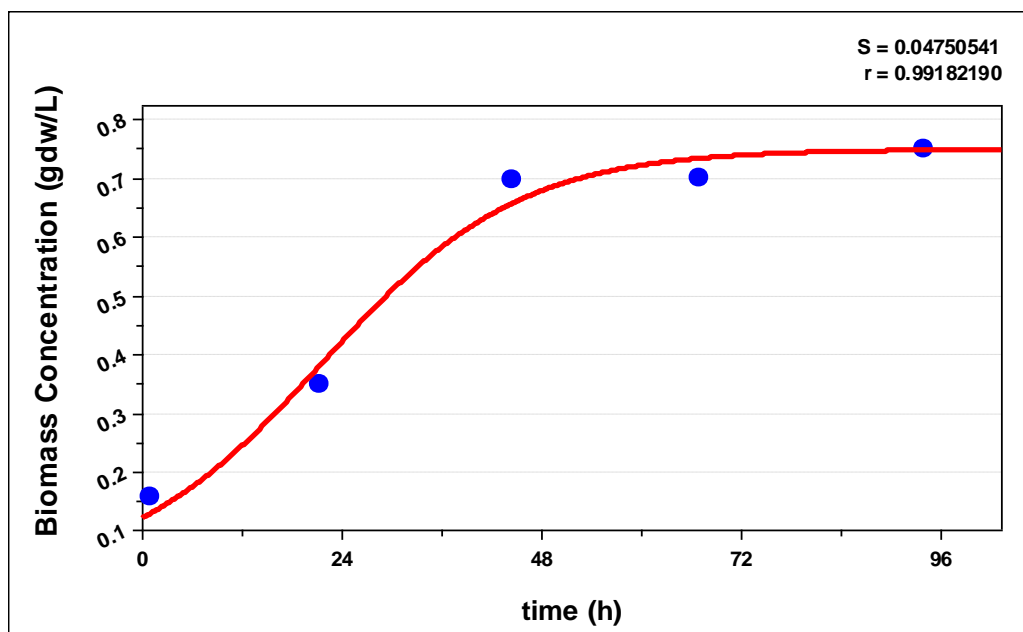


Figure I. 9 The logistic growth model of *R. capsulatus glnB* mutant in 3 mM NH_4Cl containing medium

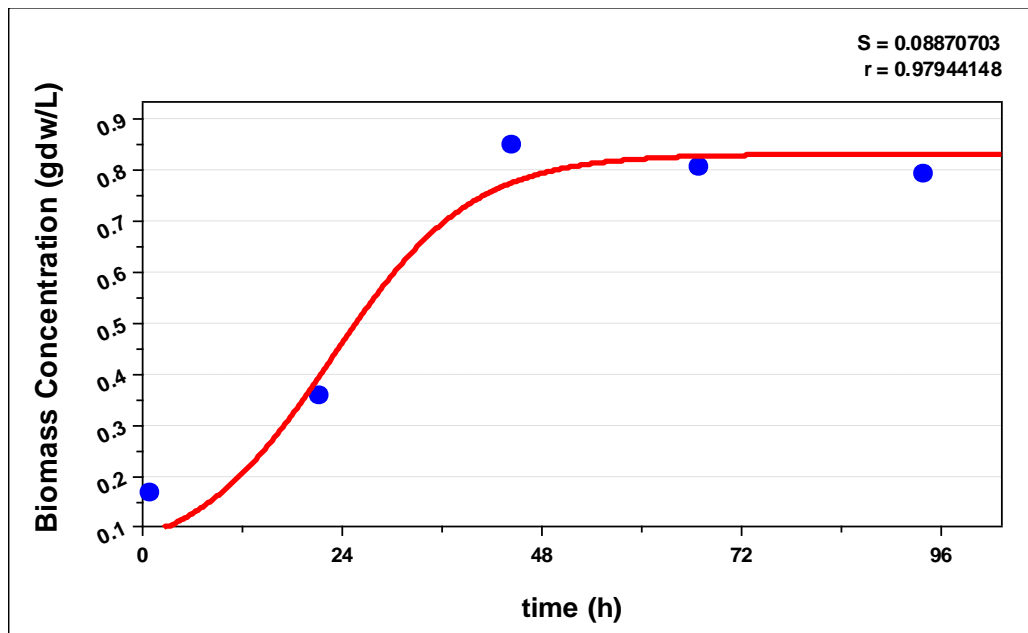


Figure I. 10 The logistic growth model of *R. capsulatus glnB* mutant in 5 mM NH_4Cl containing medium

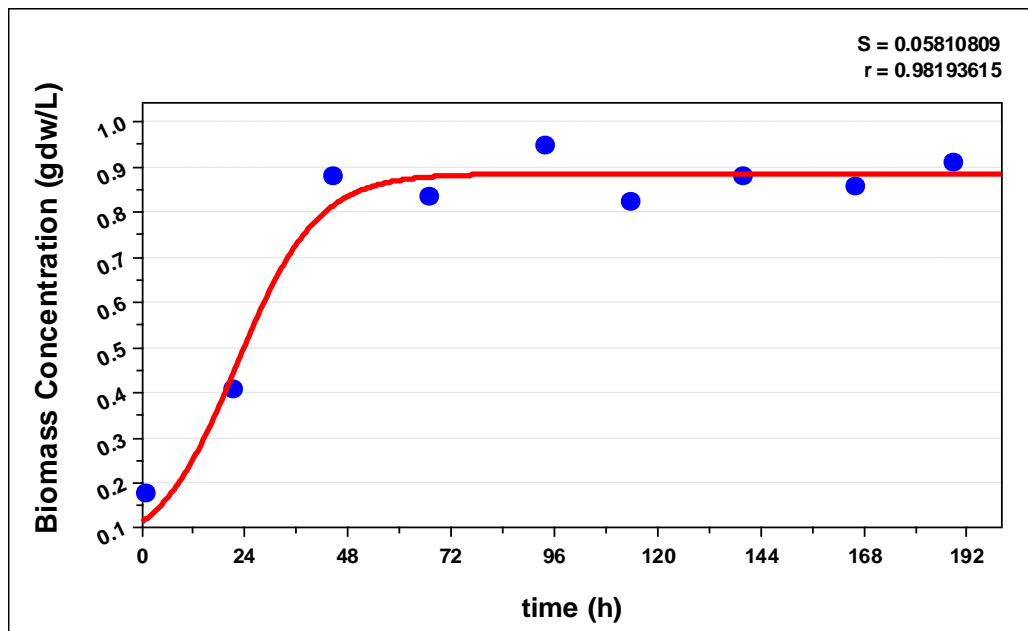


Figure I. 11 The logistic growth model of *R. capsulatus glnB* mutant in 8 mM NH_4Cl containing medium

APPENDIX J

MODIFIED GOMPERTZ MODEL

J1-J9. Curves fitted to the Modified Gompertz Model for hydrogen production of *Rhodobacter capsulatus* wild type in different concentrations of ammonium

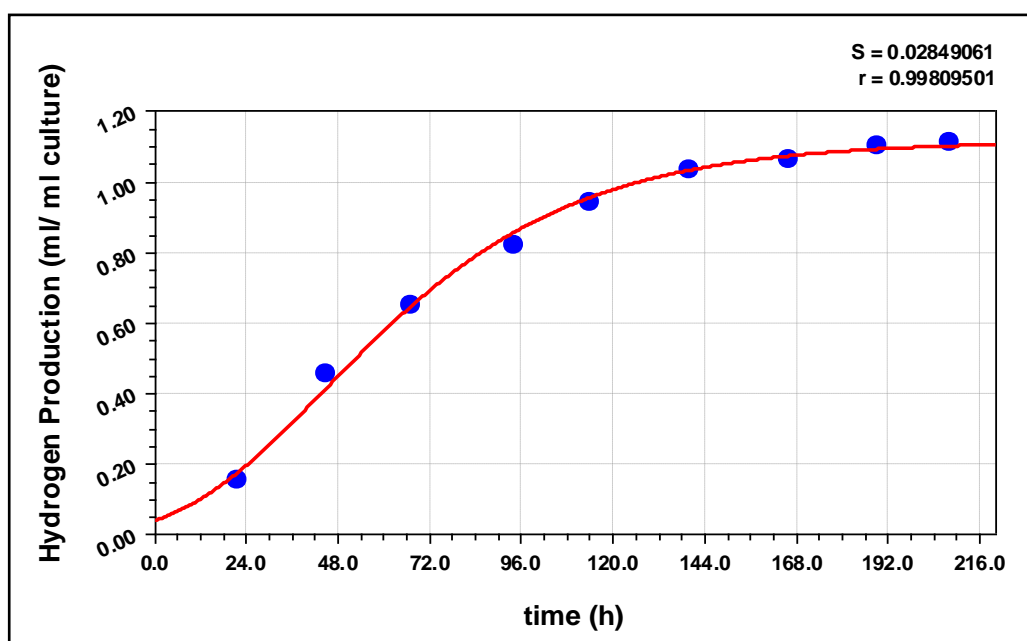


Figure J. 1 The Modified Gompertz Model of *R.capsulatus* wild type in 2 mM glutamate (control) containing medium

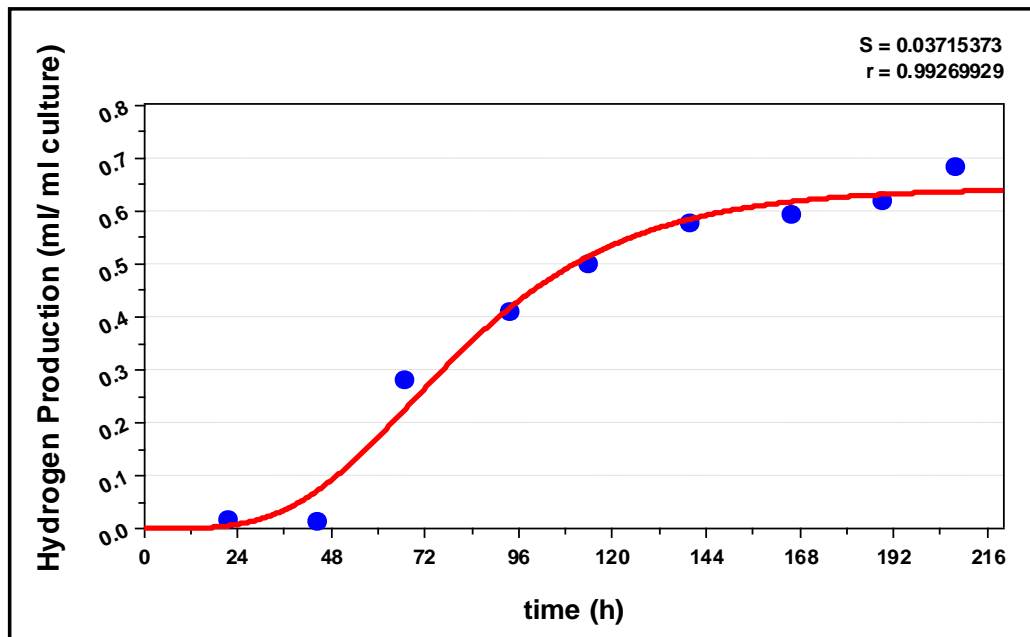


Figure J. 2 The Modified Gompertz Model of *R.capsulatus* wild type in 2 mM NH_4Cl containing medium

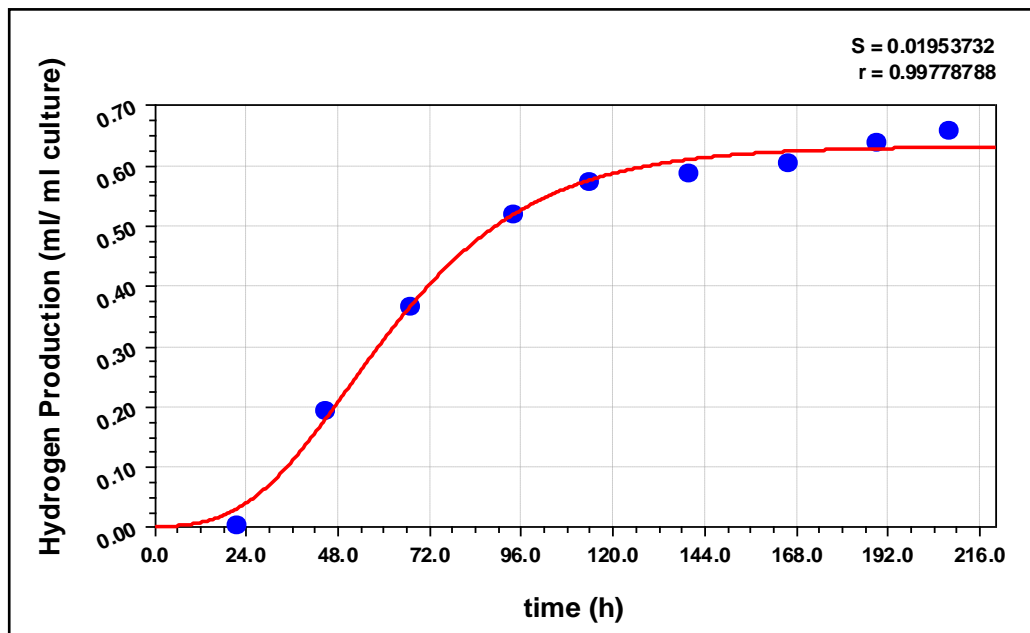


Figure J. 3 The Modified Gompertz Model of *R.capsulatus* wild type in 3 mM NH_4Cl containing medium

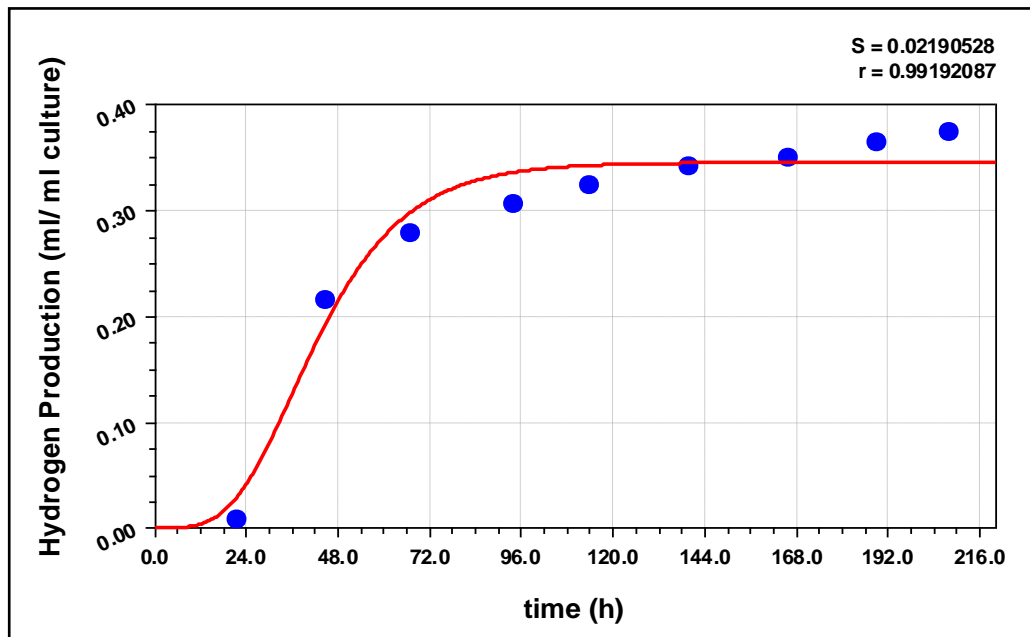


Figure J. 4 The Modified Gompertz Model of *R. capsulatus* wild type in 5 mM NH_4Cl containing medium

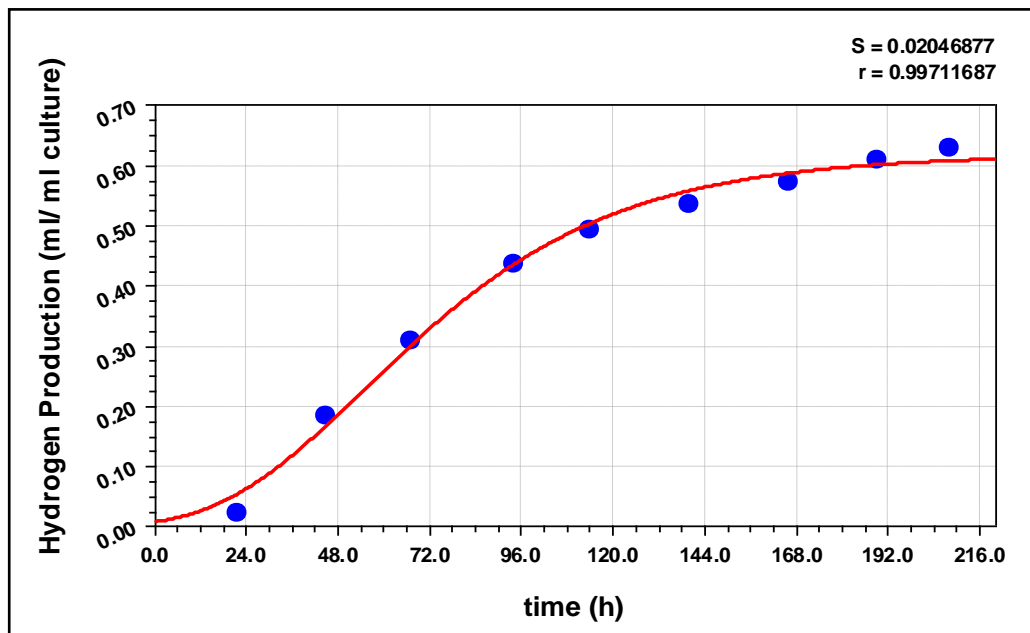


Figure J. 5 The Modified Gompertz Model of *R. capsulatus glnB* mutant in 2 mM glutamate (control) containing medium

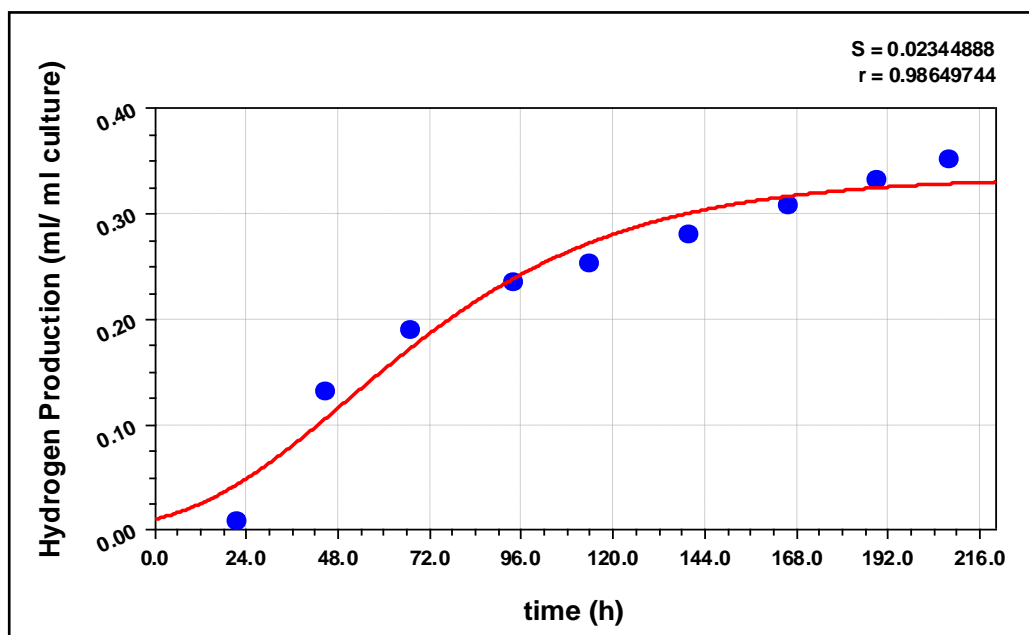


Figure J. 6 The Modified Gompertz Model of *R.capsulatus glnB* mutant in 1 mM NH_4Cl containing medium

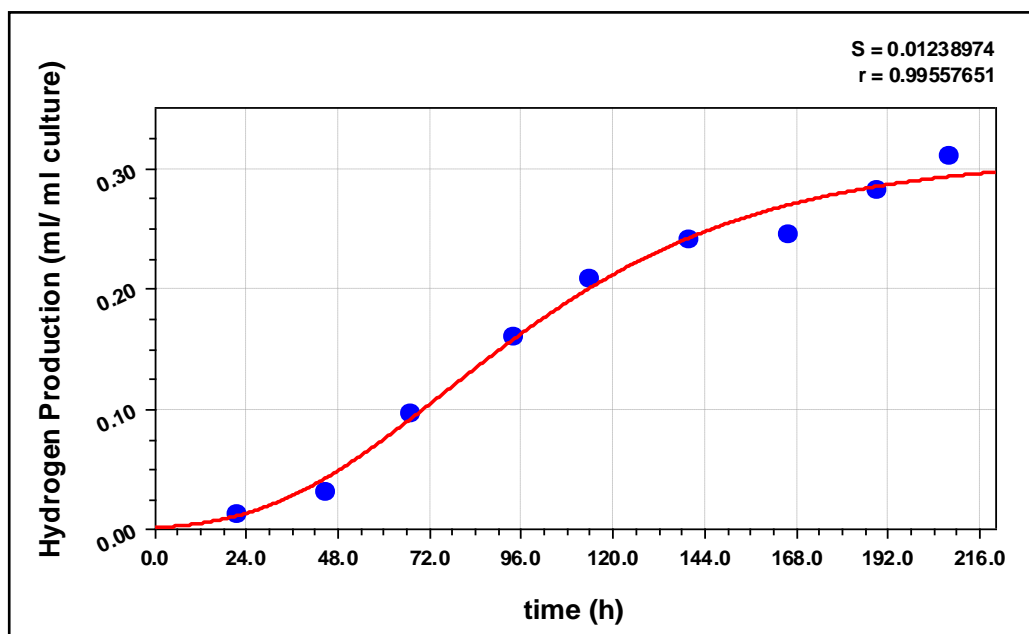


Figure J. 7 The Modified Gompertz Model of *R.capsulatus glnB* mutant in 2 mM NH_4Cl containing medium

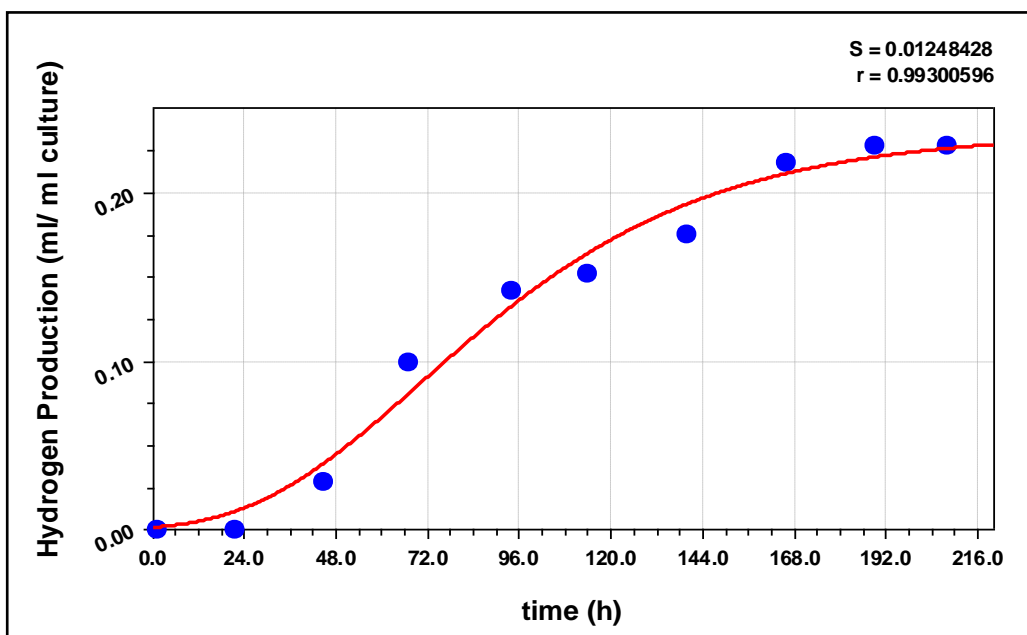


Figure J. 8 The Modified Gompertz Model of *R.capsulatus glnB* mutant in 3 mM NH_4Cl containing medium

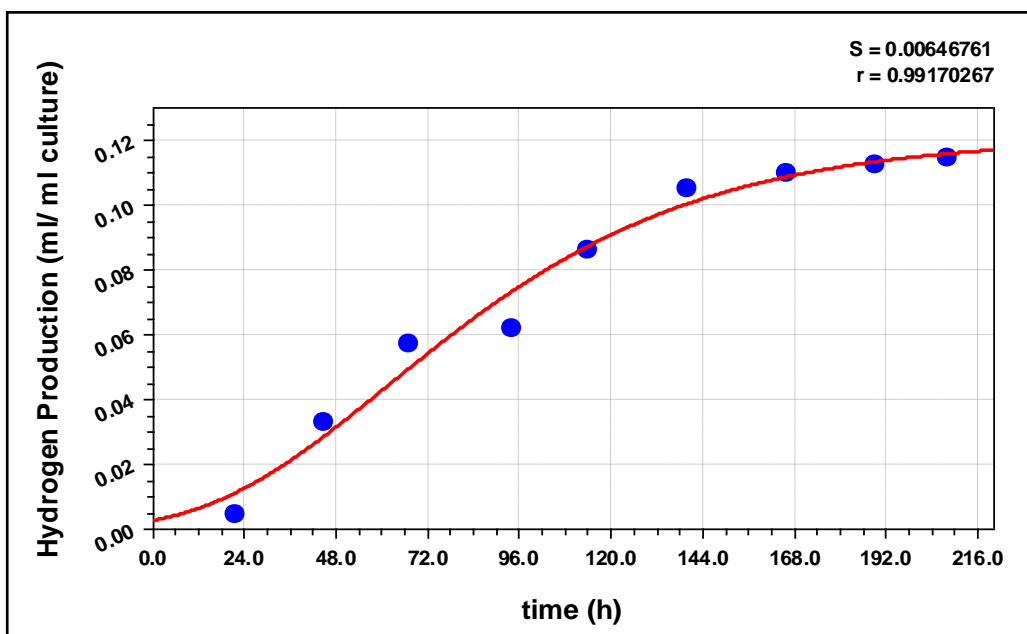
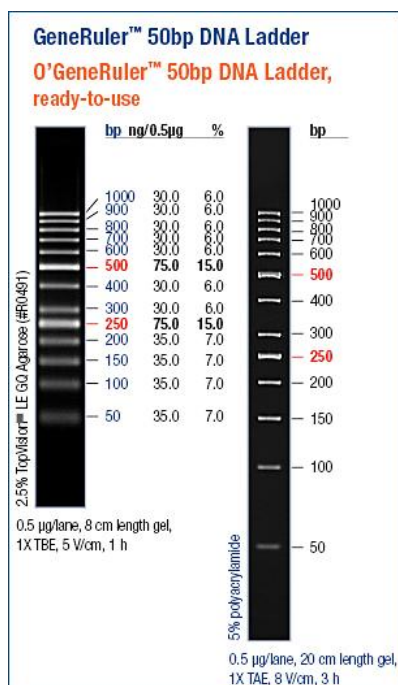


Figure J. 9 The Modified Gompertz Model of *R.capsulatus glnB* mutant in 5 mM NH_4Cl containing medium

APPENDIX K

DNA LADDERS

A



B

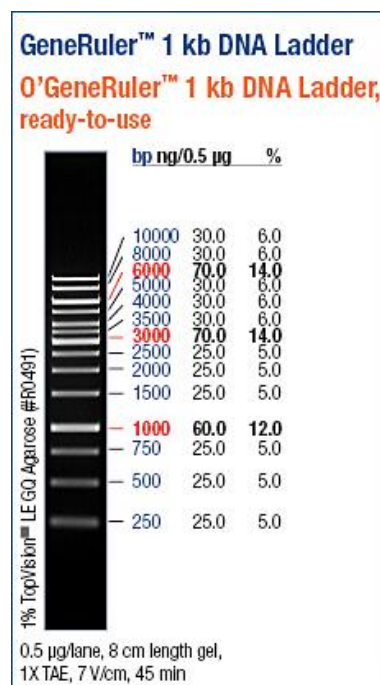


Figure K. 1 Fermentas GeneRuler 50 bp DNA Ladder (50-1000 bp) and 1 kb DNA Ladder (250-10,000 bp)